AN ABSTRACT OF THE THESIS OF

Kenneth Alan Philbrick for the degree of Master of Science in Exercise and Sport Science presented on June 6, 2008

Title: Spatial Consumption and Risk of Lower Back Disorder during Assisted Toilet Transfers On Board an Aircraft

Abstract approved:

_____

Michael J. Pavol

A major barrier to air travel for people with disabilities is the general lack of accessible lavatories on board commercial passenger aircraft. A primary reason for this lack of greater accessibility is related to space. To design an airplane lavatory that is accessible, minimizes the risk of injury to both the transferor and transferee to the extent possible, and is still consistent with the restrictive spatial requirements of airplane environments requires a broader understanding as to how the relative angle of the wheelchair to the toilet affects assisted toilet transfers.

This study investigated how the wheelchair-to-toilet angle affects both the spatial consumption required for assisted toilet transfers and the risk of injury to the transferor and transferee. Twenty-nine participants (transferors) were motion captured in a laboratory environment while conducting assisted toilet transfers using a pivot transfer technique at relative wheelchair-to-toilet angles of 0º, 45º, 90º, and 180º. A 95th percentile male dummy represented the transferee. A novel, three-dimensional computer-based spatial mapping technique was developed to compute the spatial volume requirements of assisted toilet transfers from the motion capture data.

The wheelchair-to-toilet angle directly affected the total spatial volume needed to conduct an assisted toilet transfer. The total rectangular area required to perform an assisted toilet transfer using a pivot transfer technique progressively increased as the wheelchair-to-toilet angle rose from 0° to 180°. However, the three-dimensional volume required for an assisted transfer differs between transfer angles, is non-rectangular, and varies in spatial area over the height of the transfer volume.

The wheelchair-to-toilet angle also affected the magnitude of the transferor's kinematic risk factors for lower back disorder. Eight of the fourteen analyzed kinematic risk factors for lower back disorder were affected. Of these risk factors, the wheelchair-to-toilet angle primarily affected the transferor's odds of being at high risk of lower back disorder through its effect on the transferor's maximum load moment arm. Surprisingly, the magnitude of the transferor's maximum load moment arm was inversely related to the wheelchair-to-toilet angle. After accounting for the effects of the wheelchair-to-toilet angle and the direction of assisted transfer, associations were also found between the transferor's kinematic risk factors for lower back disorder and the transferor's standing height.

The results of this study suggest that accessible lavatories can be designed for use in constrained environments by designing the lavatory to support assisted transfers at a single optimal wheelchair-to-toilet angle. The results further suggest that, in using a pivot transfer technique, the 180º orientation is an optimal transfer orientation. Finally, it is suggested that transferors short in stature and physically capable of conducting assisted transfers should be preferentially selected to assist in assisted transfers, as they are predicted to have a lower risk of lower back disorder than taller transferors.

Spatial Consumption and Risk of Lower Back Disorder during Assisted Toilet Transfers On Board an Aircraft

by
Kenneth Alan Philbrick

A THESIS

submitted to

Oregon State University

in partial fulfillment of
the requirements for the
degree of

Master of Science

Presented June 6, 2008
Commencement June 2009

Master of Science thesis of Kenneth Alan Philbrick presented on June 6, 2008.

APPROVED:

Major Professor, representing Exercise and Sport Science

Chair of the Department of Nutrition and Exercise Sciences

Dean of the Graduate School

I understand that my thesis will become part of the permanent collection of Oregon State University libraries. My signature below authorizes release of my thesis to any reader upon request

Kenneth Alan Philbrick, Author

ACKNOWLEDGEMENTS

This thesis would not have been possible without significant support and encouragement from the faculty at Oregon State University, friends, and family.

I would like to specifically thank Mike Pavol Ph.D. (advisor). Dr. Pavol's unending support and guidance has been instrumental in the success of this and other works.

I would further like to thank my friends and past and present colleagues in the OSU Biomechanics Lab. Brian Higginson, Josh Baxter, Lisa Welsh, Kristof Kipp, Melissa Mache, and Norio Kadono, the support, friendship, and jokes you have provided have been invaluable.

Finally, I would like to thank my parents, David and Cathey, and brother John for their unending support during the development and authorship of this work and their ongoing support of my graduate studies.

Finally, I would like to thank the Oregon State University National Center for Accessible Transportation, for the funding that supported this research (funded by grant H133E030009 from the U.S. Dept. of Education, NIDRR).

TABLE OF CONTENTS

Page

Introduction 1

Literature Review 4

Prevalence of Disability 4

Federal Accessibility Legislation 4

Spatial Consumption 7

Risk of Lower Back Disorder 8

Kinetic and Kinematic Risk Factors for Lower Back Disorder 9

Assessing Lower Back Disorder Risk 12

Validity of the Model for Lower Back Disorder Developed by Marras *et al.* (1995) 13

Perceived Exertion 16

Biomechanics of Assisted Toilet Transfers 17

Purpose and Hypotheses 19

Purpose 19

Research Hypotheses 21
Spatial Consumption 21
Risk of Injury to the Transferor 21
Risk of Injury to the Transferee 22

Materials and Methods 23

Human Participants 23

Instruments and Apparatus 24
Experimental Setup 24
Experimental Protocol 26
Pre-Trial 27
Assisted Transfer Data Collection 29
Post-Trial Data Collection 31

Data Analysis 32

TABLE OF CONTENTS (Continued)

Page

Spatial Consumption 34

Statistical Analysis 39
Qualitative Spatial Requirements of Assisted Transfers 39
Transferor's Kinematic Risk Factors for Lower Back Disorder, Perceived Exertion, and the Vertical Acceleration of the Transferee 40

Assumptions 43

Delimitations 44

Results 45

Spatiotemporal Consumption 45

Transferor Kinematics 57

Transferee Kinematics 67

Characteristics of the Transferor as Predictors of Risk Factors for Lower Back Disorder 67

Discussion 77

Spatial Requirements for Assisted Toilet Transfers 77

Risk of Injury during Assisted Toilet Transfers 84

Limitations 102

Future Research 106

Conclusion 110

References 114

LIST OF FIGURES

Figure Page

1 – Experimental lavatory design 24

2 – Software's graphical representation of the three-dimensional model of an assisted transfer for a participant at a fixed point in time. 36

3 – Illustration of the calculation of the area occupied by the participant, wheelchair, and dummy at two experimental heights. 37

4 – Percentile planar intersection map taken below and above the knee 38

5 – Mapping representative of that to be used to express the combined percentage of time that any location in a plane at a specified height was occupied across all participants..... 39

6 – Spatial consumption at 1 cm from the floor as a function of transfer angle, area occupied by the wheelchair's wheels and the feet of the transferor and dummy. 48

7 – Spatial consumption at 20 cm from the floor, as a function of transfer angle; the area occupied by the wheelchair's leg struts and the mid calf of the transferor and dummy. 49

8 – Spatial consumption at 44 cm from the floor, seat height of the wheelchair, as a function of transfer angle. 50

9 – Spatial consumption at 62 cm from the floor, transferor and dummy pelvis height, as a function of transfer angle. 51

10 – Spatial consumption at 75 cm from the floor, transferor lower trunk to mid trunk height, as a function of transfer angle. 52

11 – Spatial consumption at 86 cm from the floor, transferor lower trunk to mid trunk height, as a function of transfer angle..... 53

12 – Spatial consumption at 105 cm from the floor, seated dummy head height, as a function of transfer angle. 54

13 – Spatial consumption at 118 cm from the floor, area used by the transferor's upper trunk and dummy head, as a function of transfer angle. 55

14 – Spatial consumption at 138 cm from the floor, upper trunk and head height of the transferor, as a function of transfer angle. 56

LIST OF FIGURES (Continued)

Figure Page

15 – Standing height vs. transfer leg position 98

LIST OF TABLES

Table Page

1 – Minimum spatial requirements for an assisted toilet transfer, as determined by Warren *et al.* (1991) 7

2 – Participant Descriptive Statistics, mean (SD) 24

3 – Participant Motion Capture Marker Set 26

4 – Dummy Motion Capture Marker Set 26

5 – Tape Measure and Caliper Measurements 31

6 – The minimum rectangular dimensions required to conduct assisted toilet transfers as a function of wheelchair-to-toilet angle 57

7 – P-Value for statistical confidence that the parameter affected transferor lower back disorder risk factors. 58

8 – Effect of Transfer Direction and Angle on Transferor Kinematics, Mean (SD) ... 65

9 – Effect of Transfer Direction and Wheelchair-to-Toilet Angle on Transferor Kinematics, Mean (SD) 66

10 – Effect of Transfer Direction and Angle on Transferee Acceleration, Mean (SD) 67

11 – P-Value for statistical confidence that the parameter affected kinematic risk factors for lower back disorder in the transferor. 69

12 – Regression coefficients and standard errors for models to predict the values of kinematic risk factors for lower back disorder from characteristics of the transferor, after accounting for the main effects of the wheelchair-to-toilet angle (not shown) and the direction of assisted transfer. 76

LIST OF APPENDICES

Appendix Page

A – Pivot Transfer Technique 121

B – Select High Resolution Spatiotemporal Maps 124

C – Spatial Modeling Software 133

Overview 134

Geometric Bounding Solids 137

Percentile Planar Intersection Map 139

Visualization of a Volume Object's Three Dimensional Volume 143
Single Motion Capture Frame Visualization 143
Single Trial Visualization 145
Percentile Spatial Volume used Across Multiple Motion Capture Trials 148

Implementing Spatial Language Parser and Execution Engine 148
Implementing the Java Component 149
C++ Spatial Language Parser 152
Antler 3 Spatial Language Grammar 153

D – Spatial Consumption Language Programming Guide 155

Language Overview 155
End of Line and Comment Syntax 155
Variable and Types 156
Numbers 157
Strings 158
Numeric Vectors 158

Volume Objects 159
Solid Code Block Reference 161

Internal Variables 165
Dynamic Motion Capture Marker Positions 165
Internal Model State 167

Internal Functions 167
General Math Functions 167
Trig Functions 169
Vector Functions 171
String Functions 173
Data Access Functions 174

LIST OF APPENDICES (Continued)

Appendix Page

Debug Output Function 176
Model State Functions 176
Reference Object Drawing Functions 176

Language Execution Model 179

Example Source 181
Volume Objects 181
Reference Objects 182

E – 2007 Northwest Biomechanics Symposium Abstract 184

LIST OF APPENDIX FIGURES

Figure Page

16 – The transferor positioned the wheelchair for the assisted transfer..... 121

17 – The transferor raised the armrests, moved the feet to the floor, and raised the footrest..... 121

18 – Grasping the gait belt, the transferor slid the transferee forward. 122

19 – The transferor rotated the transferee towards the toilet, keeping the transferee seated on the wheelchair. 122

20 – The transferor positioned him/herself halfway between the wheelchair and toilet using either the straddle or interlaced leg position..... 123

21 – Grasping the gait belt, the transferor lifted the dummy, keeping his/her back straight. The straddle leg position is shown..... 123

22 – Starting with his/her pelvis oriented to divide the transfer angle in half, the transferor kept his/her back straight and pivoted, twisting at the arms and legs, to transfer the transferee from the wheelchair to the toilet..... 123

23 – Spatial Consumption at 1 cm for 0º Transfer..... 125

24 – Spatial Consumption at 75 cm for 0º Transfer..... 126

25 – Spatial Consumption at 1 cm for 45º Transfer..... 127

26 – Spatial Consumption at 75 cm for 45º Transfer..... 128

27 – Spatial Consumption at 1 cm for 90º Transfer..... 129

28 – Spatial Consumption at 75 cm for 90º Transfer..... 130

29 – Spatial Consumption at 1 cm for 180º Transfer..... 131

30 – Spatial Consumption at 75 cm for 180º Transfer..... 132

31 – Screen shot of user interface of the spatial modeling software..... 133

32 – High-level block diagram of the spatial modeling software 135

33 – A subset of the geometric solids supported by the spatial modeling software, visualized using the spatial modeling software (left to right): capsule, ellipsoid, box, and tapered box (back row); capsule, cone, and cylinder (middle row); custom foot object, and aligned stadium (front row) 137

LIST OF APPENDIX FIGURES (Continued)

Figure Page

34 – Volume objects are represented as a union of the core geometric bounding solids. 138

35 – Visualization of the binary area occupied by the participant, wheelchair, and dummy for a single frame at two experimental heights. 139

36 – Percentile planar intersection map taken below and above the knee for a single trial. 140

37 – Graphical representation of the assisted transfer three-dimensional model. ... 143

38 – Convex geometric solids have only two edge points (top and bottom), concave solids can have more than two..... 144

39 – Graphical representation of the total volume of a single trial of assisted transfer. 145

40 – A two dimensional representation of the oct-tree expanded to describe the nodes in grey is shown below, the numbers within each node represent the node's level of sub-division..... 146

41 – A two-dimensional representation of an adaptive oct-tree. 147

42 – Total spatial volume and 95% spatial volume for 29 assisted transferors conducting two assisted transfers between the wheelchair and toilet at the 90º wheelchair-to-toilet angle. 148

43 – Lexical analysis, conversion of the input stream into token blocks. 151

44 – The stages of parsing, raw text, lexical analysis, generation of parse trees, creation of the optimized C++ execution stream, and finally stack based execution. 153

LIST OF APPENDIX TABLES

Table Page

13 – Examples of comment syntax 156

14 – Examples of variable usage 156

15 – Examples of correct number syntax 157

16 – Operator precedence (first to last executed) 157

17 – Examples of expression and resulting value based upon operator precedence 157

18 – Examples of string syntax 158

19 – Examples of numeric vector arithmetic 159

20 – Example of input CSV data file and the resulting dynamically defined internal variables 166

21 – Pseudo code representation of volume object hierarchy execution. 180

Spatial Consumption and Risk of Lower Back Disorder during Assisted Toilet Transfers On Board an Aircraft

Introduction

A major barrier to air travel for people with disabilities is the general lack of accessible lavatories in commercial passenger aircraft (Charles 1999, Greenberger 1999, Wald 2003, Strickman 2005). Recognizing the importance of lavatory accessibility, the Aircraft Carrier Access Act (ACAA), passed by Congress in 1986, requires all twin-aisle aircraft built or refurbished after 1992 to include an accessible lavatory (U.S. Government 1986). Notably, however, definitions and requirements outlining accessibility were omitted, as were any requirements for accessible lavatories in single-aisle aircraft. This has led to inconsistent implementation of accessible lavatories in aircraft and a lack of their inclusion on the majority of domestic aircraft.

The primary reason for this is related to space. Traditionally, accessible lavatories outside the airplane environment have been designed such that no serious spatial constraints have been imposed on assisted transfers. However, in the airplane lavatory, this is not an option, as space is at a high premium. It was estimated in 1993 that one row of three coach seats had an annual value of approximately $300,000 in commercial aircraft revenue (U.S. Department of Transportation 1993). Thus, unlike in traditional accessible lavatories, the overall footprint of an accessible aircraft lavatory needs to be minimized to the extent possible. A key design variable thought to define the size of an accessible lavatory is the minimum achievable wheelchair-to-toilet angle (Warren and Valois 1991, ATAA

1992, U.S. Department of Transportation 1993). Proposed designs for accessible lavatories that do not require additional spatial volume beyond what is already provided in traditional aircraft lavatories have required assisted transfer at large wheelchair-to-toilet angles, e.g. 180º, using transfer techniques thought by some to be unsafe (ATAA 1992). Previous estimates of the spatial requirements of assisted transfers were reported as purely rectangular areas and only for 0º and 90º assisted transfers (Warren and Valois 1991). To realistically design accessible lavatories for spatially restricted environments, design data are needed for a wider range of transfer angles and that report more detailed spatial requirements. Most likely, the true spatial requirements of assisted transfers are not rectangular. Through an improved understanding of how the wheelchair-to-toilet angle affects the spatial requirements of assisted transfers, compact, spatially conscious lavatories can be designed by more closely fitting lavatory components, such as a sink, around unused portions of the actual volume required for assisted transfers.

Minimization of the spatial requirements is not the only concern in an accessible aircraft lavatory. Assisted wheelchair transfers are recognized to place the transferor at a high risk of developing lower back disorder (Garg *et al.* 1992, Marras *et al.* 1999, Owen 2000, Barondess *et al.* 2001, Santaguida *et al.* 2005, Miller *et al.* 2006). Biomechanical analyses of assisted wheelchair-to-toilet transfers have estimated that the spine of the transferor experiences 886 N – 1147 N of shear force and 4406 N – 6718 N of compressive force (Garg *et al.* 1992, Marras *et al.* 1999). Comparing these levels to the thresholds at which National Institute for Occupational Safety and Health (NIOSH 1981) reports spinal damage to be initiated (shear threshold: 750 N – 1000 N; compression threshold: 3400 N – 6400 N), it becomes obvious that assisted transfers induce forces at or above the threshold for damage,

potentially resulting in lower back disorder. With respect to the assisted wheelchair-to-toilet transfer, it is currently unknown how the wheelchair-to-toilet angle affects the transferor's risk of lower back disorder. A component of this study is to investigate this relationship with the aid of a predictive model for lower back disorder developed by Marras *et al*. (1995).

Beyond minimizing the risk of injury to the transferor, the risk of injury to the individual being transferred must also be minimized. Chronic wheelchair use has been found to result in a significant reduction in bone mineral density at the hip and spine (Goemaere *et al.* 1994, Goktepe *et al.* 2004) and reduced bone mineral density is widely acknowledged to decrease the fracture strength of bone (Cummings *et al.* 2002, Syed and Khan 2002). This suggests that an accessible lavatory design should allow the wheelchair to be oriented relative to the toilet such that the accelerations, and thus forces, at the hip and spine of the person being transferred are minimized. Currently, it is unknown how the wheelchair-to-toilet angle affects transferee acceleration during an assisted transfer.

The purpose of this study was to investigate how the wheelchair-to-toilet orientation affects the spatial requirements of an assisted toilet transfer and the risk of injury to both the transferor and the transferee during the transfer. It is the hope that this research will lead to greater lavatory accessibility in commercial passenger aircraft.

Literature Review

Prevalence of Disability

The 2000 U.S. Census estimated that roughly 19.3% of the population had a disability (U.S. Census Bureau 2000). Breaking disability down into sub-groups, the 2004 American Community Survey found that approximately 3.4% (9 million) of a sample of Americans over the age of 5 years had a physical disability and 2.3% (6 million) had a "self-care" disability (U.S. Census Bureau 2004). There has been some debate as to the actual trends in disability, but it is undeniable that people with disabilities represent a considerable portion of the population (U.S. Census Bureau 2000, Freedman *et al.* 2002, Freedman *et al.* 2004, U.S. Census Bureau 2004, Chernew *et al.* 2005, Lakdawalla *et al.* 2005). Despite the size of the population with disabilities, numerous barriers continue to exist for people with disabilities with regards to commercial passenger air travel. One of the primary barriers is the general lack of accessible lavatories on board aircraft.

Federal Accessibility Legislation

Passed in 1990, the Americans with Disabilities Act (ADA) established a new set of guidelines requiring minimum accommodations for people with disabilities at both public and commercial facilities (U.S. Government 1990). The general goal of these guidelines was to empower individuals with disabilities to function in both public and commercial venues with a greater degree of dignity and self-sufficiency. The guidelines outlined in the ADA Accessibility Guidelines are quite broad, influencing the design of everything from lavatories to automated teller machines, but they contain a number of notable exceptions. One such exception exempts aircraft from

the requirements outlined in the guidelines. By omitting aircraft from the scope of the ADA, the accessibility requirements for aircraft have been left to a previously- and loosely-defined regulation included in the Aircraft Carrier Access Act (ACAA) (U.S. Government 1986).

The ACAA, passed by Congress in 1986, recognized the importance for commercial public air travel to be accessible to people with disabilities (U.S. Government 1986). The regulations in the ACAA stipulate rules governing moveable armrests, priority seating, and onboard wheelchairs, and require all twin-aisle aircraft built or refurbished after 1992 to include an accessible lavatory. By limiting the accessible lavatory requirement to twin-aisle aircraft, the legislation has, in effect, exempted the single-aisle aircraft that comprise the majority, 70% (Bureau of Transportation Statistics, 2006), of the domestic aircraft fleet from any accessible lavatory requirement.

Furthermore, in contrast to the more recently enacted ADA, the ACAA provides no definitions of or requirements for an accessible aircraft lavatory. The ACAA makes only vague claims of accessibility and never mentions the need to accommodate an assisted transfer. The net effect has been to allow the airline industry the freedom to dictate the definition of an accessible aircraft lavatory and has resulted in a lack of industry standardization (ATAA 1992, Decker 1993). For the assisted caregiver, this lack of standardization decreases the extent to which experience with one carrier's lavatory is transferable. Lack of familiarity and associated psychosocial stress could potentially increase lower back disorder risk during a transfer (Chaffin and Park 1973, Marras *et al.* 1995, Norman *et al.* 1998, Marras *et al.* 2000b).

Design guidelines for aircraft lavatories have been suggested by two committees that investigated the design of accessible lavatories in both twin- and single-aisle aircraft (ATAA 1992, U.S. Department of Transportation 1993). In 1992, as part of an effort to clarify the requirements for an accessible lavatory, a committee led by the airline industry and disability interest groups published suggested guidelines for the design of accessible lavatories for twin-aisle aircraft (ATAA 1992). A number of lavatory designs were proposed in the twin-aisle committee's final report; however these designs appear to have been the result of committee consensus and not ergonomic evaluation. The importance of using research to guide design was demonstrated by a study that found that the benefit of ergonomic interventions could be predicted using ergonomic models (Marras *et al.* 2000a). The study further found that ergonomic interventions implemented based on intuition often resulted in no measurable change in actual or predicted lower back disorder risk.

In 1992, a federal advisory committee was also formed to investigate the feasibility of accessible lavatories on single-aisle aircraft (U.S. Department of Transportation 1993). The committee hypothesized that the risk of injury to the transferor increased as the angle between the wheelchair and toilet increased; a hypothesis that will be investigated in this study. It was further concluded, based on research by Warren *et al.* (1991), that an accessible lavatory could be provided in single aisle-aircraft without a reduction in aircraft seating capacity but that the lavatory would require assisted transfers at large wheelchair-to-toilet angles, e.g. 180^{o}, using transfer techniques considered by some to be unsafe (ATAA 1992). The largest lavatory designs, allowing for the smallest angle between the wheelchair and toilet, required the removal of three coach seats or two first-class seats (U.S. Department of Transportation 1993). In 1993 dollars, it was estimated that these seats had an

annual value of $300,000 (U.S. Department of Transportation 1993). Designs resulting in no impact on seating capacity were proposed but, in each of these, an 180º transfer was required for an assisted toilet transfer. Given that the angle between the wheelchair and toilet had been hypothesized to be directly related to the risk of injury during a transfer, some committee members speculated as to the true level of accessibility afforded by lavatories requiring 180º transfers. To date, there are no data that definitively define the spatial requirements of assisted toilet transfers or how the orientation angle of the wheelchair relative to the toilet affects the risk of injury during these transfers. By more precisely understanding these variables, accessible lavatories can be designed using the principles of ergonomics.

Spatial Consumption

To the author's knowledge, there has been only one study that attempted to quantify the total space required during an assisted toilet transfer (Warren and Valois 1991). That study was commissioned by disability interest groups as input to the committee addressing lavatory accessibility guidelines for twin-aisle aircraft, and was attached to the committee's report (ATAA 1992). The study found that the minimum space required for an accessible lavatory varied with the degree of assistance required by the user and with the angle between the wheelchair and toilet. A 90º fully assisted transfer was found to require more space than a similar 0º transfer (Table 1).

Table 1 – Minimum spatial requirements for an assisted toilet transfer, as determined by Warren *et al.* (1991)

Transfer Type	Minimum spatial requirement
0º fully assisted transfer	1.22 m^2 (1.07 m x 1.14 m)
90º fully assisted transfer	1.42 m^2 (1.17 m x 1.22 m)

The results of Warren *et al.* (1991) would suggest that the space required for an assisted toilet transfer is rectangular. However, while a rectangular shape can obviously be fit around any boundary, the precise shape utilized during an assisted toilet transfer is most likely not rectangular. It is one goal of this study to calculate the precise spatial volume required for an assisted transfer.

Also of note is that no apparent attempt was made by Warren *et al.* (1991) to test 45º or 180º transfers. While 180º assisted transfers might very well prove to be less than optimal from a transferor injury perspective, accessible lavatories requiring such transfers have been proposed to require no more space than traditional aircraft lavatories (ATAA 1992). It is the goal of the current study to collect data for both the spatial requirements and injury risk of 45º and 180º transfers, as well as for transfers at 0º and 90º orientations.

Risk of Lower Back Disorder

It has been estimated that over 80% of adults in the United States will, at some time, experience lower back disorder (Marras 2000). The National Health Interview Survey estimated that 2/3 of all incidence of lower back disorder is a result of repeated action undertaken while at work (Barondess *et al.* 2001). Data from worker compensation claims indicate that lower back disorder represents 16% – 19% of the total number of worker's compensation claims but 33% – 41% of the total costs (Marras 2000). When broken down by occupation and gender, the occupational categories with the highest rates of lower back disorder are construction and nursing for men and women, respectively (Barondess *et al.* 2001). Among nursing personnel, nursing assistants at long-term care facilities are at the highest risk of lower back disorder (Garg *et al.* 1992, Marras *et al.* 1999, Barondess *et al.* 2001).

Assisted transfers have been identified as a primary cause of the high rates of lower back disorder in nursing personnel. In an ergonomic evaluation, nursing assistants in a nursing home were found to perform an average of 12 assisted transfers per 4-hour shift and, besides rating these as their most stressful tasks, 51% had visited a healthcare provider for lower back disorder (Garg *et al.* 1992). While a nursing home and an aircraft lavatory are obviously different environments, the risk of injury to the transferor is likely very similar, as the kinetics and kinematics of assisted transfers are likely very similar in both domains.

Kinetic and Kinematic Risk Factors for Lower Back Disorder

Medically diagnosing the precise anatomical origins of lower back disorder has proven quite elusive; estimates for the percentage of cases with an anatomical diagnosis have ranged from 30% – 50% (Punnett *et al.* 1991, Marras 2000). In the majority of cases, lower back disorder appears to be an internal structural fatigue failure due to repeated exposure and not the result of a single catastrophic incident (Marras *et al.* 1995, Norman *et al.* 1998, Marras 2000, Marras *et al.* 2000a, Barondess *et al.* 2001). While more difficult to quantify, a study by Norman *et al.* (1998) clearly made the link between cumulative exposure and lower back disorder by demonstrating a high odds ratio between integrated lumbar moment and lower back disorder. In light of the longitudinal nature of the disorder, ergonomic job evaluations, case studies, and the like have identified a number of kinematic and kinetic risk factors correlated with lower back disorder. These risk factors include: lifting frequency (Chaffin and Park 1973, Binckmann *et al.* 1987, Marras *et al.* 1995, Marras *et al.* 2000a), load moment (Chaffin and Park 1973, Garg *et al.* 1992, Marras *et al.* 1995, Davis *et al.* 1998), minimum required body strength (Chaffin and Park 1973),

and trunk kinematics variables that include the peak positions and average velocities in flexion, lateral bending, and twisting (Punnett *et al.* 1991, Marras *et al.* 1995). Excluding lifting frequency, transferors experiencing increased magnitudes of each of these kinematics variables have greater risk of developing lower back disorder. The relationship between lifting frequency and lower back disorder is "J" shaped (Chaffin and Park 1973). Both infrequent lifters (0 – 50 times a day) and frequent lifters (> 100 times per day) report a higher occurrence of lower back disorder than those lifting with moderately frequency (50 - 100 times a day). Based upon this, it has been suggested that moderate lifting reduces lower back disorder risk by inducing neuromuscular adaptations (Chaffin and Park 1973).

While a diagnosis of the anatomical origins of lower back disorder is often indeterminate (Punnett *et al.* 1991, Marras 2000), a general biomechanical explanation has been put forth for the origins of lower back disorder. The hypothesis is that spinal damage at the vertebral end plate reduces the flow of micronutrients to the inter-vertebral disks. This reduction in nutrients then leads to atrophy and degeneration of the disks (Lotz *et al.* 1998). Disk degeneration and atrophy is thought to be one pathway through which lower back disorder, taking the form of disc protrusions, disk herniation, and instability of the spinal system, is thought to occur (Marras 2000).

Cadaver studies and animal tissue studies have had some success in identifying the physical thresholds at which damage can be expected to begin being manifested (Barondess *et al.* 2001). The National Institute for Occupational Safety and Health (NIOSH 1981) concluded, based on published data, that between 3400 N and 6400 N of spinal compression is the threshold at which damage at the vertebral endplate begins to occur. At 6400 N, damage is thought to have begun in roughly

50% of individuals under 40 years of age. NIOSH further concluded that the threshold for spinal damage from shear forces is between 750 N and 1000 N. Repeated exposure has been found to dramatically reduce the resistance of the vertebral end plates to compression, with spinal tolerance reduced by 30% after 10 loading cycles and by 50% after 5000 loading cycles (Binckmann *et al.* 1987).

Important contributors to the loading of the spine include the load moments created by external forces and the weight of the upper body, as well as movement speed and non-sagittal trunk positions. Greater trunk velocities have been shown to result in greater spinal compression during lifting (Granata and Marras 1999, Davis and Marras 2000). Non-neutral, non-sagittal trunk positions have also been shown to elevate the risk of lower back disorder over that associated with pure flexion by significantly increasing trunk muscle co-contraction (Punnett *et al.* 1991, Marras and Granata 1995, Marras *et al.* 1995, McGill *et al.* 1996, Granata and Marras 1999). Comparisons of static and dynamic postures have shown that dynamic twisting results in spinal compression roughly double that of the similar posture held statically (Marras and Granata 1995). Punnett *et al.* (1991) found the odds ratio associated with the reporting of lower back disorder to be nearly equal for twisting/lateral bending as for severe flexion, with the odds ratios being 5.7 and 5.9, respectively. A simplified model to predict spinal compression as a function of the resultant flexion, lateral bending, and twisting moments was derived by McGill *et al.* (1996), using electromyography (EMG) and a 90-muscle model. The results indicated that non-sagittal forces contribute significantly to the compression experienced in the lower back; a pure moment of 160 Nm in extension would generate the same compressive force as the combination of 100 Nm in extension and 50 Nm in both lateral bending and twisting. As part of a large evaluation into the risk factors for developing lower

back disorder, Marras *et al.* (1995) found non-sagittal twisting and lateral velocities to be two of five components in a model that best discriminated between individuals with high versus low odds of developing lower back disorder.

Assessing Lower Back Disorder Risk

To quantify how the risk of developing lower back disorder in the transferor is affected by the spatial arrangement of the wheelchair and toilet, a risk model is needed linking measurable variables during lifting with the associated likelihood of developing lower back disorder. Ergonomic studies have sought to predict the odds of developing lower back disorder through injury risk models. Early work in this area, associated a significantly increased risk of lower back disorder with greater time spent in non-neutral trunk positions, such as those arrived at through sagittal flexion, lateral bending, and twisting (Punnett *et al.* 1991). Later work to generate more detailed risk models with better predictive power has found that no single kinematics variable strongly predicts lower back disorder but, when kinematic risk factors are combined into multivariate models, stronger predictive models could be created (Marras *et al.* 1995, Norman *et al.* 1998).

A lower back disorder risk model constructed by Norman *et al.* (1998) was based on the ergonomic evaluation of hourly employees at a large automotive manufacturing plant. In total, more than 230 workers and more than 1000 tasks were examined. Four factors were found to account for 89% of the variance in the incidence of lower back disorder in a multivariate logistic regression model. The model strongly implicated both peak and cumulative spinal loading as being separate predictive risk factors for lower back disorder. The four factors making up the model are: peak shear force, integrated lumbar moment over the duration of the lift, peak

torso angular flexion velocity, and mean hand force over the course of the lift. According to the model, the odds ratio for lower back disorder between the low- and high-risk jobs was slightly greater then 6.0.

Another risk model for lower back disorder, constructed by Marras *et al.* (1995), consists of a pair of multivariate logistic regression equations that quantify the odds of being at high and at medium versus low risk of lower back disorder in industrial lifting jobs. The model was derived from the measurement of workplace factors and trunk kinematics in over 400 industrial lifting jobs across 48 industries. The wide breadth of industrial jobs sampled provides the model with considerably greater ability to generalize than would be expected for a single-industry evaluation. Variables included in the model were chosen from among those measured to maximize the odds ratio between jobs associated with high and low risk of lower back disorder. The model includes five variables: lift rate, average twisting velocity, maximum moment, maximum sagittal flexion, and maximum lateral bending velocity, with greater values of each variable associated with greater odds of being at high risk of lower back disorder. According to this model, the odds ratio for lower back disorder between the low- and medium-risk jobs was 6.3, whereas the odds ratio for lower back disorder between the low- and high-risk jobs was 10.6.

Validity of the Model for Lower Back Disorder Developed by Marras *et al.* (1995)

The initial accuracy of the lower back disorder model proposed by Marras *et al.* (1995) was assessed by testing 100 industrial jobs of known lower back disorder risk. The model correctly identified low-, medium-, and high-risk jobs 87%, 49%, and

78% of the time, respectively. These results suggested that the model has validity for the determination of low versus high risk of lower back disorder.

While the models by Norman *et al.* (1998) and Marras *et al.* (1995) were derived independently using different methods, both models share logical similarity in the identified kinematics and kinetic variables used in their logistic models. This logical agreement provides a very basic form of replication. Both models directly implicate maximum sagittal flexion as a key variable in lower back disorder risk. The linkage of mean hand force and integrated lumbar moment to lower back disorder by the model of Norman *et al.* is also similar to the linkage of maximum moment and lift rate to the risk for lower back disorder in the model of Marras *et al.* The real difference, conceptually, between the models is in the representation of non-sagittal plane movement. The model by Marras *et al.* directly implicates non-sagittal plane movement with the inclusion of average twisting velocity and maximum lateral bending velocity, whereas the model by Norman *et al.* largely ignores non-sagittal movement.

Logistic regression models assume that a sigmoid relationship exists between their respective independent variables and the dependent variable. While such a relationship is consistent with the epidemiological data for four of the five variables included in the model of Marras *et al.*, the "J" shaped relationship observed between lifting frequency and lower back disorder (Chaffin and Park 1973) would violate this assumption. To test the possibility that a model construct other than logistic regression would more accurately predict the risk of lower back disorder, the data Marras *et al.* used to generate their model was used as a training set for a computer neural network (Zurada *et al.* 1997). A strength of the neural network approach is its ability to construct non-linear relationships between the independent variables and

the risk of lower back disorder. The results of a split-half validation of the neural network model indicated that its predictive value was slightly less than that of the logistic regression model, thus providing further support for the logistic model.

The predictive validity of the model proposed by Marras *et al.* (1995) was assessed as part of a longitudinal ergonomic intervention study into the lower back disorder reporting rates in sixteen industries before and after ergonomic interventions (Marras *et al.* 2000a). The study first assessed the reported rates of lower back disorder and used the model to predict the odds of being at high risk of lower back disorder for 142 employees spread across the industries. Then, following ergonomic interventions designed by individuals employed at the different companies, the post-intervention lower back disorder rates and the model-predicted odds of being at high risk of lower back disorder were re-assessed. A regression analysis found the relationship between changes in model-predicted risk of lower back disorder and actual lower back disorder reporting had an r^2 of 0.23, thus indicating that the model could account for 23% of the variance in the changes in lower back disorder incidence. Because non-modifiable characteristics, such as strength and vertebral surface area, are logically connected to the risk of lower back disorder, the model of lower back disorder risk derived by Marras *et al.* likely describes more than 23% of the modifiable variance in lower back disorder risk during lifting. As such, the model proposed by Marras *et al.* will be used in the present study to evaluate the effect of observed differences on the risk of lower back disorder during an assisted toilet transfer.

Perceived Exertion

A psychosocial component to lower back disorder risk has been suggested by research in which job-induced psychological stress was found to be correlated with the incidence of lower back disorder (Herrin *et al.* 1986). Psychosocial stress has also been found to increase muscular co-activation, and thus spinal loading, during lifting in individuals with some personality types (Marras *et al.* 2000b). One means of quantifying the psychophysical stress associated with a lifting task is the maximum acceptable weight of lift (MAWL), which represents the maximum load a person feels comfortable lifting under a given set of conditions (Davis *et al.* 2000). Others have employed the Borg scale (Borg 1982, Borg 1998) to quantify perceived exertion during lifting tasks in which the weight was fixed (Garg and Owen 1992, Garg *et al.* 1992). MAWL has been found to closely relate to the magnitude of muscular strain, more so than to the magnitude of spinal loading (Davis *et al.* 2000). These results suggest that perceived exertion would incorrectly assess the relative risk of lower back disorder during lifts in which muscular strain is independent of spinal loading. Nevertheless, the logical connection between external loads, muscular contraction, and spinal loading would suggest that perceived exertion reflects a component of the risk of lower back disorder during lifting. In keeping with this, MAWL was one of the sources of data used in the development of the NIOSH lifting guidelines (NIOSH 1981). Perceived exertion as measured by the Borg scale has also been found to be moderately correlated (0.72) with spinal compression (Garg *et al.* 1992). Arguably, the reporting of perceived exertion during lifting offers an insight complementary to the traditional biomechanical analyses for evaluating the risk of lower back disorder. To the extent possible, accessible lavatories should be designed such that the

transferor's perceived exertion is minimized, thereby minimizing that component of lower back disorder risk described by perceived exertion.

Biomechanics of Assisted Toilet Transfers

Absent external forces and moments, spinal compression has been estimated at approximately 534 N during quiet standing (McGill *et al.* 1996). However, during assisted transfers, spinal compression in the transferor increases dramatically as spinal muscles operating at small moment arms, 5 cm – 7.5 cm, attempt to counteract large external moments (McGill *et al.* 1996, Norman *et al.* 1998). Non-sagittal plane movements, such twisting or bending, during assisted transfers and the dynamic nature of the task would be expected to result in increased co-contraction, further increasing spinal compression. However, the biomechanics of one-person assisted transfers between a wheelchair and a toilet has received little study to date.

Garg *et al.* (1992) estimated total spinal compression induced during assisted toilet-to-wheelchair transfers of 25^{th} – 90^{th} percentile individuals as being 4,406 N – 5,575 N. Assisted toilet transfers of a 50^{th} percentile individual were associated with 4810 N of spinal compression and 886 N of shear in the transferor. However, the extent to which toilet transfers were typically conducted with one or two transferors is unclear and it is further unclear what the mean wheelchair-to-toilet angle was during the transfers. Using an EMG-driven model, Marras *et al.* (1999) estimated both shear and compression forces during one-person assisted transfers of a 50 kg individual, using a hug technique, between a hospital chair and a toilet. Spinal forces in the transferor were estimated as 1005 N – 1147 N in lateral shear, 776 N – 1137 N in anteroposterior shear, and 6062 N – 6718 N in compression, depending on the direction of transfer and the degree to which the transfer required lifting or lowering.

The angle of transfer used in that study was not reported. Comparing the spinal forces experienced by the transferor in these studies with the thresholds at which NIOSH (1981) reports spinal damage being initiated (shear threshold: 750 N – 1000 N; compression threshold: 3400 N – 6400 N), it becomes obvious that assisted transfers induce forces at or above the threshold for damage; potentially leading to lower back disorder.

Beyond kinematic and kinetic measurements of spinal loading, evidence exists for a relationship between perceived exertion and lower back disorder related to assisted transfers. In a study of assisted transfers conducted by nursing home attendants in a nursing home, assisted wheelchair-to-toilet transfers had some of the highest perceived exertion scores and perceived exertion was found to be moderately correlated (0.72) with lower back compression (Garg and Owen 1992, Garg *et al.* 1992).

With regard to the safety of the transferor, assisted transfers clearly represent a task that places the individual at a high risk of lower back disorder. Despite this, there has been limited study of the factors that influence the risk of injury to the transferor during a one-person assisted toilet transfer. In particular, there has been no systematic study of the effects of the wheelchair-to-toilet angle on the risk of lower back disorder to the transferor. Nor has any study to date addressed the risk of injury to the transferee during an assisted transfer.

Purpose and Hypotheses

Purpose

If new regulations are to expand the inclusion of accessible lavatories on aircraft, designs must be created which are both ergonomic and spatially consistent with the realities of the aircraft environment. However, as stated, there is currently a lack of understanding as to how the wheelchair-to-toilet angle affects the spatial requirements of assisted transfers and the risk of injury during these transfers. The purpose of this study is to determine how the spatial relationship of the wheelchair to the toilet affects the total spatial requirements, the transferor's risk factors for low back disorder, and the risk of injury to the transferee during assisted toilet transfers. A secondary goal of this research is to identify characteristics of the transferor that, after accounting for the effects of the wheelchair-to-toilet angle and direction of assisted transfer, are associated with the transferor's risk of lower back disorder. Specifically, this research will address the following questions:

- What are the spatial requirements for a toilet transfer, as a function of the wheelchair-to-toilet angle?
- How does the angle of the wheelchair relative to the toilet and the direction of the assisted transfer affect:
  - The transferor's kinematic risk factors for lower back disorder: duration of transfer, maximum load moment arm, integrated load moment arm, maximum angles of lumbar flexion, extension, twisting, and bending, maximum velocities of lumbar flexion and extension, maximum and average lumbar twisting velocities, and maximum and average lumbar bending velocities?
  - The perceived exertion of the transferor?

  - The vertical acceleration of the transferee, as an indicator of both the risk of injury to the transferee and the roughness of the transfer?

- After accounting for the main effects of both the wheelchair-to-toilet angle and direction of assisted transfer, is there an association between the transferor's standing height, the transferor's use of the interlaced or straddle leg position, the transferor's self-reported previous experience in conducting assisted transfers and the transferor's resulting kinematic risk factors for lower back disorder, the transferor's perceived exertion, or the vertical acceleration of the transferee.

Through a better understanding of how the spatial relationship between a wheelchair and toilet affects these variables, new accessibility regulations can be created and accessible lavatories can be designed to minimize the lavatory spatial requirements while also minimizing the risks of injury to the transferor and transferee during assisted toilet transfers. Through an improved understanding of the association between assisted transfer technique and the injury risk during assisted transfers, transfer technique recommendations can be made to improve the safety of assisted transfers across all wheelchair-to-toilet angles. Finally, an improved understanding of how the transferor's standing height is related to the risk of injury during assisted transfers could result in selection criteria through which transferors having reduced risk of developing lower back disorder could be preferentially selected. Overall, it is the long-term goal of this research to improve lavatory accessibility in commercial passenger aircraft and in other environments with spatial restrictions.

Research Hypotheses

Spatial Consumption

Qualitatively, it was hypothesized that the 95th percentile spatial consumption volume would be non-rectangular and would change in area over the height of the transfer volume. It was also hypothesized that the 95th percentile spatial consumption required for assisted transfers would qualitatively decrease as the wheelchair-to-toilet angle increased.

Risk of Injury to the Transferor

It was hypothesized that statistically significant differences would be observed in the measures listed below between toilet transfers conducted at wheelchair-to-toilet angles of 0º, 45º, 90º, and 180º.

1. The transferor's kinematic risk factors for lower back disorder: maximum load moment arm; integrated load moment arm; maximum angles of lumbar flexion, extension, bending, and twisting; maximum lumbar flexion and extension velocities; and the maximum and average lumbar bending and twisting velocities.
2. The transferor's perceived exertion during the transfer.

However, because the experimental lifting condition would be unconstrained and there would be minimal difference, 4 cm, in toilet and wheelchair floor-to-seat height, it was hypothesized that there would be no detectable difference in any of the previously listed measures with respect to the direction of assisted toilet transfer.

It was further hypothesized that, after accounting for the main effects of both the wheelchair-to-toilet angle and the direction of assisted transfer, the transfer technique used by the transferor (straddled vs. interlaced leg position), the

transferor's standing height, and the transferor's self-reported previous experience in conducting transfers would all have statistically significant associations with and describe separate components of the variance in the transferor's kinematic risk factors for lower back disorder and perceived exertion.

Risk of Injury to the Transferee

It was hypothesized that statistically significant differences in the maximum vertical acceleration of the transferee would be observed between toilet transfers conducted at wheelchair-to-toilet angles of 0º, 45º, 90º, and 180º. It was also hypothesized that, because the experimental lifting condition would be unconstrained and there would be minimal difference in toilet and wheelchair floor-to-seat height, there would be no detectable difference in the vertical acceleration of the transferee with respect to the direction of assisted transfer. Finally, it was hypothesized that, after accounting for the main effects of both the wheelchair-to-toilet angle and the direction of assisted transfer, the transferor's technique, standing height, and self-reported previous experience would all have statistically significant associations with the maximum vertical acceleration of the transferee.

Materials and Methods

Human Participants

Twenty-nine healthy adults (18 – 38 years of age) were recruited to participate in this study (Table 2). Participants were recruited using word of mouth and fliers posted around the campus of Oregon State University. Participants were required to have no previous history of back injury or chronic lower back pain. They were required to be experienced and accustomed to lifting weights of 11.3 kg (25 lbs) or more at least twice per week over the preceding month through participation in a regular strength training program or the equivalent. Individuals under the influence of drugs or medications that impair physical or mental function and individuals with self-reported musculoskeletal, neurological, or cardiopulmonary pathology were excluded from participating. No attempt was made to control the relative numbers of men and women who enrolled in this study. Qualifying participants were tested in order of their making an appointment, regardless of sex. Participants received $40 as compensation for their participation in the study. Institutional Review Board (IRB) approval for the study was obtained. Prior to involvement in the study, all participants provided their written informed consent and completed a health history questionnaire. As part of the questionnaire, participants were asked to report (yes/no) any prior experience in conducting assisted transfers in the previous calendar year.

Table 2 – Participant Descriptive Statistics, mean (SD)

Female	(n)	6
Male	(n)	23
Age	(years)	24.7 (5.4)
Height	(cm)	181 (9)
Weight	(kg)	79.4 (12.7)
Prior Transfer Experience	(yes / no)	8 / 21

Instruments and Apparatus

Experimental Setup

This study investigated assisted toilet transfers of travelers with disabilities in an aircraft lavatory through experiments conducted in a laboratory environment. The outer dimensions of two experimental lavatories (1 m x 1.2 m and 1.2 m x 1 m) were marked on the laboratory floor using masking tape. The lavatory toilet was simulated by a wooden toilet frame and an aircraft toilet seat (Boeing, Seattle, WA). The toilet was mounted to the floor in a "corner" of the lavatory (Figure 1).

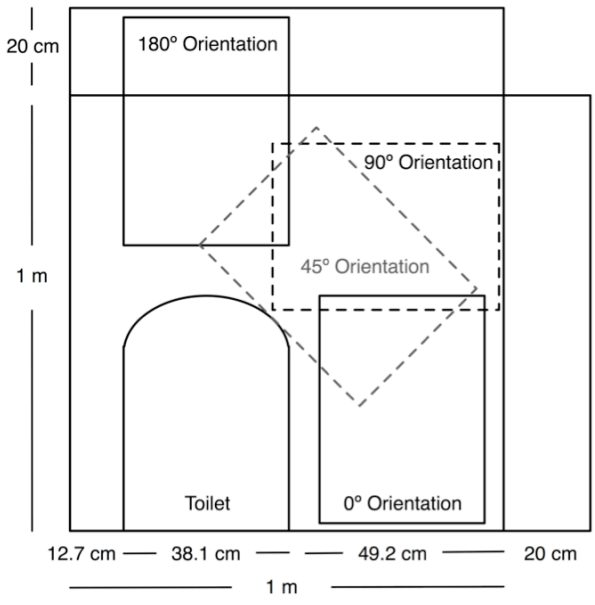

Figure 1 – Experimental lavatory design

A 66 kg anthropometric dummy (Simulaids, Saugerties, NY) with the approximate body dimensions of a 95th percentile male was used to simulate the transferee. Due to limitations in dummy articulation, the dummy's forearms were removed and the associated weight was replaced through a weight belt about the dummy's waist. In addition to the basic apparel worn by the dummy, a gait belt was secured around the dummy's waist for use during the assisted transfers. For the safety of the participants, the dummy was loosely tethered to the ceiling via a chest harness and dynamic climbing rope. The rope tethering the dummy had sufficient slack to allow for unencumbered transfers while restricting the distance the dummy could travel in the event of a fall. A standard aircraft onboard wheelchair (Innovint Aircraft Interior, Hamburg, Germany) was used as the experimental wheelchair. A uniaxial accelerometer (PCB Piezotronics, Depew, NY) was attached to the middle of the dummy's chest to measure the vertical accelerations experienced by the dummy. Vertical acceleration was recorded at 600 Hz and used to quantify the risk of injury to the traveler with disabilities during the assisted transfers, as well as the roughness of the assisted transfers.

A nine-camera red-light motion capture system (Vicon, Lake Forest, CA) was used to record, at 60 Hz, the positions of the participant, dummy, and wheelchair in three dimensions over time. Spherical reflective markers, 9.5 mm in diameter, were attached to the skin and clothing of the participant at specified locations (Table 3) with double-sided tape. Elastic bands were used to secure markers around both the chest and head. Similar markers were attached to the dummy (Table 4) and three markers were attached to the cross members of the wheelchair.

Table 3 – Participant Motion Capture Marker Set

Segment	Marker Location	Marker Count
Head	Left & Right Anterior, Left & Right Posterior	4
Trunk	C7, T5, T10, Left & Right Back, Asymmetric Middle Back	6
Pelvis	Left & Right Anterior & Posterior Superior Iliac Spines, Left & Right Pelvis	6
Left & Right Arm	Shoulder, Upper Arm, Elbow, Wrist	8
Left & Right Thigh	Greater Trochanter, Thigh, Lateral Femoral Epicondyle	6
Left & Right Leg	Tibia, Lateral Malleolus	4
Left & Right Foot	Heel, 2nd and 5th Metatarsal Head	6
	Total	**40**

Table 4 – Dummy Motion Capture Marker Set

Segment	Marker Location	Marker Count
Head	Top	1
Neck	Left & Right	2
Shoulder	Left & Right	2
Left & Right Leg	Knee, Tibial Tubercle, Tibia	6
Left & Right Foot	Lateral Malleolus, Heel, Toe	6
	Total	**17**

Experimental Protocol

The experiment investigated how the wheelchair-to-toilet angle (0º, 45º, 90º, and 180º) and the direction of transfer (wheelchair-to-toilet, toilet-to-wheelchair) affects the space required for an assisted toilet transfer, the estimated risk of lower back disorder to the transferor, and the vertical acceleration of the transferee, an indicator of the risk of injury to the individual being transferred and the roughness of the transfer. A secondary goal of this research was to determine the effect of the transferor's leg position, transferor's standing height, and transferor's self-reported

prior experience in conducting assisted transfers on the transferor's risk factors for lower back disorder, transferor's perceived exertion, and the vertical acceleration experienced by the transferee, after controlling for the effect of the wheelchair-to-toilet angle and the direction of assisted transfer.

Pre-Trial

On arrival, participants provided informed consent in writing, signing a copy of the study's IRB-approved informed consent document. In addition to providing written informed consent, participants completed a health history questionnaire to verify that they qualified for inclusion in the study. Participants were instructed in proper lifting technique and in the one-person assisted transfer technique (Takeda 1977, McConnell 1995, McConnell 2002, Hess *et al.* 2007) through an instructional video (Appendix A). The assisted transfer technique shown on the video instructed participants to:

1. Stand in front of the dummy.
2. Reposition the dummy forward on the wheelchair/toilet seat, if desired, by leaning the dummy forward and then grasping and lifting it by the gait belt.
3. Rotate the dummy on the wheelchair/toilet seat to place its legs midway between their initial and final seated positions.
4. Stabilize the legs of the dummy using either an interlaced leg position, positioning one of the dummy's knees between the knees of the participant, or a straddle leg position, positioning both of the dummy's knees between the knees of the participant.
5. Lean the dummy forward while grasping the gait belt.
6. Lift and shift the dummy using a squat technique.

7. Lower the dummy onto the toilet/wheelchair seat.
8. Reposition the dummy, if necessary.

Prior to participation, participants were led through the following warm-up exercises to prepare them for lifting:

1. 5 minutes of brisk walking
2. One set of 15 body-weight squats. Keeping the back straight, participants flexed and extended their knees and hips to lower and raise their body.
3. One set of 15 stiff-legged body-weight dead lifts. Keeping the back straight, participants flexed and extended at the hips to lower and raise the trunk.
4. One set of 10 squats with an 11.3 kg weight held at forearm length in front of the torso. Between squats, participants stepped from side to side.
5. One set of 10 stiff-legged dead lifts with a weight of 11.3 kg held at forearm length in front of the torso.

After this set of warm-up exercises, participants were asked to rate their perceived exertion on a 6 – 20 visual analog Borg Scale of Perceived Exertion (Borg 1982, Borg 1998) and were asked whether they experienced any pain. Participants reporting Borg ratings of 16 (very hard) or greater or who felt any pain would have been excluded from participation in the study. No one was excluded for this reason.

Following the warm-up exercises, the participants performed two practice transfer trials. During the two practice trials, participants were coached in proper lifting and transfer technique and deviations from proper technique were verbally corrected. After each transfer, participants were asked whether they experienced any pain. A “yes” answer would have resulted in exclusion from further participation in the study. None of the participants reported experiencing pain.

Following the two practice transfers, the participant performed a standing static trial. The participant stood still in a known orientation for 2 – 3 seconds while reference static motion capture data was collected. The results from the static trial were then visually inspected to verify that all of the markers were correctly detected by the motion capture system and that the participant was free of reflective noise, such as from reflective surfaces on shoes. If noise from reflective clothing was detected, masking tape was used to cover the material, after which the static trial was repeated until successfully completed.

Assisted Transfer Data Collection

Data collection consisted of eight assisted transfers, one from the wheelchair to the toilet and one from the toilet to the wheelchair for each wheelchair-to-toilet angle of interest. Both the order in which the wheelchair-to-toilet orientations (0°, 45°, 90°, 180°) were attempted and the initial position of the dummy (toilet or wheelchair) were randomized.

The experiment proceeded as follows. With the dummy in its initial randomly selected position on the wheelchair or toilet, the participant was asked to position the wheelchair for an assisted transfer at the first randomly selected wheelchair-to-toilet angle of interest. Participants were required to position the wheelchair at the specified angle of transfer and within either of the lavatory boundaries outlined on the floor. However, participants were encouraged to translate the wheelchair front-to-back and side-to-side to place it at a self-selected optimal position. The one exception to this was the 180° transfer. For the 180° transfer, the wheelchair was positioned directly opposite the toilet, partially outside both lavatory boundaries. Prior to the 180° transfer, participants were only allowed to adjust the front-to-back position

of the wheelchair. Participants were then asked to plan their transfer to attempt to stay within the taped lavatory boundary and to use as little space as safely possible. After describing their plan, participants received feedback from the experimenters regarding ways of potentially performing the transfer in a safer manner and participants were allowed to modify their plan if they so desired. The positions of the motion capture markers and dummy acceleration data were then recorded as the participant transferred the dummy. At the conclusion of the transfer, the participants were asked whether they had experienced any pain and to report their perceived exertion using the 6 – 20 point visual analog Borg scale of perceived exertion (Borg 1982, Borg 1998). None of the participants reported experiencing pain. If any had, their data collection session would have been ended.

After a minimum of two minutes passed, the participant was asked to transfer the dummy back to its initial position, again using as little space as safely possible. The same basic procedures were followed as for the initial transfer. Marker position, dummy acceleration, and perceived exertion data were collected for the return transfer. After a minimum of two minutes passed, the data collection procedure was repeated at the next randomly selected wheelchair-to-toilet angle.

Prior to experimentation, it was hypothesized that the risk of injury during assisted transfers at the 180° wheelchair-to-toilet angle would be greater than at the other orientations. Due to this hypothesis, after having them position the wheelchair for a 180° transfer, participants were asked if they would like to attempt the transfer. The participants were verbally instructed that not attempting the 180° transfer would not affect the compensation that they would receive for their participation in the study nor would it affect the number of transfers that they would be asked to attempt. All

but one participant chose to attempt the 180° transfer. Omission of the 180° transfer resulted in the replication of the first pair of transfers at the conclusion of the 0°, 45°, and 90° transfers. Following their first assisted transfer at the 180° orientation, participants were asked whether they would like to attempt to transfer the dummy back to its initial position. All but one transferor completing the first 180° transfer chose to transfer the dummy back. As with the other transfers, if at any time the participant had reported experiencing pain, the data collection session would have been ended. None of the transferors reported experiencing pain.

Post-Trial Data Collection

At the conclusion of the eight transfers, a set of static body measurements was taken from the participant. Participant standing height, with shoes, was measured using a wall-mounted stadiometer. Mass was recorded using a digital scale. All other body measurements (Table 5) were taken with a tape measure and calipers.

Table 5 – Tape Measure and Caliper Measurements

Segment	Tape Measure and Caliper Measurements	N
Foot	Forefoot width, Heel diameter, Foot length	3
Leg	Knee width, Knee circumference, Ankle width	3
Thigh	Thigh circumference	1
Pelvis	Pelvis circumference, Buttocks depth	2
Chest	Shoulder-level depth, Upper chest width, Upper chest circumference, Waist depth, Waist circumference, PSIS to L3/L4 height	6
Head	Head width, Head depth	2
Upper Arm	Shoulder width, Proximal arm circumference, Elbow circumference	3
Forearm	Wrist circumference, Forearm length	2
	Total	**22**

Data Analysis

Post-capture power spectrum and residual analyses were conducted on the marker position data and the accelerometer data to determine appropriate data/noise cutoff frequencies. The motion capture marker position data were low-pass filtered at 6 Hz using a fourth-order no-lag Butterworth filter. The acceleration data were low-pass filtered at 15 Hz using a fourth-order no-lag Butterworth filter.

The three-dimensional marker position data were visually inspected for each participant to determine the period of the trial that was experimentally of interest. The frame range of interest for the spatial consumption analysis was determined by identifying the range of frames over which a marker on the top of the dummy's head moved. The period of interest for the analysis of lower back disorder risk was defined as the period of time over which the pelvis of the dummy was undergoing vertical motion and was not supported by the wheelchair or toilet. The range of frames for the analysis of the risk of lower back disorder thus included just those frames in which the participant was supporting the dummy whereas the range used for the spatial consumption analysis included the entire period of motion during the transfer. The frames falling outside the respective ranges of interest were excluded from the respective analyses.

The body of the transferor was modeled as a collection of rigid segments (n = 13). The segments were: head, trunk, pelvis, two upper arms, two lower arms, two thighs, two legs, and two feet. Three-dimensional locations of the joint centers between the modeled body segments were calculated for each participant for each frame of motion capture data (Vicon BodyBuilder), with the "lumbar joint" between the pelvis and trunk assumed to be located at L_3L_4. Joint center positions were calculated

by first estimating their positions in the static trial, when the participant was standing in a known position, using static body dimension measurements, the motion capture marker positions, and joint center regression models. The position of each joint center was then determined within a local coordinate system of the adjacent body segment, as constructed from the recorded marker positions. These relative positions were used to compute the global positions of the joint centers from the instantaneous positions and orientations of the local coordinate systems during the dynamic trials. Finally, from the joint center positions and, when needed, the position of a third marker attached to the body segment, the orientations of the anatomical axes of each body segment were determined.

For each assisted toilet transfer, trunk flexion, lateral bending, and twisting relative to the pelvis was calculated based on a body-fixed rotation sequence, in that order, of the trunk about its axes (Vicon BodyBuilder). Numerical differentiation of the joint angles was used to calculate joint angular velocities. Joint angular velocity data were further filtered using a seven-point moving-average filter (MATLAB, MathWorks, Natick, MA). The load moment arm was calculated as the horizontal distance between the transferor's L_3L_4 joint and the dummy's head-arms-torso center of mass. This center of mass position was extrapolated from the positions of the markers attached to the head and shoulders of the dummy.

The time required to perform an assisted transfer was calculated by dividing the total number of frames captured during the period of interest for lower back disorder risk by the frame rate of the motion capture cameras, 60 Hz. Estimates of transfer duration for trials in which the dummy was not transferred in one continuous motion were removed.

For each trial, the transferor's maximum load moment arm; maximum integrated load moment arm; maximum angles of lumbar flexion, extension, bending and twisting; maximum lumbar flexion and extension velocities; and maximum and average lumbar bending and twisting velocities were determined over the period of interest for lower back disorder risk. Integrated moment arm calculations were not performed for trials lacking an estimate of transfer duration. Left and right twisting and bending were considered equivalent (i.e. absolute values were used) in determining the maximum and/or average angles and velocities.

When needed for the lower back disorder model of Marras *et al.* (1995), the maximum load moment experienced by the transferor was estimated as the product of the maximum load moment arm over the course of the trial and the estimated force required to hold the dummy's head-arms-torso. The force exerted by the dummy's head-arms-torso was estimated based on the percentage of total body mass typically located in the head-arms-torso, according to the equation listed below (Winter 2005).

Dummy Force (N) = Dummy total mass (kg) * 9.81(m /s^2) * 0.64.

Spatial Consumption

Custom computer software was written by the author to determine the three-dimensional spatiotemporal volume required for assisted toilet transfers at each of the four experimental wheelchair-to-toilet angles. The software was written using a multi-language approach and is composed of approximately 8,000 lines of original Java source code and 14,000 lines of original C++ source code. A more complete description of the design of the software is in Appendices C and D. Prior techniques used to investigate the spatial requirements of tasks have included the use of fixed-perspective cameras (Hignett and Evans 2006) and task simulation (Warren and

Valois 1991). Studies using these techniques have, however, only reported the absolute spatial requirements of a task from a single, fixed perspective. The spatial consumption results generated using the software created for this study do not have this limitation and allow the full three-dimensional spatial requirements of an assisted transfer to be inferred from motion capture data and anthropomorphic body measurements. The software created for this study was designed as a general purpose spatial modeling tool and can be easily used to quantify the spatiotemporal requirements of any task, given both anthropometric body measurements and motion capture data for an individual performing the task. This spatial mapping technique was first presented by the author at the 2007 Northwest Biomechanics Symposium (Appendix E).

To model the unique spatial volume used by each participant in conducting an assisted transfer to and from the toilet, a custom volume model was created for each assisted transfer trial. The volume model is the combination of three sub-models that model the volume occupied by the participant, dummy, and wheelchair, respectively (Figure 2). The participant, dummy, and wheelchair were each further modeled as collections of geometrically-defined bounding primitives. Both the participant and dummy were modeled using the same 27-segment volume model, with the orientation and position of each segment determined dynamically from the filtered motion capture data. The dimensions of each segment in the models of the participant and dummy were transformed to match the respective dynamic segment dimensions of the participant and dummy, as derived from a combination of filtered motion capture data and static body measurements. The wheelchair was modeled as a collection of 33 geometric shapes and was dynamically oriented and positioned using filtered motion capture data.

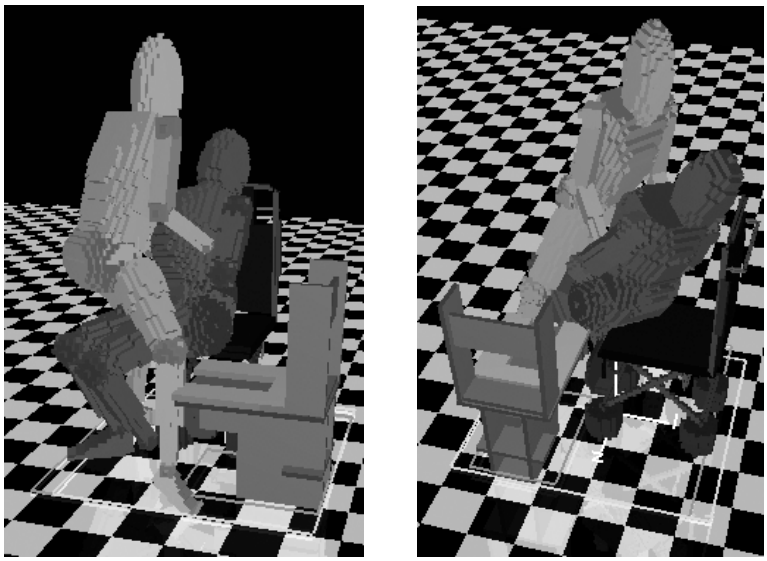

Figure 2 – Software's graphical representation of the three-dimensional model of an assisted transfer for a participant at a fixed point in time. The position of the toilet is visualized but its volume is not tracked.

To calculate the unique three-dimensional spatial volume used over the course of each trial, areas of intersection with planes parallel to the floor were calculated for the respective volume models of the participant, dummy, and wheelchair for each motion capture frame of interest. Areas of intersection were calculated for planes at 1 cm intervals over the total height of the assisted transfer volume, starting 1 cm from the floor. The area of intersection identified for each motion capture frame was the spatial area of the plane that was occupied by the union of the participant's, dummy's, and wheelchair's volume (Figure 3). This intersection mapping resulted in a binary description of the area in the plane as being either inside or outside the volume described by the participant's, dummy's, and wheelchair's volume (Figure 3). Planar intersection maps at each respective height were integrated across the motion capture frames of interest (Figures 4 – 5). The result of this, for each of the respective heights, was a single planar map that

represented the area of the plane that had intersected the volume model over the course of the transfer (Figures 4 – 5). The planar map itself represented the 400 cm x 400 cm area using a map measuring 3,000 x 3,000 pixels, with each pixel in the map representing an area measuring approximately 1.7 mm^2.

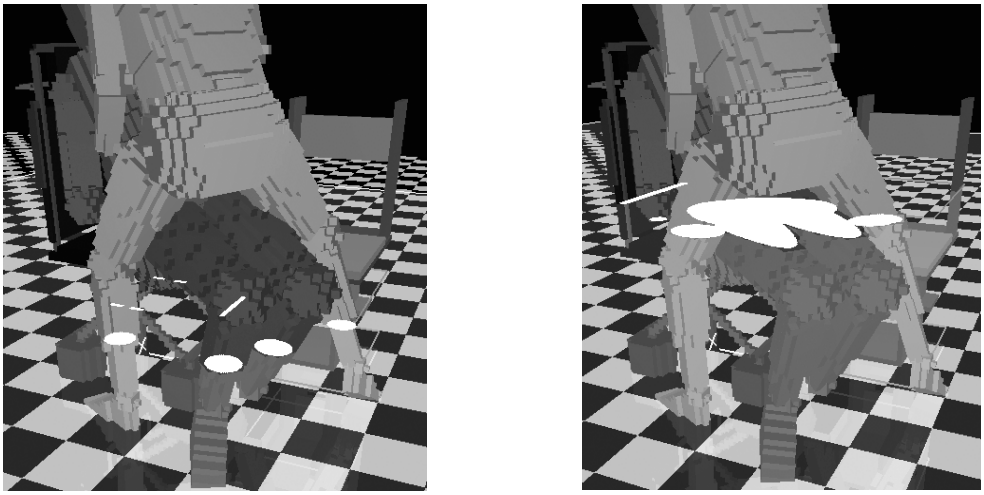

Figure 3 – Illustration of the calculation of the area occupied by the participant, wheelchair, and dummy at two experimental heights. The areas of intersection for the planes at the given heights are illustrated in white.

Following integration, each of the integrated planes was normalized by the total number of frames integrated, converting each of the planar maps into a percentile spatial consumption map for the individual trial analyzed (Figures 4 – 5). Each of the respective positions in the percentile spatial consumption map represented the area in the plane occupied over the course of the trial by a value ranging from zero, never occupied, to one, always occupied. Finally, the normalized planar maps for each height and wheelchair-to-toilet angle were averaged across participants and transfer directions. The result was a mapping of the mean percentage of time that an area at a given height from the floor was occupied over the course of all the assisted transfers conducted at a given wheelchair-to-toilet angle.

While each plane, by itself, represents just a two-dimensional area of intersection between the volume model and the plane, the volume required for an assisted transfer can be inferred by placing each plane at its respective height and integrating the voxels described between the planes across the height of the model. In addition to generating the spatial consumption maps, the software created to conduct this analysis allows for interactive visualization of the three-dimensional spatial volume and planes of intersection across individual frames, trials, and multiple trials.

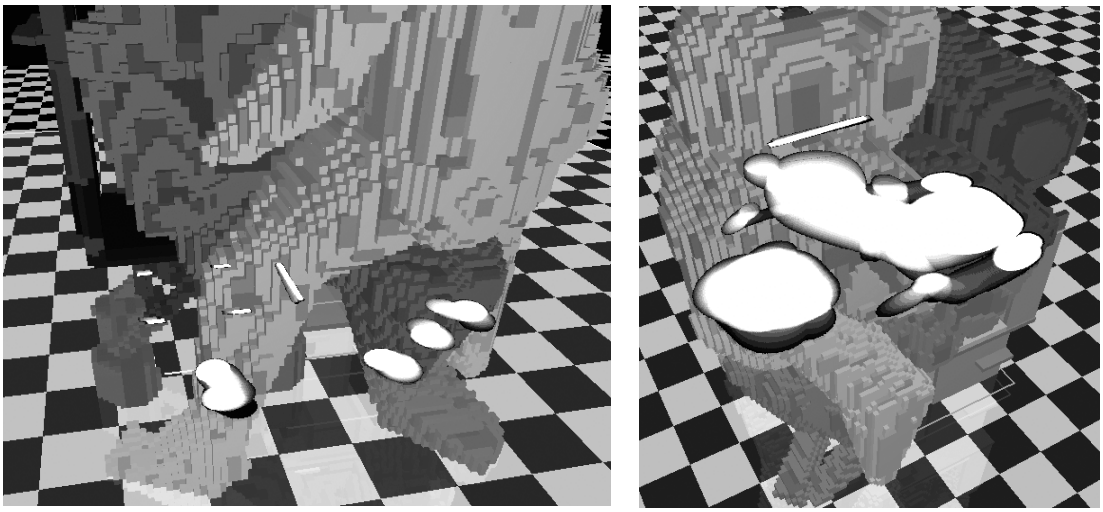

Figure 4 – Percentile planar intersection map taken below and above the knee

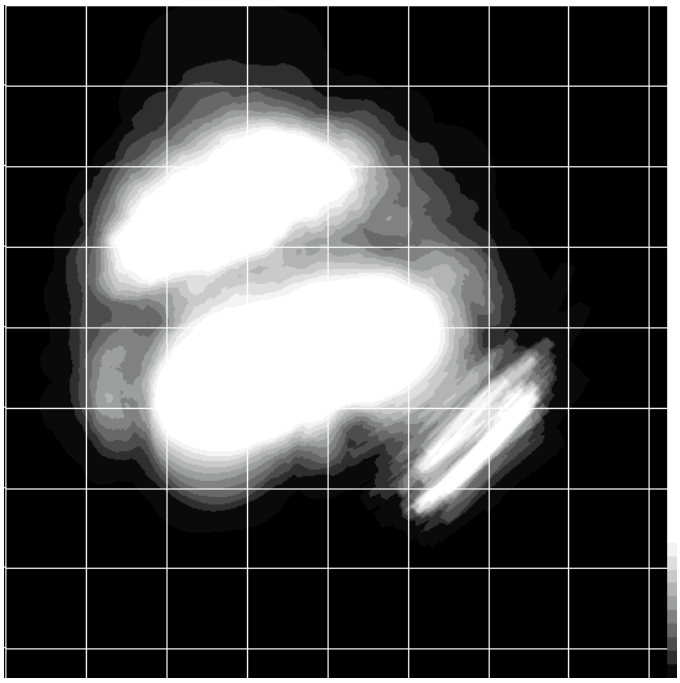

Figure 5 – Mapping representative of that to be used to express the combined percentage of time that any location in a plane at a specified height was occupied across all participants

Statistical Analysis

Qualitative Spatial Requirements of Assisted Transfers

It was hypothesized that the wheelchair-to-toilet angle would directly affect the spatial requirements of an assisted toilet transfer. Planar spatial consumption maps were computed at 1 cm intervals, starting 1 cm above the floor, to the maximum height of the assisted transfer volume, approximately 188 cm. Spatial consumption maps for key heights of interest are reported and compared qualitatively, with particular attention focused on identifying differences in the transfer volumes between the wheelchair-to-toilet angles tested (0º, 45º, 90º, and 180º). Particular attention was further directed towards identifying unused portions of the spatial volume that could function as ideal locations for lavatory fixtures, such as the sink, during accessible lavatory design.

Transferor's Kinematic Risk Factors for Lower Back Disorder, Perceived Exertion, and the Vertical Acceleration of the Transferee

Mixed-effects least-squares regression (Pinheiro and Bates 2002) was used to test for the main effects and interaction effects of the wheelchair-to-toilet angle and direction of assisted transfer on the transferor's kinematic risk factors for lower back disorder and on the maximum vertical acceleration experienced by the dummy during the assisted transfers. The wheelchair-to-toilet angle and the direction of assisted transfer were coded as four- and two-level factors, respectively. Each of the 15 response (i.e. dependent) variables was analyzed independently. Statistics were computed using S-Plus (S-Plus 8.0 for Windows, Insightful Corp, Seattle, WA) and statistical significance was defined as $P \leq 0.05$.

The distribution of each response variable across the explanatory variables was examined to determine if a transformation would improve the underlying assumptions of least-squares inference. Plots of the relationship between the response variable and both the wheelchair-to-toilet angle and the direction of assisted transfer were examined to visualize the distribution of the data. Residual versus fit plots were generated for each response variable from the full mixed-effects regression model to visualize the distribution of the fitted values across the full model. Based upon all three plots, the transfer duration, the transferor's maximum lumbar twisting angle, the transferor's lumbar angular velocities in flexion, extension, bending, and twisting, and the maximum vertical acceleration of the dummy were log-transformed to improve the equal variance and linearity assumptions rendered by least-squares inference. Response variables describing the transferor's maximum load moment arm, integrated load moment arm, and maximum lumbar angles of

flexion, extension, and bending required no transformation and were analyzed on the original scale.

Response variables were tested for the presence of influential outlying data points by examining the plots of the response, transformed as necessary, versus both the wheelchair-to-toilet angle and the direction of assisted transfer. A full fixed-effects regression model, blocked by participant, was fit and the resulting residual versus fit and Cook's distance plots were examined for influential outliers. Influential outliers were removed.

The main effects and the interaction effect of the wheelchair-to-toilet angle and the direction of assisted transfer on each of the response variables were tested individually using a full mixed-effects model. The model predicted the response variable of interest, transformed as necessary, from the fixed effects and interaction effect of the wheelchair-to-toilet angle and the direction of transfer. Random effects modeled the mean response of the transferor to control for variability in the mean response across transferors. Maximum-likelihood estimation was used to fit the model. Stepwise regression was then used to reduce the full model into its statistically significant beta terms.

Response variables affected by either the main effects or interaction effects of the wheelchair-to-toilet angle and the direction of assisted transfer were then further examined to determine the precise nature of the effect. To allow for greater control over the statistical model, indicator variables were created to represent the explanatory factor levels for both the wheelchair-to-toilet angle and the direction of assisted transfer. If the interaction effects of the wheelchair-to-toilet angle and direction of assisted transfer were significant, then eight mixed-effects regression models were created to model the relative effects across all wheelchair-to-toilet

angles and directions of assisted transfer. If the interaction effects were not significant, then the statistically significant main effects were explored. If the main effect of the wheelchair-to-toilet angle was significant, then four mixed-effects regression models were created modeling the relative main effects at each of the four wheelchair-to-toilet angles, controlling for the effect of the direction of assisted transfer. If the main effect of the direction of assisted transfer was significant, a mixed-effects regression model was created modeling assisted transfers from the wheelchair to the toilet, controlling for the main effect of the wheelchair-to-toilet angle. Statistically significant relative differences, standard deviations, and 95th percentile confidence intervals were reported.

Following the previously-described analysis, mixed-effects least-squares regression was used to control for the main effects of both the wheelchair-to-toilet angle and the direction of assisted transfer and then test for an association between the characteristics of the transferor and the response variable data sets generated as part of the preceding analysis, transformed as needed with outliers removed. The characteristics of the transferor that were examined were: transferor standing height, transferor previous experience, and transferor leg position. Two indicator variables were created to model transferor leg position (straddle/interlaced) and previous experience (yes/no). Transferors having previous experience were defined as transferors who self-reported having conducted manual assisted transfers at some time in the previous calendar year. Stepwise regression model simplification was used to reduce the full transferor characteristic model into its statistically significant components. Random effects were again used to model the mean response of the transferor, to control for variability in the mean response across transferors. The full transferor mixed-effects model used was: fixed effects= wheelchair-to-toilet angle +

direction of assisted transfer + standing height + self-reported experience + transferor leg position + (standing height x direction of assisted transfer) + (transferor leg position x direction of assisted transfer); random effects = ~ 1 | transferor (transferor's mean dependent variable response). Response variables associated with characteristics of the transferor were further examined to determine the precise nature of the associated effect. Statistically significant coefficients, standard errors, and 95th percentile confidence intervals were reported.

A logistic regression model was used to test for a relationship between the transferor's choice of transfer leg position and the main effect of the wheelchair-to-toilet angle, the direction of assisted transfer, the standing height of the transferor, and the self-reported experience classification of the transferor. Statistically significant coefficients and 95th percentile confidence intervals were reported.

Assumptions

In the design of this study, three primary assumptions were made with respect to the participant movements and transfers.

- It was assumed that participants' movements in the laboratory would be representative of the movements conducted during transfers in real-world airplane lavatories.
- The prior experience of the participants performing the experimental transfers as part of this study could be very different from that of a real-world caregiver. It was, however, assumed that the repeated-measures nature of this study would control for this by comparing participants against themselves. It was further assumed that, even in the case of the trained assisted caregiver, the

novelty of an airplane lavatory would decrease the benefit of prior experience with traditional assisted transfers.

- The study investigated lavatory spatial consumption using an unconstrained environment. It was assumed that, by using the unconstrained lavatory, participants would conduct assisted transfers in a manner that minimized their risks of injury. It was also assumed that participants would conduct assisted transfers using identical kinematics given sufficient space in an actual aircraft lavatory.

Delimitations

The following are study-specific variables directly impacting the conclusions drawn from this study:

- A dummy with the body dimensions of a 95th percentile male was used as the transfer participant. The choice of a 95th percentile dummy was designed to provide upper limits for the spatial requirements of assisted transfers. The use of the dummy instead of an actual person with disabilities could result in different measured spatial consumption and risks of injury during assisted transfers. However, the use of the dummy was more humane and reduced the intra-participant variance that would otherwise be present if the assisted transfers were tested using actual people with mobility disabilities.
- A single aircraft wheelchair (Innovint Aircraft Interior, Hamburg, Germany) was used for all trials. Assisted transfers between other wheelchair designs and an aircraft lavatory toilet could result in different risks of injury and spatial consumption than those measured in this study.

Results

Spatiotemporal Consumption

The spatial volume used during assisted toilet transfers, that is, the volume occupied by the transferor, transferee, and wheelchair, extended from the floor to a height of 188 cm – 189 cm from the floor. Spatiotemporal maps of the specific volumes used were calculated at 1 cm increments in height over the total height for each of the 0°, 45°, 90°, and 180° bi-directional transfers. Of the 188 spatiotemporal maps created, nine representative maps have been selected for presentation. The selected spatiotemporal maps are for the following heights from the floor: 1 cm, foot level (Figure 6); 20 cm, mid lower leg and wheelchair strut level (Figure 7); 44 cm, wheelchair seat height (Figure 8); 62 cm, height at which the 0° transfer appears to have required the greatest spatial area (Figure 9); 75 cm and 85 cm, heights at which the 45°, 90°, and 180° transfers appear to have required the greatest area (Figures 10 and 11); 105 cm, dummy seated head height (Figure 12); 118 cm, transferor upper trunk height (Figure 13); and 138 cm, transferor head height (Figure 14).

The spatiotemporal maps presented in Figures 6 – 14 are simplified representations in which the volume required for assisted transfers has been separated into four discrete regions. The area in black represents space occupied 5% of the time or more or, equivalently, the 95th percentile spatial area. The area in dark grey represents the area occupied between 2.5% and 5% of the time; the 95^{th} to 97.5^{th} percentile area. The area in light grey represents the area that was occupied more than 0% but less than 2.5% of the time; the 97.5^{th} to 100^{th} percentile area. Together, the black, dark grey, and light grey areas comprise the 100% spatial area. The area in white represents the area never occupied. Each map represents the

same relative experimental area and is drawn to the same scale; a grid representing 20 cm is overlaid for scale purposes. High-resolution color spatial maps have been included in Appendix B.

Taken as a whole, the spatial volume required for non-physically constrained, assisted toilet transfers appears to have been affected by the wheelchair-to-toilet angle. An effect of the wheelchair-to-toilet angle is evident in the planar spatial consumption maps at each of the heights shown. In the spatial area maps generated across the height of the transfer volume for the 0°, 45°, and 90° transfer angles, it appears that the area occupied by the transferor, as well as the area occupied by the transferee when on or near the toilet, was similar at each wheelchair-to-toilet angle. The primary difference between these angles appears to have been in the area occupied by the wheelchair and by the transferee when on or near the wheelchair. This latter area appears generally similar in overall shape across transfers, but rotated with respect to each other by the wheelchair-to-toilet angle. The spatial volume used for the 180° transfer angle appears to have a much greater depth than any of the other transfer angles. The 180° transfer volume is also very different in that the transferor and wheelchair have effectively switched places. The wheelchair-to-toilet angle appears to influence the height, 65 cm – 86 cm (Figures 9 – 11), at which each assisted toilet transfer used the greatest spatial area. The 0° transfer appears to have used the greatest area at a slightly lower height, 65 cm (Figure 9), than for the 45°, 90°, and 180° transfers, 75 cm – 86 cm (Figures 10 – 11). This appears to be due to the effect of the wheelchair-to-toilet angle on the position of the transferor's pelvis and lower back. The wheelchair-to-toilet angle further appears to have affected the volume used during an assisted transfer by constraining the transferor from moving through the volume blocked by the wheelchair.

At each respective wheelchair-to-toilet angle, the total spatial volume used in conducting the assisted transfers also appears to have been influenced by the variability in the position of the wheelchair across transfers. At a height of 1 cm (Figure 6), the wheelchair position can be inferred from the relative position of the four circular regions defining the space used by the wheelchair's castors. At a height of 20 cm (Figure 7), the spatial area used by the wheelchair's cross members can be clearly seen. It can be seen that there was considerable variability in the absolute placement of the wheelchair, which acted to increase the total spatial volume used. In addition, both heights show that increases in the wheelchair-to-toilet angle appeared to increase the overall variability in the transferor's choice in absolute wheelchair position.

There also appears to have been considerable variability in the spatial volumes used by different transferors in transferring the dummy. The nature of this variability appeared to differ across heights. Spatial maps taken at 1 cm (Figure 6) clearly show that no single foot position was used consistently and that a considerable number of foot positions were used less than 2.5% of the time. In the spatial maps from 65 cm – 86 cm (Figures 9 – 11), one can observe considerable variability in the position of the pelvis and trunk of the transferor, particularly in the direction perpendicular to the path of the transfer. In the spatial maps at 105 cm and above (Figures 12 – 14), it appears as if there is greater variability in the spatial area traversed by the transferee than in the area occupied by the body of the transferor. Finally, it appears that the initial and final seated positions of the transferee were more variable across transfers at the larger wheelchair-to-toilet angles.

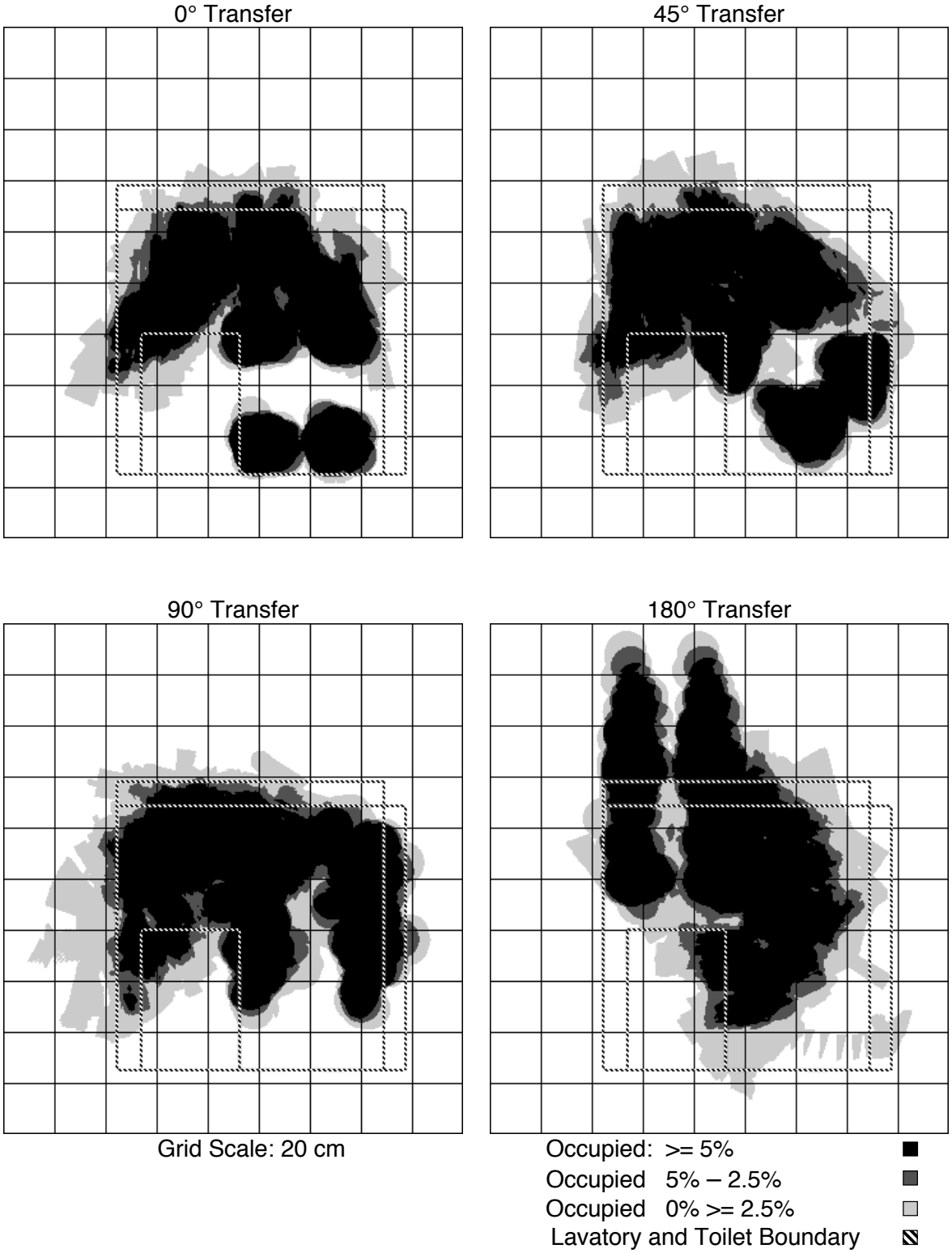

Figure 6 – Spatial consumption at 1 cm from the floor as a function of transfer angle, area occupied by the wheelchair's wheels and the feet of the transferor and dummy.

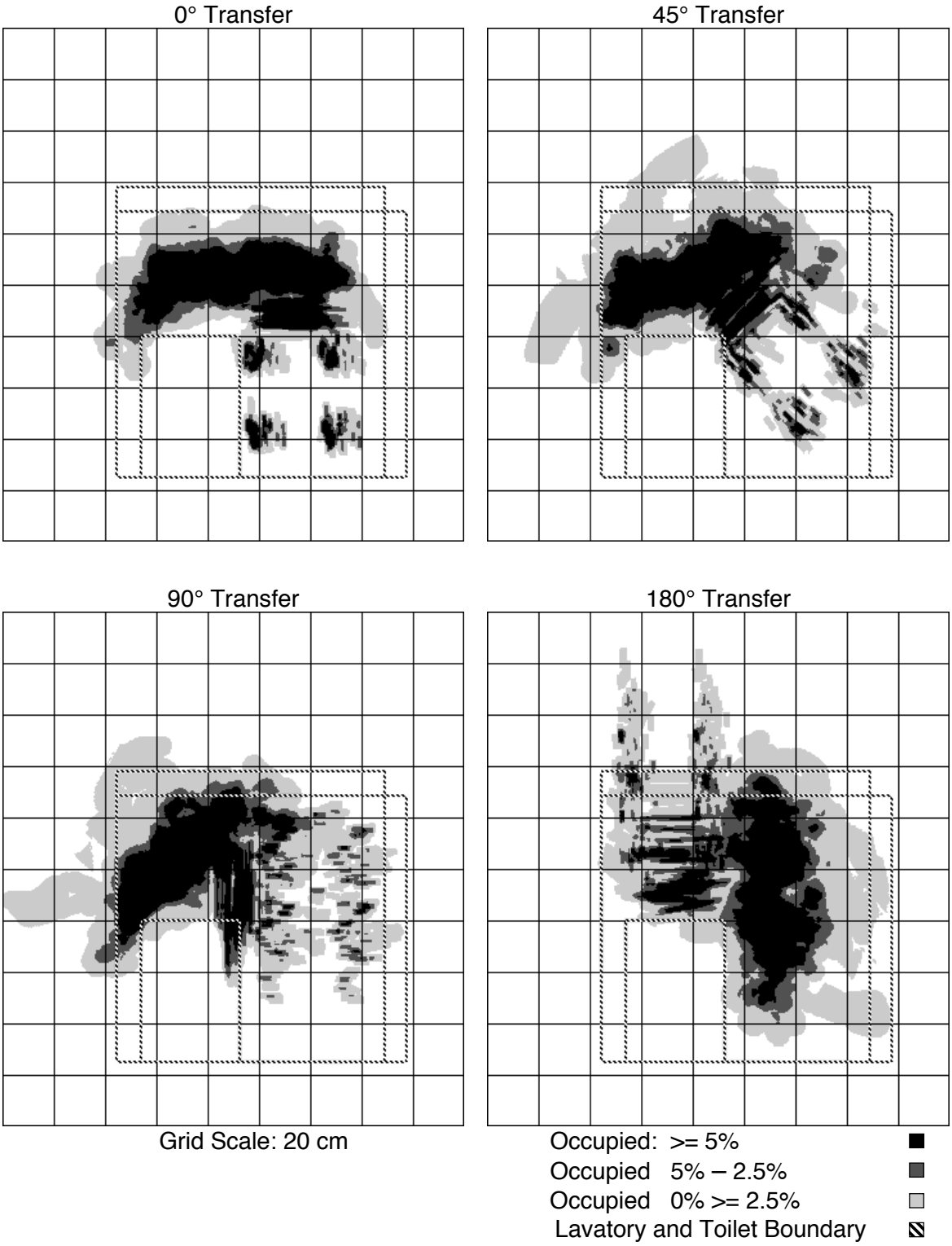

Figure 7 – Spatial consumption at 20 cm from the floor, as a function of transfer angle; the area occupied by the wheelchair's leg struts and the mid calf of the transferor and dummy.

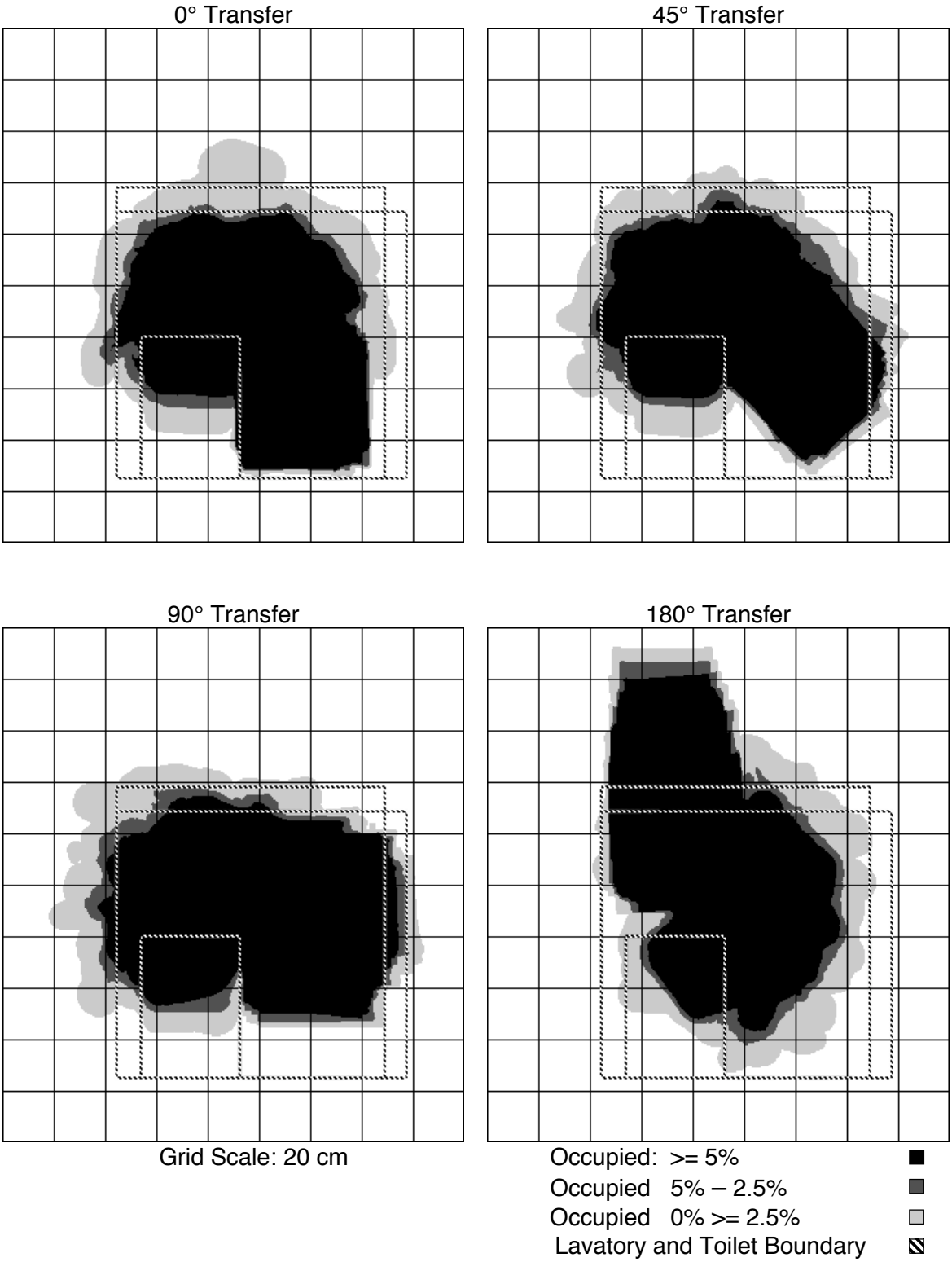

Figure 8 – Spatial consumption at 44 cm from the floor, seat height of the wheelchair, as a function of transfer angle.

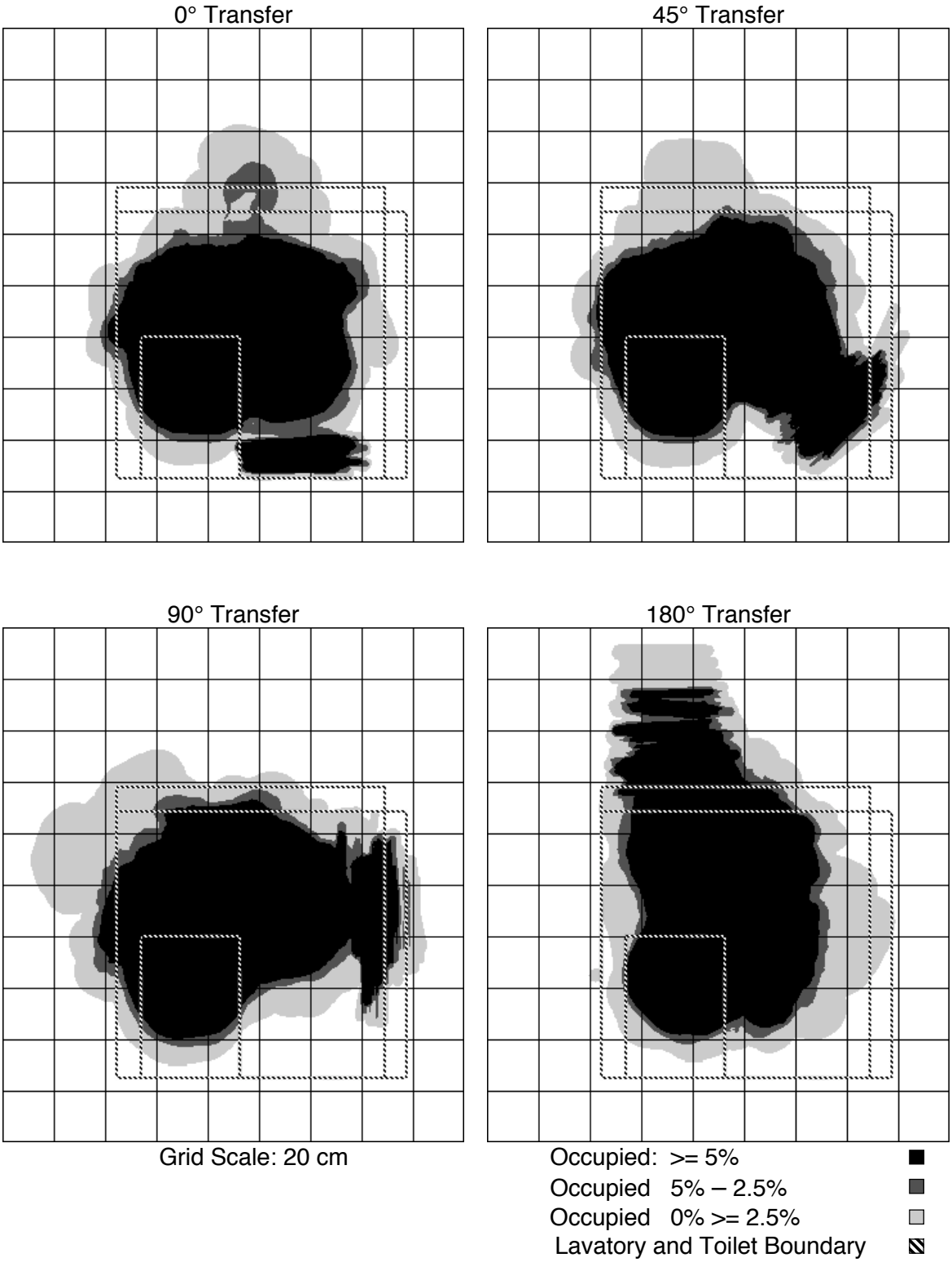

Figure 9 – Spatial consumption at 62 cm from the floor, transferor and dummy pelvis height, as a function of transfer angle.

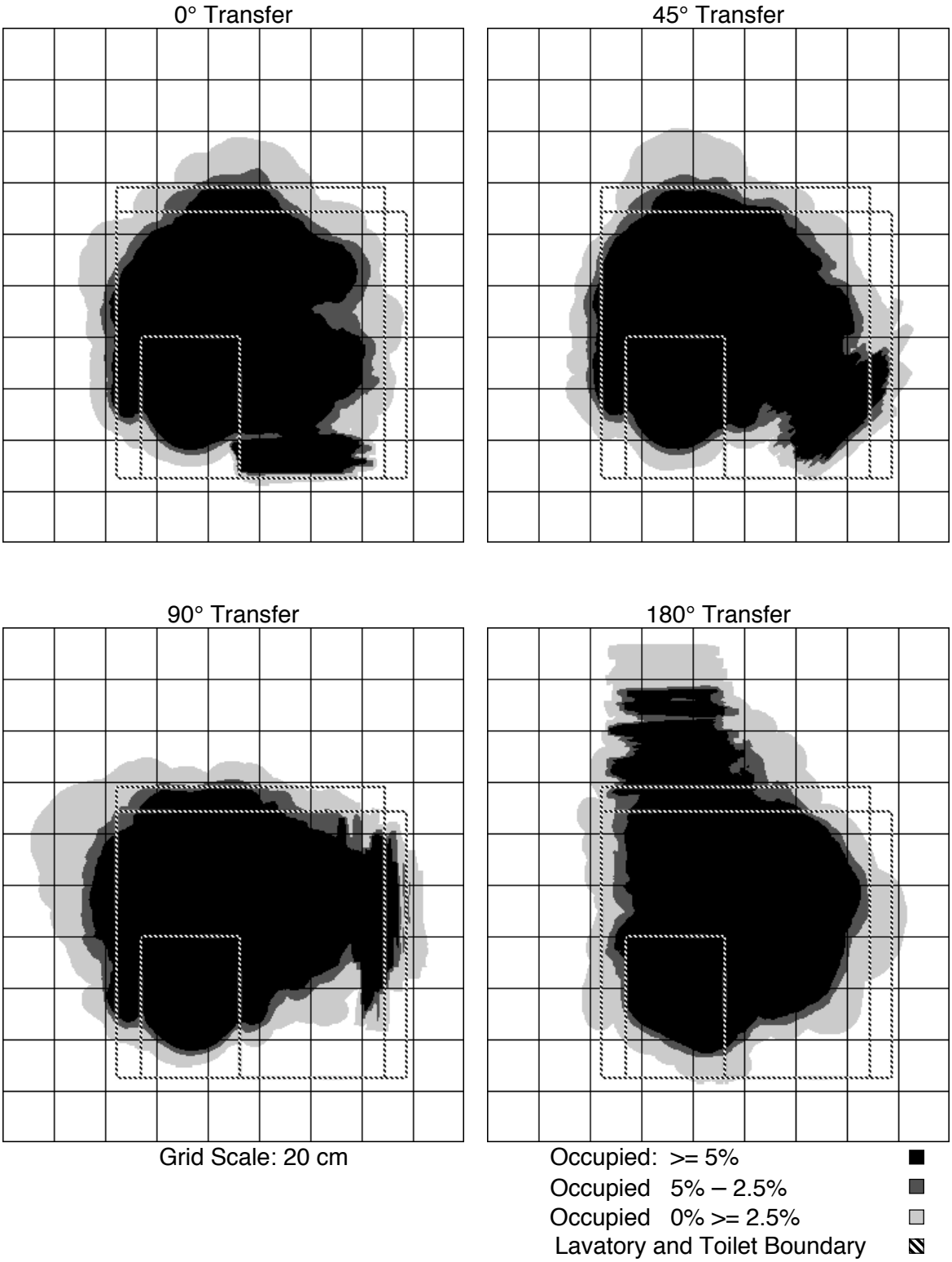

Figure 10 – Spatial consumption at 75 cm from the floor, transferor lower trunk to mid trunk height, as a function of transfer angle.

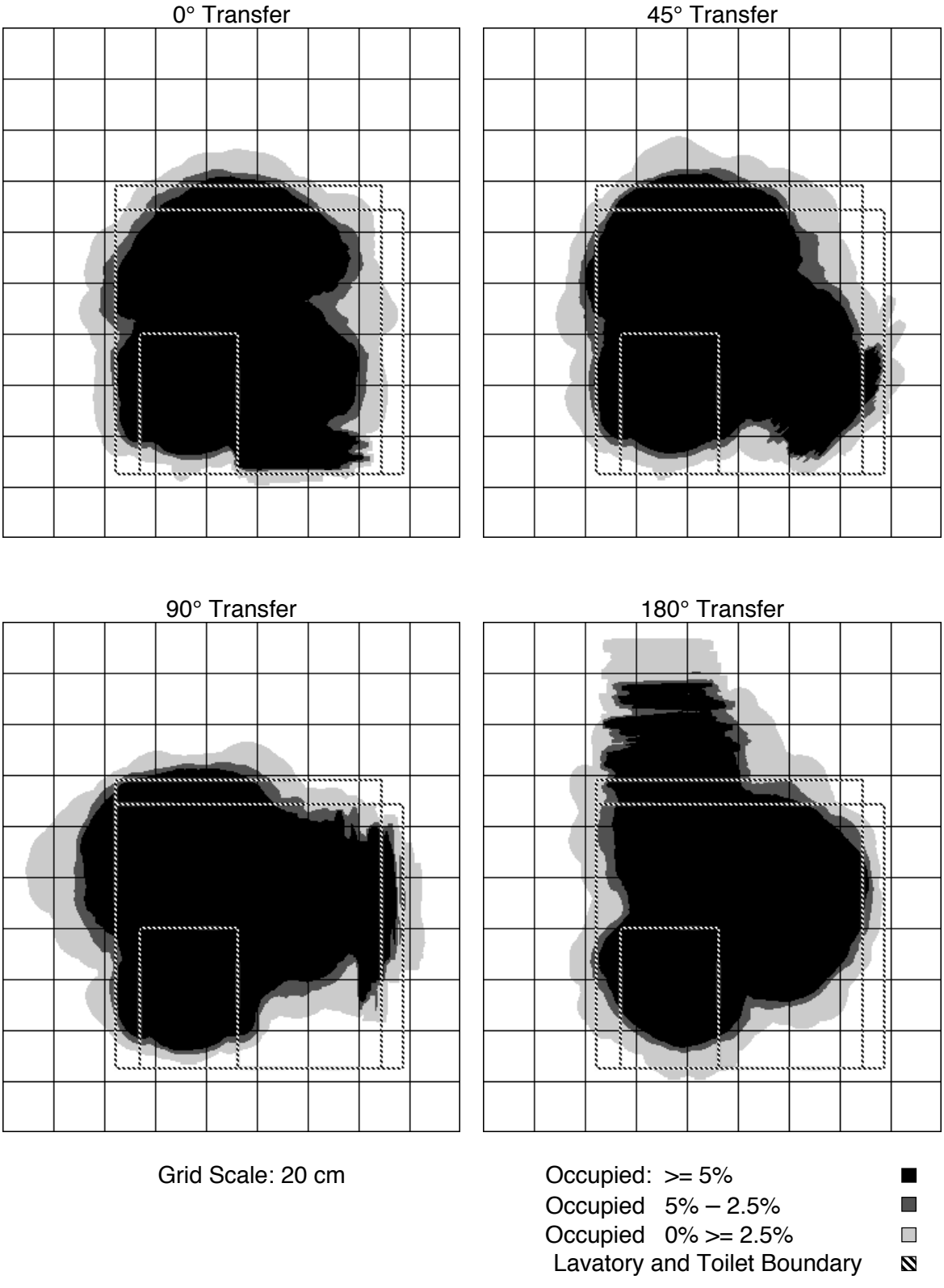

Figure 11 – Spatial consumption at 86 cm from the floor, transferor lower trunk to mid trunk height, as a function of transfer angle.

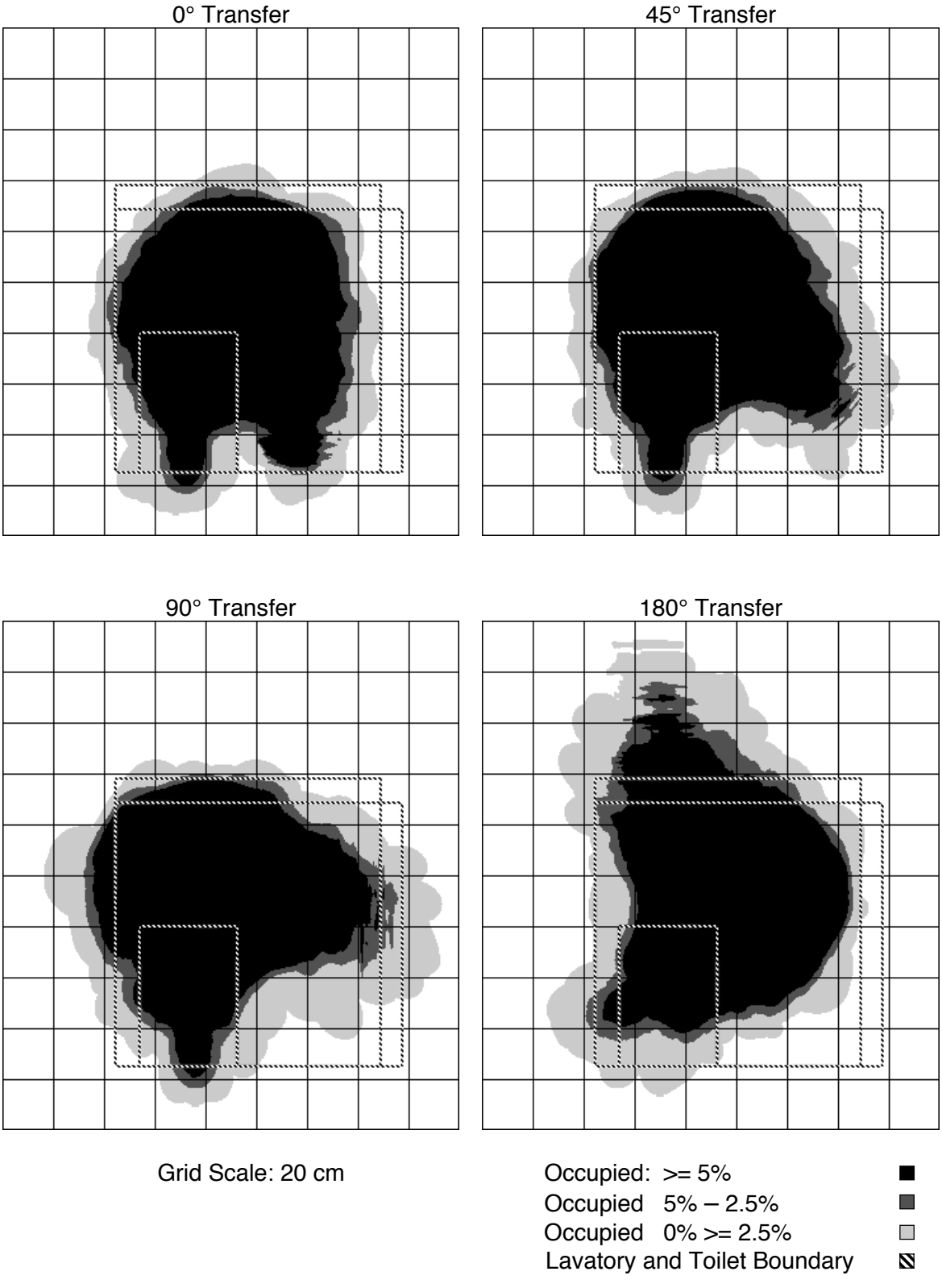

Figure 12 – Spatial consumption at 105 cm from the floor, seated dummy head height, as a function of transfer angle.

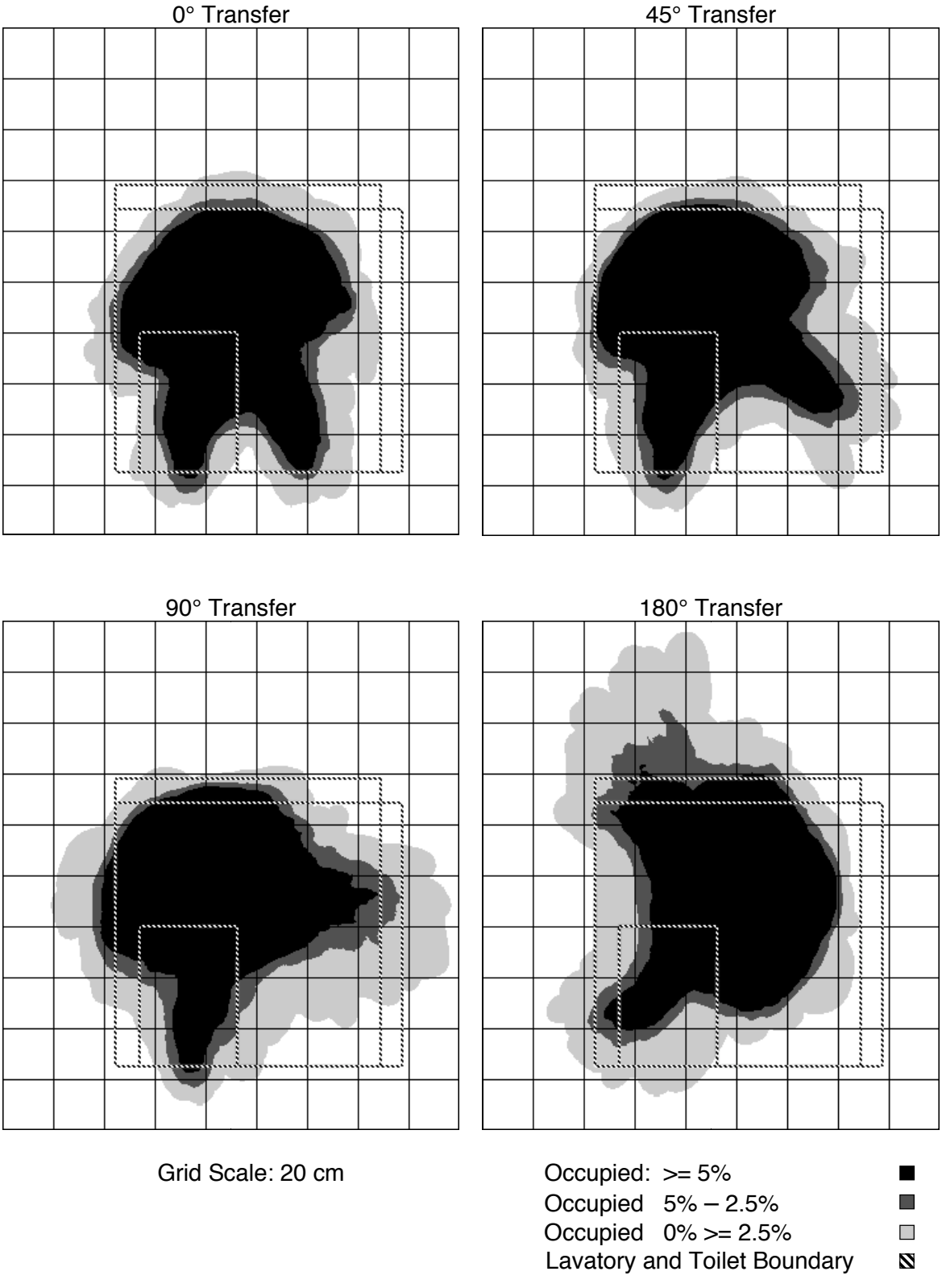

Figure 13 – Spatial consumption at 118 cm from the floor, area used by the transferor's upper trunk and dummy head, as a function of transfer angle.

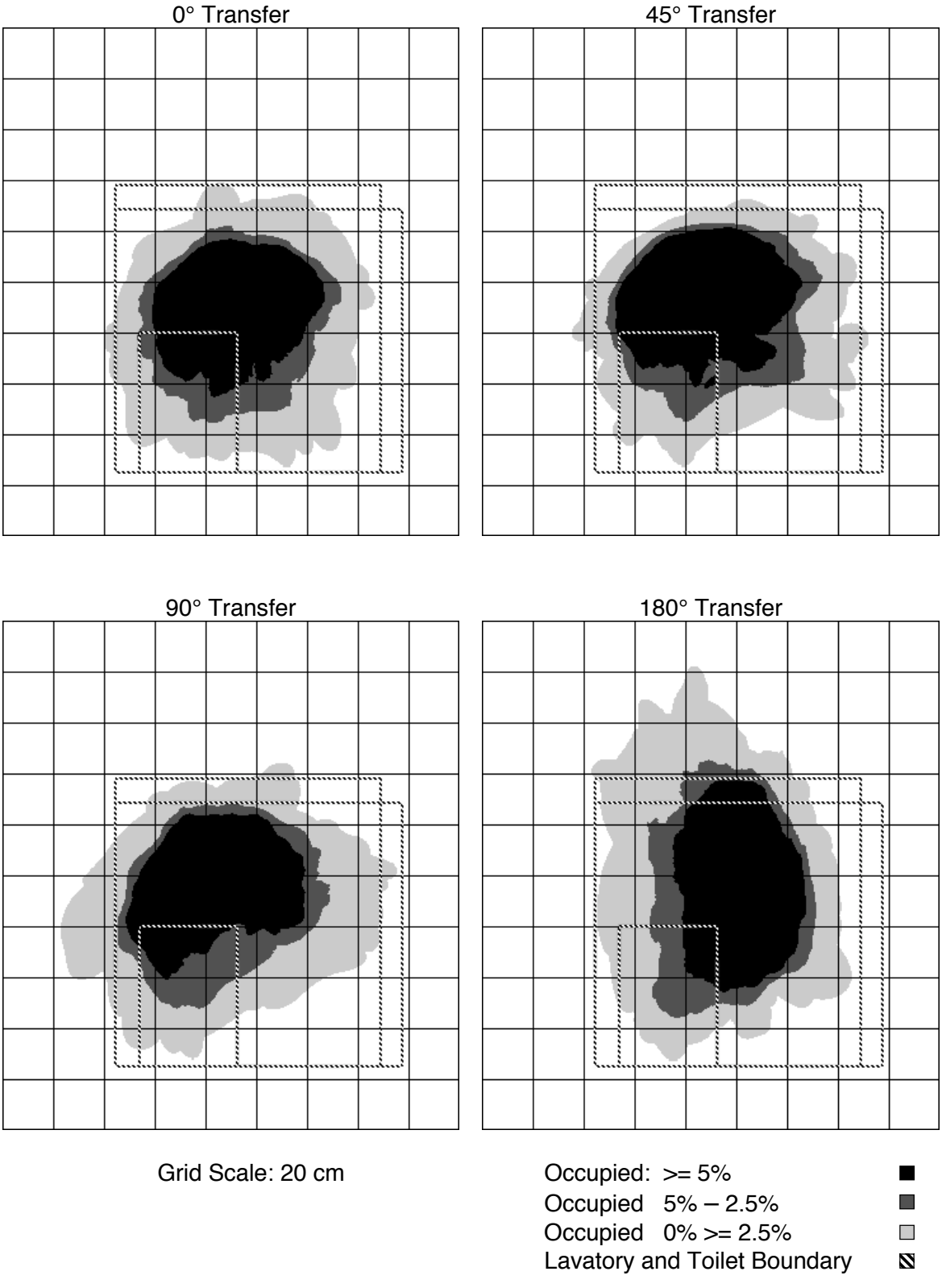

Figure 14 – Spatial consumption at 138 cm from the floor, upper trunk and head height of the transferor, as a function of transfer angle.

A rectangular footprint was fit to the spatial volume occupied 5% or more of the time across the entire height of the transfer volume to define the minimum two-dimensional rectangular area (width x depth) required to conduct an assisted transfer, for each of the transfer orientations. The minimum rectangular dimensions required for each wheelchair-to-toilet angle are listed in Table 6 below.

Table 6 – The minimum rectangular dimensions required to conduct assisted toilet transfers as a function of wheelchair-to-toilet angle

Wheelchair-to-Toilet Angle	Width (meters)	Depth (meters)
0º	1.07	1.24
45º	1.20	1.24
90º	1.29	1.25
180º	1.09	1.53

Transferor Kinematics

The wheelchair-to-toilet angle and the direction of assisted transfer affected the transferor's risk factors for lower back disorder. In general, the effects of the wheelchair-to-toilet angle and the direction of assisted transfer were independent of each other (Table 7). The lumbar flexion velocity was the only variable to exhibit an interaction between the effects of the wheelchair-to-toilet angle and direction of assisted transfer. Of the remaining variables analyzed, eight exhibited main effects of the wheelchair-to-toilet angle and five exhibited main effects of the direction of assisted transfer (Table 7). The mean and standard deviation of each of the variables, blocked by the wheelchair-to-toilet-angle and the direction of assisted transfer, are listed in Tables 8 – 9.

Table 7 – P-Value for statistical confidence that the parameter affected transferor lower back disorder risk factors.

		Direction	Angle	Direction x Angle
Transfer Duration	Log (s)*	NS	< 0.0001	NS
Max Load Moment Arm	(m)	0.0160	< 0.0001	NS
Integrated Load Moment Arm	(m•s)	NS	< 0.0001	NS
Max Lumbar Flexion Angle	(deg)	NS	NS	NS
Max Lumbar Extension Angle	(deg)	NS	NS	NS
Max Lumbar Bending Angle	(deg)	0.0068	NS	NS
Max Lumbar Twisting Angle	Log (deg)*	NS	0.0004	NS
Max Lumbar Flexion Velocity	Log (deg/s)*	NS	NS	0.0284
Max Lumbar Extension Velocity	Log (deg/s)*	0.0011	0.0145	NS
Max Bending Velocity	Log (deg/s)*	NS	NS	NS
Average Bending Velocity	Log (deg/s)*	0.0052	NS	NS
Max Twisting Velocity	Log (deg/s)*	NS	< 0.0001	NS
Average Twisting Velocity	Log (deg/s)*	0.0046	<0.0001	NS
Rating of Perceived Exertion		NS	< 0.0001	NS

* Log = Natural Logarithm
NS = Not significant (P > 0.05)

The time required to conduct an assisted transfer was directly related to the wheelchair-to-toilet angle (P < 0.0001), after controlling for the main effects of the direction of assisted transfer. The median time required to perform an assisted transfer at the 0º wheelchair-to-toilet angle was 7.7% less than that required at the 45º orientation (P = 0.0242; 95th percentile confidence interval [95% CI]: 1.1% – 13.9%), 12.3% less than that required at the 90º orientation (P = 0.0004; 95% CI: 5.9% – 19.0%), and 29.5% less than that required at the 180º orientation (P < 0.0001; 95% CI: 24.3% – 34.3%). The median time required to perform an assisted transfer at the 45º wheelchair-to-toilet angle was 23.6% less than that required at the 180º orientation (P < 0.0001; 95% CI: 18.0% – 28.8%). Similarly, the median time required to perform an assisted transfer at the 90º wheelchair-to-toilet angle was 19.6% less

than that required at the 180º orientation ($P < 0.0001$; 95% CI: 13.6% – 25.2%). There was no difference between the median time required at the 45º and 90º wheelchair-to-toilet angles ($P > 0.05$). The direction of assisted transfer did not affect the median time required for an assisted toilet transfer ($P > 0.05$) after controlling for the main effects of the wheelchair-to-toilet angle.

The maximum load moment arm experienced by the transferor was affected by both the wheelchair-to-toilet angle and the direction of assisted transfer. After controlling for the main effects of the direction of assisted transfer, the maximum load moment arm generally decreased as the angle between the wheelchair and toilet increased ($P < 0.0001$). The maximum load moment arm at the 180º wheelchair-to-toilet angle was 0.173 m less than that at 0º ($P < 0.0001$; 95% CI: 0.148 m – 0.199 m), 0.177 m less than that at 45º ($P < 0.0001$; 95% CI: 0.152 m – 0.202 m), and 0.137 m less than that at 90º ($P < 0.0001$; 95% CI: 0.112 m – 0.162 m). The maximum load moment arm at the 90º wheelchair-to-toilet angle was 0.036 m less than that at 0º ($P = 0.0044$; 95% CI: 0.012 m – 0.061 m) and 0.040 m less than that at 45º ($P = 0.0019$; 95% CI: 0.015 m – 0.064 m). The maximum load moment arm for wheelchair-to-toilet angles of 0º and 45º did not differ ($P > 0.05$). Finally, after controlling for the main effects of the wheelchair-to-toilet angle, assisted transfers from the toilet to the wheelchair had a 0.022 m greater load moment arm than those conducted in the opposite direction ($P = 0.0160$; 95% CI: 0.004 m – 0.039 m).

The integrated load moment arm of the transferor was affected by the wheelchair-to-toilet angle ($P < 0.0001$), after controlling for the main effects of the direction of assisted transfer. The mean integrated load moment arm for the 180º wheelchair-to-toilet angle was 0.278 m·s less than that experienced for the 0º

orientation ($P < 0.0001$; 95% CI: 0.203 m·s – 0.353 m·s), 0.295 m·s less than that for the 45º orientation ($P < 0.0001$; 95% CI: 0.220 m·s – 0.369 m·s), and 0.164 m·s less than that for the 90º orientation ($P < 0.0001$; 95% CI: 0.089 m·s – 0.240 m·s). The mean integrated load moment arm for the 90º wheelchair-to-toilet angle was 0.113 m·s less than that experienced for the 0º orientation ($P = 0.0034$; 95% CI: 0.039 m·s – 0.188 m·s) and 0.130 m·s less than that for the 45º orientation ($P = 0.0008$; 95% CI: 0.056 m·s – 0.204 m·s). There was no difference between the integrated moment arms for the 0º and 45º wheelchair-to-toilet angles ($P > 0.05$). The integrated moment arm was not affected by the direction of assisted transfer ($P > 0.05$) after controlling for the main effects of the wheelchair-to-toilet angle.

The mean maximum lumbar flexion angle of the transferor was 40.5º (SD = 12.1º). The mean maximum lumbar extension angle of the transferor was 29.7º (SD = 12.2º) of flexion. Neither the wheelchair-to-toilet angle nor the direction of assisted transfer affected the transferor's maximum angle of lumbar flexion or extension ($P > 0.05$).

The maximum lumbar bending angle of the transferor was affected by the direction of transfer ($P = 0.0062$), after controlling for the main effects of the wheelchair-to-toilet angle. Maximum lumbar bending was 0.85º greater for assisted transfers from the toilet to the wheelchair than for transfers in the opposite direction ($P= 0.0068$; 95% CI: 0.24º – 1.46º). The wheelchair-to-toilet angle did not affect the maximum lumbar bending angle ($P > 0.05$) after controlling for the effect of the direction of transfer.

The maximum lumbar twisting angle of the transferor was affected by the wheelchair-to-toilet angle ($P = 0.0004$), after controlling for the main effects of the

direction of assisted transfer. The median maximum angle of lumbar twisting for the 0º wheelchair-to-toilet orientation was 25.0% smaller than that for the 90º orientation (P = 0.0004; 95% CI: 12.4% – 35.7%) and 18.5% smaller than that for the 180º orientation (P = 0.0118; 95% CI: 4.7% – 30.4%). Similarly, the median maximum angle of lumbar twisting for the 45º wheelchair-to-toilet orientation was 23.6% smaller than that for the 90º orientation (P = 0.0009; 95% CI: 10.7% – 34.6%) and 17.0% smaller than that for the 180º orientation (P = 0.0231; 95% CI: 2.7% – 29.2%). There was no difference in the maximum lumbar twisting angle between either the 0º and 45º or the 90º and 180º wheelchair-to-toilet orientations (P > 0.05). Transfer direction did not affect the maximum angle of lumbar twisting (P > 0.05) after controlling for the main effects of the wheelchair-to-toilet angle.

There was an interaction between the effects of the wheelchair-to-toilet angle and direction of assisted transfer on the maximum lumbar flexion velocity of the transferor (P = 0.0284). The median maximum lumbar flexion velocity was 24.7% lower during an assisted transfer from the toilet to the wheelchair with a wheelchair-to-toilet angle of 180º than in the same direction with an angle of 0º (P = 0.0042; 95% CI: 9.0% – 37.7%). In addition, at the 180º wheelchair-to-toilet angle, the median maximum lumbar flexion velocity was 19.4% lower for assisted transfers from the toilet to the wheelchair than for those in the opposite direction (P=0.0279; 95% CI: 2.7% – 33.3%).

The maximum lumbar extension velocity of the transferor was affected by the wheelchair-to-toilet angle (P = 0.0145) and by the direction of assisted transfer (P = 0.0011). Controlling for the main effects of the direction of assisted transfer, the median maximum lumbar extension velocity for the 90º wheelchair-to-toilet angle was 17.0% lower than for the 0º orientation (P = 0.0172; 95% CI: 3.4% – 28.6%) and

21.1% lower than for the 180º orientation (P = 0.0028; 95% CI: 8.1% – 32.3%). In addition, after controlling for the main effect of the wheelchair-to-toilet angle, assisted transfers from the wheelchair to the toilet exhibited a median maximum lumbar extension velocity that was 16.5% lower than for transfers conducted in the opposite direction (P = 0.0012; 95% CI: 7.1% – 25.0%).

The mean maximum lumbar bending velocity of the transferor was 14.5 deg/sec (SD = 8.0 deg/s). Neither the wheelchair-to-toilet angle nor the direction of assisted transfer affected the transferor's maximum lumbar bending velocity (P > 0.05).

The average lumbar bending velocity of the transferor was affected by the direction of assisted transfer (P = 0.0058), after controlling for the main effects of the wheelchair-to-toilet-angle. Assisted transfers from the toilet to the wheelchair exhibited a median average bending velocity that was 6.4% greater than for transfers conducted in the opposite direction (95% CI: 3.5% – 15.4%). The wheelchair-to-toilet angle did not affect the average lumbar bending velocity (P > 0.05) after controlling for the main effects of assisted transfer direction.

The maximum lumbar twisting velocity of the transferor was affected by the wheelchair-to-toilet angle (P < 0.0001), after controlling for the main effects of the direction of assisted transfer. The median maximum lumbar twisting velocity at the 0º wheelchair-to-toilet angle was 18.1% less than that for the 90º orientation (P = 0.0008; 95% CI: 8.2% – 26.9%) and 22.1% less than that for the 180º orientation (P < 0.0001; 95% CI: 12.5% – 30.6%). The median maximum lumbar twisting velocity at the 45º wheelchair-to-toilet angle was 18.2% less than that for the 90º orientation (P = 0.0007; 95% CI: 8.3% – 26.9%) and 22.2% less than that for the 180º orientation (P = 0.0001; 95% CI: 12.6% – 30.7%). There was no difference in the transferor's median

maximum lumbar twisting velocity between either the 0º and 45º or the 90º and 180º wheelchair-to-toilet orientations ($P > 0.05$). The maximum lumbar twisting velocity was not affected by the direction of assisted transfer ($P > 0.05$) after controlling for the main effects of the wheelchair-to-toilet angle.

The average lumbar twisting velocity of the transferor was affected by both the wheelchair-to-toilet angle ($P < 0.0001$) and the direction of assisted transfer ($P = 0.0051$). Controlling for the main effects of the direction of assisted transfer, the median average lumbar twisting velocity at the 0º wheelchair-to-toilet angle was 17.6% lower than that for the 90º orientation ($P = 0.0001$; 95% CI: 9.7% – 24.7%) and 19.4% lower than that for the 180º orientation ($P < 0.0001$; 95% CI: 11.7% – 26.5%). The median average lumbar twisting velocity at the 45º wheelchair-to-toilet angle was 16.3% lower than that for the 90º orientation ($P = 0.0002$; 95% CI: 8.3% – 23.5%) and 18.2% lower than that for the 180º orientation ($P < 0.0001$; 95% CI: 10.3% – 25.4%). There was no difference in the median average lumbar twisting velocity between either the 0º and 45º or the 90º and 180º wheelchair-to-toilet orientations ($P > 0.05$). Controlling for the main effects of the wheelchair-to-toilet angle, assisted transfers from the toilet to the wheelchair were associated with 9.0% greater median average lumbar twisting velocities than those in the opposite direction ($P = 0.0051$; 95% CI: 2.9% – 14.7%).

The rating of perceived exertion (RPE) reported by the transferors immediately following an assisted transfer was affected by the wheelchair-to-toilet angle ($P < 0.0001$), after controlling for the main effects of the direction of assisted transfer. The mean RPE for the 0º wheelchair-to-toilet angle was 0.8 points lower than that for the 180º orientation ($P < 0.0001$; 95% CI: 0.4 – 1.1 points). The mean RPE for the 45º wheelchair-to-toilet angle was 0.6 points lower than that for the 180º orientation ($P =$

0.0002; 95% CI: 0.3 – 1.0 points). The mean RPE for the 90º wheelchair-to-toilet angle was 0.5 points lower than that for the 180º orientation (P = 0.0061; 95% CI: 0.1 – 0.8 points). The direction of assisted transfer did not affect the transferor's RPE after controlling for the main effects of the wheelchair-to-toilet angle.

Table 8 – Effect of Transfer Direction and Angle on Transferor Kinematics, Mean (SD)

Variable		Direction	Wheelchair-to-Toilet Angle 0°	45°	90°	180°
Transfer Duration	(s)	T→W	1.9 (0.5) †‡§	1.9 (0.5) *§	2.1 (0.6) *§	2.5 (0.8) *†‡
		W→T	1.8 (0.5) †‡§	2.1 (0.5) *§	2.2 (0.7) *§	2.6 (0.7) *†‡
Max Load Moment Arm	(m)	T→W ¶	0.606 (0.118) ‡ §	0.622 (0.102) ‡§	0.577 (0.121) *†§	0.414 (0.100) *†‡
		W→T	0.591 (0.104) ‡§	0.582 (0.119) ‡§	0.550 (0.128) *†§	0.417 (0.104) *†‡
Integrated Load Moment	(m•s)	T→W	0.931 (0.283) ‡§	0.918 (0.257) ‡§	0.822 (0.278) *†§	0.571 (0.228) *†‡
		W→T	0.877 (0.277) ‡§	0.936 (0.316) ‡§	0.769 (0.310) *†§	0.650 (0.307) *†‡
Max Lumbar Flexion Angle	(deg)	T→W	40.9 (12.9)	40.8 (12.0)	41.1 (13.1)	39.4 (10.9)
		W→T	40.1 (10.8)	40.2 (13.8)	41.3 (12.8)	40.5 (11.2)
Max Lumbar Extension Angle #	(deg)	T→W	30.3 (14.3)	29.9 (12.3)	30.5 (13.0)	28.6 (10.9)
		W→T	31.2 (11.0)	29.4 (12.4)	29.9 (12.8)	27.4 (11.3)
Max Lumbar Bending Angle	(deg)	T→W ¶	7.2 (3.5)	6.3 (2.5)	6.9 (3.5)	6.1 (2.8)
		W→T	5.9 (2.9)	5.2 (2.6)	5.6 (2.2)	6.7 (3.1)
Max Lumbar Twisting Angle	(deg)	T→W	5.0 (4.0) ‡§	4.4 (3.1) ‡§	6.2 (3.4) *†	5.6 (3.0) *†
		W→T	4.8 (3.4) ‡§	5.4 (3.5) ‡§	5.9 (3.8) *†	5.5 (2.6) *†

* ($P < 0.05$) vs. 0° † ($P < 0.05$) vs. 45° ‡ ($P < 0.05$) vs. 90° § ($P < 0.05$) vs. 180° ¶ ($P < 0.05$) vs. W→T

T→W toilet to the wheelchair transfer W→T wheelchair to the toilet transfer

Positive values correspond to lumbar flexion

Table 9 – Effect of Transfer Direction and Wheelchair-to-Toilet Angle on Transferor Kinematics, Mean (SD)

Variable		Direction	Wheelchair-to-Toilet Angle 0°	45°	90°	180°
Max Lumbar Flexion Velocity #	(deg/s)	T→W	23.8 (11.0) §	22.0 (12.1)	20.2 (8.7)	17.3 (7.1) *
		W→T	19.5 (8.7)	20.8 (13.0)	20.4 (11.8)	22.4 (11.7) ¶
Max Lumbar Extension Velocity	(deg/s)	T→W ¶	19.4 (9.8) ‡	17.6 (9.4)	17.1 (10.4) *§	17.5 (5.9) ‡
		W→T	14.8 (8.6) ‡	15.5 (9.0)	13.4 (7.7) *§	17.9 (8.8) ‡
Max Bending Velocity	(deg/s)	T→W	15.5 (7.8)	14.3 (7.4)	15.7 (8.3)	13.8 (5.6)
		W→T	13.4 (7.7)	13.0 (8.2)	14.9 (11.3)	15.2 (6.4)
Average Bending Velocity	(deg/s)	T→W ¶	5.5 (2.2)	5.0 (2.3)	5.5 (2.6)	5.0 (2.1)
		W→T	5.0 (2.5)	4.3 (2.1)	4.4 (2.3)	4.9 (1.8)
Max Twisting Velocity	(deg/s)	T→W	10.1 (6.4) ‡§	9.6 (6.4) ‡§	11.5 (5.3) *†	12.2 (7.1) *†
		W→T	8.8 (4.9) ‡§	9.4 (6.0) ‡§	10.6 (6.7) *†	11.9 (7.5) *†
Average Twisting Velocity	(deg/s)	T→W ¶	3.2 (1.6) ‡§	3.2 (1.9) ‡§	4.0 (2.0) *†	3.9 (2.0) *†
		W→T	2.9 (1.6) ‡§	3.1 (2.0) ‡§	3.4 (1.9) *†	3.6 (1.7) *†
Rating of Perceived Exertion		T→W	10.8 (2.2) §	11.0 (2.1) §	11.2 (2.3) §	11.5 (2.1) *†‡
		W→T	10.8 (2.3) §	10.8 (2.4) §	10.9 (2.5) §	11.5 (2.2) *†‡

* ($P < 0.05$) vs. 0° † ($P < 0.05$) vs. 45° ‡ ($P < 0.05$) vs. 90° § ($P < 0.05$) vs. 180° ¶ ($P < 0.05$) vs. W→T
T→W toilet to the wheelchair transfer W→T wheelchair to the toilet transfer
($P < 0.05$) for wheelchair-to-toilet angle × direction of transfer interaction

Transferee Kinematics

The mean value of the maximal vertical acceleration of the transferee (i.e. the anthropometric dummy) during the assisted transfers was 0.38 G (SD = 0.22). Neither the wheelchair-to-toilet angle nor the direction of assisted transfer affected the acceleration of the dummy during the assisted transfers ($P > 0.05$). Characteristics of the transferor, namely body height, leg position during the transfer, and self-reported prior experience conducting assisted transfers, were also unrelated to the vertical acceleration experienced by the dummy ($P > 0.05$). The mean and standard deviation of the transferee's acceleration, blocked by the wheelchair-to-toilet-angle and the direction of assisted transfer, is listed in Table 10.

Table 10 – Effect of Transfer Direction and Angle on Transferee Acceleration, Mean (SD)

			Wheelchair-to-Toilet Angle			
Variable		Dir.	0º	45º	90º	180º
Transferee Acceleration	(G)	T→W	0.31 (0.23)	0.33 (0.23)	0.37 (0.27)	0.28 (0.15)
		W T	0.35 (0.25)	0.33 (0.24)	0.34 (0.18)	0.40 (0.21)

Characteristics of the Transferor as Predictors of Risk Factors for Lower Back Disorder

The transferor's choice of leg position, straddle vs. interlaced, was associated with the transferor's standing height and self-reported prior experience, yes vs. no, in conducting assisted transfers. Both a greater standing height and prior experience increased the odds that the transferor used the straddle leg position during assisted transfer ($P < 0.000$). A 1 cm increase in transferor's standing height increased the odds that the transferor used the straddle leg position over the interlaced leg position 1.14 fold (95% CI: 1.08 – 1.18 fold). Reporting prior experience conducting assisted

transfers increased a transferor's odds of using the straddle position 3.62 fold (95% CI: 1.78 – 7.39 fold) after accounting for the main effect of the transferor's standing height. The transferor's choice of leg position was not related to either the wheelchair-to-toilet angle or the direction of assisted transfer ($P > 0.05$).

Characteristics of the transferor were associated with the kinematic measures of lower back disorder risk, beyond the main effects of the wheelchair-to-toilet angle and the direction of assisted transfer. As a whole, the transferor's kinematic risk factors for lower back disorder were associated with his or her standing height and with the leg position used during the transfer (Table 11). The transferor's standing height was associated with nine of the fourteen risk factors analyzed. The transferor's leg position was associated with seven of the fourteen risk factors analyzed, and this effect interacted with the direction of assisted transfer for four of the seven factors. No interaction was observed between transferor standing height and transfer direction. The transferor's self-reported prior experience in conducting assisted transfers was associated only with the integrated load moment arm. Regression coefficients and standard errors for models used to predict the value of the transferor's kinematic risk factors for lower back disorder from the characteristics of the transferor are shown in Table 12.

Table 11 – P-Value for statistical confidence that the parameter affected kinematic risk factors for lower back disorder in the transferor.

Variable		Height	Height x Direction	Leg Position	Leg Position x Direction	Experience
Transfer Duration	Log (s)*	NS	NS	0.0006	0.0138	NS
Max Load Moment Arm	(m)	0.0002	NS	0.0076	0.0075	NS
Integrated Load Moment	(m•s)	NS	NS	0.0023	< 0.0001	0.0169
Max Lumbar Flexion Angle	(deg)	0.0004	NS	NS	NS	NS
Max Lumbar Extension Angle	(deg)	0.0001	NS	NS	NS	NS
Max Lumbar Bending Angle	(deg)	NS	NS	0.0018	NS	NS
Max Lumbar Twisting Angle	Log (deg)*	0.0085	NS	0.0215	0.0217	NS
Max Lumbar Flexion Velocity	Log (deg/s)*	NS	NS	NS	NS	NS
Max Lumbar Extension Velocity	Log (deg/s)*	NS	NS	0.0077	NS	NS
Max Bending Velocity	Log (deg/s)*	0.0013	NS	NS	NS	NS
Average Bending Velocity	Log (deg/s)*	0.0012	NS	NS	NS	NS
Max Twisting Velocity	Log (deg/s)*	< 0.0001	NS	NS	NS	NS
Average Twisting Velocity	Log (deg/s)*	0.0003	NS	NS	NS	NS
Rating of Perceived Exertion		NS	NS	NS	NS	NS

* Log = Natural Logarithm
NS = Not significant (P > 0.05)

The time required to conduct an assisted transfer was associated with an interaction between the transferor's leg position and the direction of transfer (P = 0.0138) after controlling for the main effects of the wheelchair-to-toilet angle. The median time required to conduct an assisted transfer from the toilet to the wheelchair using the straddle leg position was 16.1% less than for transfers in the same direction using the interlaced leg position (95% CI: 7.4% – 24.0%); 7.7% less than for transfers in the opposite direction using the straddle leg position (95% CI: 1.4% – 13.6%); and 12.3% less than for transfers in the opposite direction using the interlaced leg position (95% CI: 3.1% – 20.6%). The transferor's standing height and reported prior experience were unrelated to the time required for an assisted transfer after controlling for the wheelchair-to-toilet angle and the interaction between the direction of assisted transfer and the transferor's leg position (P > 0.05).

The maximum load moment arm experienced by the transferor was related to the transferor's standing height (P = 0.0002) and an interaction between transferor's leg position and the direction of assisted transfer (P = 0.0075) after controlling for the main effects of the wheelchair-to-toilet angle. A 1 cm increase in transferor's standing height was associated with a 0.72 cm increase in the maximum load moment arm experienced by the transferor (95% CI: 0.39 cm – 1.05 cm). The maximum load moment arm during assisted transfers from the toilet to the wheelchair for transferors using the interlaced leg position was 4.9 cm greater than during transfers using the straddle leg position in the same direction (P = 0.0076; 95% CI: 1.4 cm – 8.5 cm); 4.7 cm greater than during transfers in the opposite direction using the same leg position (P = 0.0004; 95% CI: 2.2 cm – 7.2 cm); and 4.8 cm greater than during transfers using the straddle leg position in the opposite direction (P = 0.0074; 95% CI: 1.4 cm – 8.2 cm). The transferor's reported prior experience was unrelated to the transferor's

maximum load moment arm ($P > 0.05$), after controlling for the wheelchair-to-toilet angle, the direction of transfer, the transferor's standing height, and the interaction between transfer direction and transferor's leg position.

The integrated load moment arm experienced by the transferor was related to the transferor's self-reported previous experience ($P = 0.0169$) and an interaction between the transferor's leg position and the direction of assisted transfer ($P < 0.0001$) after controlling for the main effects of the wheelchair-to-toilet angle. Transferors reporting prior experience conducting assisted transfers experienced a 0.215 m·s greater integrated load moment arm during assisted transfers than those reporting no prior experience ($P = 0.0169$; 95% CI: 0.045 m·s – 0.385 m·s). The integrated load moment arm during assisted transfers from the toilet to the wheelchair for transfers using the interlaced leg position was 0.149 m·s greater than during transfers in the opposite direction using the same leg position ($P = 0.0001$; 95% CI: 0.076 m·s – 0.222 m·s); and 0.161 m·s greater than during transfers in the same direction using the straddle leg position ($P = 0.0023$; 95% CI: 0.060 m·s – 0.262 m·s). In contrast, the integrated load moment arm during assisted transfers from the toilet to the wheelchair using the straddle leg position was 0.097 m·s smaller than during transfers in the opposite direction using the same leg position ($P = 0.0063$; 95% CI: 0.029 m·s – 0.165 m·s). The standing height of the transferor was unrelated to the integrated load moment arm ($P > 0.05$) after controlling for the wheelchair-to-toilet angle, the transferor's reported prior experience, and the interaction between the direction of assisted transfer and the transferor's leg position.

The maximum lumbar flexion angle exhibited by the transferor was directly related to the transferor's standing height ($P = 0.0004$) after controlling for the main

effects of the wheelchair-to-toilet angle and the direction of assisted transfer. A 1 cm increase in standing height was associated with a 0.785º increase in maximum lumbar flexion (95% CI: 0.396º – 1.173º). The transferor's leg position and reported prior experience were unrelated to the transferor's maximum angle of lumbar flexion after controlling for the wheelchair-to-toilet angle, the direction of assisted transfer, and the transferor's standing height ($P > 0.05$).

The maximum lumbar extension angle exhibited by the transferor was directly related to the transferor's standing height ($P = 0.0001$) after controlling for the main effects of the wheelchair-to-toilet angle and the direction of assisted transfer. A 1 cm increase in standing height was associated with a 0.852º decrease in maximum lumbar extension (95% CI: 0.484º – 1.220º). The transferor's leg position and reported prior experience were unrelated to the transferor's maximum angle of lumbar extension after controlling for the wheelchair-to-toilet angle, the direction of assisted transfer, and the transferor's standing height ($P > 0.05$).

The maximum lumbar bending angle exhibited by the transferor was associated with the transferor's leg position ($P = 0.0018$) after controlling for the main effects of the wheelchair-to-toilet angle and the direction of assisted transfer. Assisted transfers using the straddle leg position had maximum lumbar bending angles 1.5º smaller than transfers using the interlaced leg position (95% CI: 0.58º – 2.4º). The transferor's standing height and reported prior experience were unrelated to the maximum angle of lumbar bending after controlling for the wheelchair-to-toilet angle, the direction of assisted transfer, and the transferor's leg position ($P > 0.05$).

The maximum lumbar twisting angle exhibited by the transferor was inversely related to the transferor's standing height ($P = 0.0085$) and demonstrated an interaction between the transferor's leg position and the direction of assisted transfer

(P = 0.0217) after controlling for the main effects of the wheelchair-to-toilet angle. A 1 cm increase in transferor standing height was associated with a 15.4% decrease in the median maximum lumbar twisting angle (95% CI: 2.2% – 107.6%). The median maximum lumbar twisting angle during transfers from the toilet to the wheelchair for transferors using the interlaced leg position was 23.1% lower than during transfers in the same direction using the straddle leg position (P = 0.0215; 95% CI: 4.2% – 38.3%); and 16.9% lower than during transfers in the opposite direction using the same leg position (P = 0.0257; 95% CI: 2.5% – 29.2%). The transferor's reported prior experience was unrelated to the transferor's maximum twisting angle (P > 0.05) after controlling for the wheelchair-to-toilet angle, the direction of transfer, the transferor's standing height, and the interaction between transfer direction and transferor's leg position.

The transferor's maximum lumbar flexion velocity was not related to the transferor's standing height, leg position, and reported prior experience (P > 0.05) after controlling for the main effects of the wheelchair-to-toilet angle and the direction of assisted transfer.

The maximum lumbar extension velocity exhibited by the transferor was related to the transferor's leg position (P = 0.0077) after controlling for the main effects of the wheelchair-to-toilet angle and the direction of assisted transfer. Transferors using the straddle leg position had a 21.8% lower median maximum lumbar extension velocity than transferors using the interlaced leg position (95% CI: 6.6% – 34.5%). The transferor's standing height and reported prior experience were unrelated to the transferor's maximum lumbar extension velocity after controlling for the wheelchair-to-toilet angle, the direction of assisted transfer, and the transferor's leg position (P > 0.05).

The maximum lumbar bending velocity exhibited by the transferor was inversely related to the transferor's standing height ($P = 0.0013$) after controlling for the main effects of the wheelchair-to-toilet angle and the direction of assisted transfer. A 1 cm increase in standing height associated with an 8.4% decrease in median maximum lumbar bending velocity (95% CI: 2.5% – 27.9%). The transferor's leg position and reported prior experience were unrelated to the transferor's maximum lumbar bending velocity after controlling for the wheelchair-to-toilet angle, the direction of assisted transfer, and the standing height of the transferor ($P > 0.05$).

The average lumbar bending velocity exhibited by the transferor was inversely related to the transferor's standing height ($P = 0.0012$) after controlling for the main effects of the wheelchair-to-toilet angle and the direction of assisted transfer. A 1 cm increase in standing height was associated with a 7.5% decrease in median average lumbar bending velocity (95% CI: 2.4% – 23.0%). The transferor's leg position and reported prior experience were unrelated to the transferor's average lumbar bending velocity after controlling for the wheelchair-to-toilet angle, the direction of assisted transfer, and the standing height of the transferor ($P > 0.05$).

The maximum lumbar twisting velocity was inversely related to the transferor's standing height ($P < 0.0001$) after controlling for the main effects of the wheelchair-to-toilet angle and the direction of assisted transfer. A 1 cm increase in standing height was associated with a 22.9% decrease in median maximum twisting velocity (95% CI: 6.9% – 76.1%). The transferor's leg position and reported prior experience were unrelated to the transferor's maximum lumbar twisting velocity after controlling for the wheelchair-to-toilet angle, the direction of assisted transfer, and the transferor's standing height ($P > 0.05$).

The average lumbar twisting velocity was inversely related to the transferor's standing height ($P < 0.0003$) after controlling for the main effects of the wheelchair-to-toilet angle and the direction of assisted transfer. A 1 cm increase in standing height was associated with a 16.8% decrease in median average twisting velocity (95% CI: 4.3% – 66.3%). The transferor's leg position and reported prior experience were unrelated to the transferor's average lumbar twisting velocity after controlling for the wheelchair-to-toilet angle, the direction of assisted transfer, and the transferor's standing height ($P > 0.05$).

The transferor's rating of perceived exertion (RPE) was not related to the transferor's standing height, leg position, and reported prior experience ($P > 0.05$) after controlling for the main effects of the wheelchair-to-toilet angle and the direction of assisted transfer.

Table 12 – Regression coefficients and standard errors for models to predict the values of kinematic risk factors for lower back disorder from characteristics of the transferor, after accounting for the main effects of the wheelchair-to-toilet angle (not shown) and the direction of assisted transfer.

		Height (m)	Leg Position (Straddle)	Direction (W T)	Leg Position (Straddle) x Direction (W T)	Experience (Yes)
Transfer Duration	Log (s)*	NS	-0.176 (0.051)	-0.045 (0.037) †	0.125 (0.050)	NS
Max Load Moment Arm	(m)	0.720 (0.164)	-0.049 (0.018)	-0.047 (0.013)	0.048 (0.018)	NS
Integrated Load Moment Arm	(m•s)	NS	-0.161 (0.052)	-0.149 (0.038)	0.246 (0.052)	0.215 (0.084)
Max Lumbar Flexion Angle	(deg)	78.464 (19.204)	NS	NS	NS	NS
Max Lumbar Extension Angle ‡	(deg)	85.203 (18.158)	NS	NS	NS	NS
Max Lumbar Bending Angle	(deg)	NS	-1.500 (0.475)	-0.833 (0.308)	NS	NS
Max Lumbar Twisting Angle	Log (deg)*	-2.735 (0.964)	0.263 (0.113)	0.186 (0.083)	-0.263 (0.113)	NS
Max Lumbar Extension Velocity	Log (deg/s)*	NS	-0.229 (0.095)	-0.186 (0.057)	NS	NS
Max Bending Velocity	Log (deg/s)*	-2.124 (0.594)	NS	NS	NS	NS
Average Bending Velocity	Log (deg/s)*	-2.012 (0.554)	NS	-0.140 (0.045)	NS	NS
Max Twisting Velocity	Log (deg/s)*	-3.132 (0.593)	NS	NS	NS	NS
Average Twisting Velocity	Log (deg/s)*	-2.822 (0.678)	NS	-0.094 (0.033)	NS	NS

Leg Position: Straddle leg position = 1; Interlaced leg position = 0
Direction: W T (wheelchair to the toilet transfer) = 1; T W (toilet to wheelchair transfer) = 0
* Log = Natural Logarithm
† Direction coefficient not statistically significant (P > 0.05)
‡ Positive values correspond to lumbar flexion

Discussion

Spatial Requirements for Assisted Toilet Transfers

Wheelchair users face numerous barriers during commercial air travel. The general lack of accessible lavatories on board commercial passenger aircraft is one such barrier. Current ACAA lavatory accessibility regulations require only twin-aisle aircraft to have an accessible lavatory on board. The effect of this has been to exempt all single-aisle passenger aircraft, approximately 70% of the total domestic passenger air service (U.S. Bureau of Transportation Statistics, 2006), from the accessible lavatory requirement (Strickman 2005). Absent regulations, airlines have been reluctant to include a lavatory that can accommodate an assisted toilet transfer on board commercial passenger aircraft. This reluctance is due, in part, to the perceived spatial requirements for wheelchair-accessible lavatories and the increased spatial requirements of existing designs. While wheelchair-accessible lavatories are generally perceived to have greater spatial requirements than non-accessible lavatories, the spatial requirements of assisted toilet transfers and the factors that affect them are poorly understood.

Only one previous study has examined the spatial requirements of assisted toilet transfers (Warren and Valois 1991). That study reported the minimum rectangular spatial footprint required for an assisted toilet transfer. Based on these findings, it has been suggested that the increased lavatory dimensions required to successfully accommodate assisted toilet transfers would require the removal of a row of three coach seats. In 1993, it was estimated that these seats had an approximate value of $300,000 in annual commercial aircraft revenue (U.S. Department of Transportation 1993). One limitation to this previous study is that it

only investigated the spatial requirements of 0º and 90º assisted toilet transfers; the spatial volume required for assisted transfers at wheelchair-to-toilet angles of 45º and 180º were not investigated. Furthermore, the previous study only reported the spatial requirements of assisted transfers as the minimum rectangular spatial area required to conduct an assisted transfer. However, while a rectangular shape can obviously be fit around any boundary, one might reasonably surmise that the precise shape utilized during an assisted toilet transfer is most likely not rectangular. It is believed that through a more thorough understanding of the spatial requirements of assisted toilet transfers, lavatories can be designed that are compatible with spatially constrained environments and that provide sufficient spatial volume to conduct an assisted toilet transfer.

The goal of the present study was thus to improve the understanding of the effect of the wheelchair-to-toilet angle on the spatial volume required for an assisted toilet transfer and on the transferor's associated risk of lower back disorder. Twenty-nine participants were motion captured while performing assisted toilet transfers bi-directionally at wheelchair-to-toilet angles of 0º, 45º, 90º, and 180º. The transferors were verbally encouraged to use as little space as safely possible and to attempt to stay within one of two hypothetical lavatory boundaries that had been taped to the floor. However, the spatial volume used by each of the transferors was not physically constrained. It was believed that by doing this, the resulting motion of the transferor would strike an "acceptable" balance between minimizing the spatial volume they used and minimizing their risk of lower back injury. A novel, three-dimensional computer-based spatial mapping technique was developed to compute the spatial volume requirements of tasks from motion capture data. Using this technique, the

spatiotemporal volume employed in conducting assisted transfers at each of the four experimental wheelchair-to-toilet angles was computed.

The spatial volume used during the assisted toilet transfers was stratified as percentile spatial volumes representing the total percentage of time that a given volume was used across participants. Spatiotemporal maps were reported for the 95th percentile spatial area, 97.5th percentile area, and the 100th percentile area (Figures 6 – 14; high resolution color spatial maps included as Appendix B). The 100th percentile spatial area describes the total spatial volume used across all transferors over the entire experiment, i.e. spatial area used by even a single transferor for even a single frame of motion capture (1/60th of a second) would be included in the 100th percentile spatial area. The 100th percentile spatial area thus logically does not describe the true minimum volume needed by a transferor to conduct assisted transfers, as it is the union of both this theoretical minimum volume and other, nonessential space used when the transferor moved outside of this volume. Therefore, the 95th percentile spatial area, comprising the spatial area occupied 5% or more of the time, was used instead to represent the spatial requirements of assisted transfers. It is believed that the 95th percentile spatial area encompasses the functional spatial volume required by almost all individuals for almost all assisted transfers, without including the volume described by extraneous transferor movements. Notably, there was not a large difference between the 95th and 97.5th spatial areas, suggesting that the precise choice of criterion threshold was not critical in determining the spatiotemporal area required for assisted toilet transfers.

Previous research has found that, at a wheelchair-to-toilet angle of 0^{o}, a minimum area of 1.07 m x 1.14 m is required for an assisted toilet transfer and that, at

an angle of 90º, the minimum area required is 1.17 m x 1.22 m (Warren and Valois 1991). The present results are consistent with the prior findings. Fitting a rectangular footprint to the 95th percentile spatial area at the 0º wheelchair-to-toilet angle, a 1.07 m x 1.24 m spatial area (width x depth) was required; at the 45º wheelchair-to-toilet angle, a 1.20 m x 1.24 m spatial area (width x depth) was required; at the 90º wheelchair-to-toilet angle, a 1.29 m x 1.25 m spatial area (width x depth) was required; and at the 180º wheelchair-to-toilet angle, a 1.09 m x 1.53 m spatial area (width x depth) was required. Similar to the previous findings, the rectangular area required for a toilet transfer tended to increase for a larger wheelchair-to-toilet angle (Figures 6 – 14). Transfers at the 0º wheelchair-to-toilet orientation required the least absolute area, with both the smallest width and depth of any orientation. Transfers at the 45º and 90º orientations required a rectangular area with a similar depth and greater width than at the 0º orientation. Transfers at the 180º orientation required the greatest rectangular area, having a width similar to the 0º orientation and the largest depth of any orientation.

A typical airline lavatory measures approximately 1 m x 1.2 m. Based upon this, a typical airline lavatory has sufficient total spatial volume to support the 95th percentile transfer volume required at the 0º transfer orientation, but not at the other wheelchair-to-toilet angles tested. However, in addition to providing the volume required for an assisted transfer, accessible airplane lavatories must also fit lavatory fixtures within the lavatory volume. Based solely on the preceding analysis, the total volume required for a lavatory supporting assisted transfers at the 0º transfer orientation would exceed the dimensions of a typical aircraft lavatory, as lavatory fixtures would have to be placed outside of the rectangular spatial volume required for assisted transfers so as to not impede the kinematics of assisted toilet transfers. This

is consistent with previous conclusions that the inclusion of an accessible aircraft lavatory will result in a loss of seating capacity.

In keeping with this, and in contrast to both the current and previous findings, an ergonomic investigation of caregivers who routinely conducted assisted toilet transfers in a nursing home environment reported that lavatories measuring 1.4 m x 1.5 m in area provided insufficient space to conduct an assisted toilet transfer with the wheelchair in the lavatory (Owen and Garg 1991). The caregivers were reported to position the wheelchair in the lavatory doorway and then manually carry the transferee between the wheelchair and toilet. Grab bars were reportedly present; however, it is unclear from the published report to what extent lavatory fixtures, such as sinks, were also present within the lavatory volume. If lavatory features such as sinks were placed within the lavatory volume, the total spatial volume available for assisted transfers would have been less than the total spatial dimensions of the lavatory. This may explain the differences between studies. Logically, if lavatory fixtures are placed within the accessible lavatory volume, they should be positioned such that the spatial volume needed to conduct an assisted toilet transfer is not impeded. Ideally, lavatory fixtures could be positioned to facilitate assisted transfers.

The dimensions required to conduct an assisted toilet transfer have thus far been discussed with respect to a rectangular bounding area. However, the results of the spatiotemporal mapping clearly show that the spatial volume required for an assisted toilet transfer is not rectangular and changes in both shape and dimension as a function of height. This suggests that lavatory fixtures could potentially be incorporated, at least partially, within the bounding rectangle of the transfer volume, if their placement was made in a manner that did not impede the kinematics of the transfers.

As determined in the present study, the spatial volume used during an assisted toilet transfer was a function of the physical dimensions of the transferee, transferor, and wheelchair, as well as the wheelchair-to-toilet angle. Spatiotemporal maps taken across the assisted transfer volume showed that the spatial volume used during the transfers differed between wheelchair-to-toilet orientations and also contained a fairly large variability across transfers. This is particularly visible with regards to the absolute position of the wheelchair at each of the transfer orientations and in the foot and leg placement of the transferors. Differences in the body dimensions of the transferors could logically have been responsible for a component of this variability. Based upon these results, lavatories designed to support an assisted transfer at a given wheelchair-to-toilet angle must thus support a variety of wheelchair placements and transferor foot placements in order for the lavatory to be accessible. Furthermore, if lavatory fixtures are placed partially within the bounding rectangles identified in the present study, they must be placed such that they do not impinge upon the transfer kinematics of most transferors.

Across all experimental participants, the wheelchair-to-toilet angle appeared to directly affect the portion of the rectangular volume used during assisted toilet transfers. The spatial maps for the 0º wheelchair-to-toilet angle suggest that a volume along the right side of the lavatory, diagonally opposite the toilet, in Figures 6 – 14 was relatively unused and could potentially serve as a lavatory fixture location without requiring altered transfer kinematics. At a 45º wheelchair-to-toilet angle, the unused volume appears similar to that at 0º. However, unlike for the 0º wheelchair-to-toilet angle, the diagonal placement of the wheelchair at 45º blocked the area behind the wheelchair from general use. Thus, for the 45º orientation, although the spatial volume behind the wheelchair is not used during assisted transfers, it is also not

readily accessible. As a consequence, lavatory features needed during lavatory use cannot be placed there. Assisted transfers at the 90º wheelchair-to-toilet angle appeared to leave the volume along the wall immediately to the right of the toilet in Figures 6 – 14 unused. Based upon this, lavatories designed to specifically accommodate the 90º wheelchair-to-toilet angle could place lavatory features, such as a sink, adjacent to the toilet to facilitate their use while remaining seated on the toilet. The spatial volume required for transfers at a 180º wheelchair-to-toilet angle appeared to extend into the space outside the theoretical boundaries of the lavatory (e.g. into the aisle of the aircraft) to a greater extent than any of the other transfers. However, the 180º transfer also visually appears to use the least volume within the boundaries of the theoretical lavatory. Designing for a 180º wheelchair-to-toilet angle thus appears to enable placement of lavatory features both diagonally across from the toilet, similar to the 0º and 45º transfer orientations, and immediately adjacent to the toilet, similar to the 90º transfer orientation.

For transfers at the 180º wheelchair-to-toilet angle, the wheelchair was placed directly opposite the toilet and extending slightly outside of the theoretical lavatory volume. This wheelchair placement suggests that the spatial volume required for a 180º transfer could be partially provided by temporarily utilizing space in the aisle of the aircraft. A hypothetical assisted transfer session could be conducted as follows: the wheelchair would be moved into position for the transfer; the traveler would be transferred from the wheelchair to the toilet; the wheelchair would be moved out into the aisle; the lavatory door would be closed, providing the privacy required for lavatory use. From a spatial consumption point of view, this scenario effectively utilizes existing space and would result in the smallest total lavatory spatial volumes. However, while compelling from a spatial consumption standpoint, this transfer

scenario has a number of drawbacks. Moving the wheelchair into the aisle during lavatory use could inhibit movement along the aisle by both flight attendants and passengers for the duration of the lavatory use; assisted toileting has been reported to require in excess of four minutes (Owen and Garg 1991). A possible remedy could be to place the accessible lavatory in the aft-most section of the airplane, where use of the space outside the lavatory would not inhibit movement through the aisle. Even if the temporary utilization of aisle space did not impede the mobility of others, the use of the aisle space during the initial stages of assisted toileting could sharply reduce the level of privacy offered during lavatory usage. Curtains might partially mitigate the reduction in privacy. However, even with curtains, aisle-based assisted transfers would offer significantly less privacy than transfers conducted in a totally enclosed lavatory. This reduced level of privacy could potentially render the lavatory inaccessible, even if the spatial volume is sufficient, if it created psychological barriers for either the transferor or transferee.

Taken together, the spatial consumption results of this study suggest that in designing accessible lavatories for use in constrained environments, such as passenger aircraft, the total spatial volume required for the lavatory can be minimized by optimizing the lavatory's layout to support assisted transfers at a single optimal wheelchair-to-toilet transfer angle. The present results importantly provide design data upon which to base new designs for accessible lavatories.

Risk of Injury during Assisted Toilet Transfers

In addition to providing sufficient space to conduct an assisted toilet transfer, a truly accessible lavatory should, to the extent possible, mitigate the risk of injury to the transferor and transferee. Of particular concern is the risk of lower back injury to the

transferor. Lower back disorders are very common. Approximately 80% of individuals are estimated to experience lower back disorder at some time during their lives (Marras 2000). However, while back injuries are nearly ubiquitous, 50% to 70% of the cases are idiopathic; the anatomical origins cannot be diagnosed (Punnett *et al.* 1991, Marras 2000). Biomechanically, it is hypothesized that the majority of lower back disorder cases are a result of chronic damage to the vertebral endplates induced by high compressive forces generated by the internal musculature during lifting (Lotz *et al.* 1998, Marras 2000).

The biomechanics of lifting have been extensively studied in an attempt to understand the etiology of lower back disorder. Risk factors for lower back disorder have been experimentally identified and risk models have been developed and validated through studies of occupational lifting and the associated incidence of lower back disorder (Marras *et al.* 1995, McGill *et al.* 1996, Zurada *et al.* 1997, Norman *et al.* 1998, Granata and Marras 1999, Marras *et al.* 2000a). Recognized risk factors for lower back disorder include large magnitudes of: maximum load moment (Chaffin and Park 1973, Garg *et al.* 1992, Marras *et al.* 1995, Davis *et al.* 1998); integrated load moment (Norman *et al.* 1998); maximum angles and velocities of lumbar flexion, extension, bending, and twisting (Punnett *et al.* 1991, Marras *et al.* 1995, Granata and Marras 1999); and the average angular velocities of lumbar twisting and bending (Punnett *et al.* 1991, Marras *et al.* 1995, Granata and Marras 1999).

Occupations that involve routine engagement in manually-performed assisted patient transfers have some of the highest incidence of lower back disorder (Garg *et al.* 1992, Marras *et al.* 1999, Barondess *et al.* 2001). Based upon such epidemiological data and experimental studies, the biomechanics of manually-performed assisted patient transfers are recognized to place the transferor at high risk

for the development of lower back disorder (Owen and Garg 1991, Garg and Owen 1992, Garg *et al.* 1992, Marras *et al.* 1999, Hess *et al.* 2007). Assisted toilet transfers of 25^{th} – 90^{th} percentile individuals has been estimated to expose the transferor to spinal compression and shear forces at or in excess of the thresholds at which NIOSH reports spinal damage to be initiated (Owen and Garg 1991, Garg and Owen 1992, Garg *et al.* 1992, Marras *et al.* 1999).

Few studies have examined the biomechanics of assisted transfers between a wheelchair and toilet. Prior studies have primarily investigated the effect of transfer technique on the transferor's injury risk and perceived exertion while conducting assisted toilet transfers (Owen and Garg 1991, Garg and Owen 1992, Garg *et al.* 1992, Marras *et al.* 1999). These studies have largely suggested that manually-performed assisted transfers place the transferor at a high risk for lower back disorder but also that the use of assistive devices, such as a walking belt, can reduce the transferor's relative risk of lower back disorder. No prior work, however, has investigated how environmental factors affect the injury risk during assisted toilet transfers. If accessible lavatories are to be designed for constrained environments that support only a single "optimal" angle of assisted transfer, it is essential that the effects of the wheelchair-to-toilet angle on the transferor's kinematic risk factors for low back disorder be understood.

At the outset, it was hypothesized that increases in the wheelchair-to-toilet angle would alter the transferors' lumbar kinematics during the assisted toilet transfers in a manner consistent with a greater risk of lower back disorder. The findings of this study do not support this hypothesis. Of the fourteen risk factors for lower back disorder analyzed, five had a direct relationship with the transfer angle: transfer duration, all measures of lumbar twisting (maximum angle, maximum

velocity, and average velocity), and the transferor's rating of perceived exertion. However, the transferors' maximum lumbar flexion, extension, and bending angles were not affected by the wheelchair-to-toilet angle, nor were their maximum lumbar flexion and bending velocities. Furthermore, in direct contrast to the proposed hypothesis, risk factors relating to the transferor's maximum load moment arm, integrated load moment arm, and extension velocity had an inverse relationship with the wheelchair-to-toilet angle.

The total time required for an assisted transfer is believed to be an injury risk factor for both the transferee and transferor. Longer transfer durations require the transferor to have greater muscular endurance to avoid injury and have the potential to expose the spine to damaging loads for longer periods of time. In unstable environments, like an airplane, longer transfer durations also increase the chance that an unexpected perturbation could arise and result in a catastrophic loss of balance. The total time required to transfer the transferee between the toilet and wheelchair was directly related to the wheelchair-to-toilet angle; greater angles required greater time. This is because, in using the pivot transfer technique (Appendix A), larger transfer angles required the transferor to move the transferee through a longer distance. Using transfer duration as an injury risk factor for both the transferor and transferee, the greater duration of the 180º transfer would suggest elevated injury risk. However, the mean difference in transfer duration between the 180º wheelchair-to-toilet angle and the 0º orientation was less than 1 second. This suggests that while differences in transfer duration were observed, the differences did not notably affect the transferor's and transferee's risk of injury.

The mean transfer duration ranged from 1.8 to 2.6 s across conditions, whereas it has been reported that moving the transferee to the toilet prior to toileting

requires the transferor to support at least part of the body weight of the transferee for approximately 32 s (Owen and Garg 1991). The large difference in transfer duration between the current work and the prior ergonomic evaluation suggests that, in the prior evaluation, there were tasks associated with the assisted toilet transfer other than the transfer itself for which support was provided. The extent to which these "associated tasks" could be conducted in a manner that does not require lifting by the transferor is unknown. However, it does seem logical to assume that any increase in the transfer duration due to "associated tasks" would be independent of the wheelchair-to-toilet angle. This would suggest that any associated increase in the transferor's and transferee's risk of injury would be the same across all wheelchair-to-toilet angles.

The maximum load moment arm describes the maximum horizontal distance between the transferor's L_3L_4 joint and the dummy's head-arms-torso center of mass. The maximum load moment arm is a key component in the calculation of the maximum load moment, a major risk factor for lower back disorder. The transferor was found to move progressively closer to the transferee as the wheelchair-to-toilet angle increased above 45º. This finding is consistent with previous research in which it was found that people moving boxes positioned at a 90º angle from them had a smaller horizontal distance between the center of mass of the load and the L_4L_5 vertebral joint than when lifting boxes positioned at 0º and at 45º (Banaag 1988). The previous research further found that the maximum acceptable weight that could be repeatedly lifted decreased as the lifting angle increased. This suggests that while assisted transfers at wheelchair-to-toilet angles of 90º and 180º had lower peak load moment arms than at 0º and 45º, the maximum acceptable weight that could be transferred at these larger angles might be lower. It is unclear what mechanism was

responsible for the transferor's decrease in maximum load moment arm at larger wheelchair-to-toilet angles. It could be that greater pre-rotation of the dummy on the seat or toilet prior to transferring allowed the transferor to achieve a closer body position as the wheelchair-to-toilet angle increased. Another possible hypothesis is that the transferors' conscious or unconscious perception of an assisted transfer's lower back disorder risk could affect their trunk kinematics and, thus, their overall lower back disorder risk. This hypothesis would support the observation by Hess *et al.* (2007) that transferors conducting assisted bed-to-wheelchair transfers reduced their maximum trunk flexion, a lower back disorder risk factor, in response to increased transferee weight. However, it is currently unknown to what extent the transferor's perception of a lift's injury risk affects his or her lifting kinematics, nor the extent to which transferors would alter their kinematics if the risks were brought to their attention.

The maximum load moment exerted on the transferor by the transferee during an assisted transfer is a risk factor for lower back disorder, as it is directly related to the maximum spinal compressive force experienced by the transferor (Chaffin and Park 1973, Marras *et al.* 1995, Norman *et al.* 1998). Maximum load moment is one of five predictors of the probability of being at high risk for lower back disorder in a logistic regression model developed by Marras *et al.* (1995). Absent kinetic measurements, it was assumed that the force exerted on the transferor by the dummy during lifting was equal to the weight of the dummy's head-arms-torso, a constant 437.5 N, over the duration of the lift. Based on this assumption, the logistic regression model of Marras *et al.* (1995) was used to estimate the effect of the mean differences in maximum load moment arm between wheelchair-to-toilet angles on the transferor's probability of being at high risk for lower back disorder. The model

predicts that the increase in maximum load moment arm between the 0º and 90º wheelchair-to-toilet angles increased the transferors' odds of being at high risk of lower back disorder by a factor of 1.68. This model also predicts that the increases in maximum load moment arm for the 0º, 45º, and 90º wheelchair-to-toilet angles relative to the 180º orientation increased the transferors' respective odds of being at high risk of lower back disorder by factors of 14.9, 15.6, and 9.3, respectively. Based purely on the estimated load moment, the 180º transfer is predicted to have placed the transferor at the lowest risk of developing lower back disorder. Nevertheless, the model estimates that the load moment experienced at the 180º transfer is still dangerous. The model estimates that the probability of being at high risk for lower back disorder during the 180º transfer was 0.968 (SD 0.043). Based upon this, it is estimated that only 1 out of approximately every 31.3 individuals conducting the 180º transfer are at a low risk for lower back disorder. This suggests that, ultimately, a "no-lift" solution to toilet transfers is needed.

The integrated load moment, a measure of cumulative loading is recognized to describe a component of lower back disorder risk that is independent from that described by peak loading or maximum load moment (Norman *et al.* 1998). Kinetic data were not captured for the present task as part of this study, so the integrated load moment arm, the product of the duration of the assisted transfer and the mean load moment arm, was used as a relative measure of the cumulative loading. Based on this, it might be expected that the previously identified relationship between the wheelchair-to-toilet angle and the assisted transfer duration would also be observed with the integrated load moment arm. However, in contrast to transfer duration, where a direct relationship with angle occurred, the integrated moment arms at the 0º, 45º, and 90º wheelchair-to-toilet angles were found to be greater than the integrated

moment arm for transfers at the 180º wheelchair orientation. This implies that the average load moment arm experienced by the transferor over the duration of the 180º transfer was significantly smaller than that experienced at the other transfer angles. These findings combined with the aforementioned results for the maximum load moment arm suggest that the 180º transfer exposes the transferor to a lower peak spinal compression and a lower cumulative spinal compression, despite the fact that the 180º transfer requires the longest transfer duration. This would suggest that transferors were at a lesser risk for lower back disorder when conducting the 180º transfer than when conducting assisted transfers at the 0º, 45º, and 90º orientations.

The wheelchair-to-toilet angle directly affected the transferor's maximum lumbar twisting angle and the maximum and average twisting velocity. Larger magnitudes and velocities of lumbar rotation in flexion-extension, bending, and twisting during lifting tasks are recognized as risk factors for lower back disorder, particularly when they occur in combination (Punnett *et al.* 1991, Marras *et al.* 1995). Studies of dynamic lifting have found that twisting or bending significantly elevate spinal compression over that during lifts restricted to the sagittal-plane by increasing co-contraction of the trunk musculature (Davis and Marras 2000). In the present study, all measures of lumbar twisting were slightly greater for assisted transfers at the 90º and 180º wheelchair-to-toilet angles than at the 0º and 45º orientations. Nevertheless, the small magnitudes of the differences in the maximum twisting angle and velocities across the wheelchair-to-toilet angles strongly suggests that the effect of the wheelchair-to-toilet angle on these risk factors did not notably alter the transferors' risk of lower back disorder. The effect of the differences in the transferor's lumbar twisting, across wheelchair-to-toilet angles, on the transferors' odds of being at high risk for lower back disorder was estimated using the logistic

regression model developed by Marras *et al.* (1995). The maximum difference in the absolute magnitude of lumbar twisting occurred between the 0º and 90º orientations. This difference, 1.15º, is estimated to result in a 1.12-fold elevation in the odds of the transferor being at high risk for lower back disorder for the 90º orientation compared to the 0º orientation. The maximum difference in both maximum and average twisting velocity occurred between the 180º and 0º orientations. These differences in twisting velocity, 2.6 deg/s and 0.7 deg/s, respectively, are estimated to elevate the transferor's odds of being at high risk for lower back disorder 1.04- and 1.09-fold for the 180º orientation compared to the 0º orientation. Furthermore, considering the wheelchair-to-toilet angle did not affect any measure of lumbar bending (i.e. maximum angle, maximum velocity, and average velocity), it appears that the wheelchair-to-toilet angle has only a marginal effect on the lumbar angular kinematics that influence the transferor's risk of lower back disorder.

The lack of a large effect of the wheelchair-to-toilet angle on the transferor's peak lumbar motion is surprising, as it means that the transferor's lumbar motion was essentially unaffected by the 180° range of wheelchair-to-toilet angles. The marginal effect of the wheelchair-to-toilet angle on the transferor's twisting kinematics was likely a direct result of the pivot transfer technique used. Prior to the experiment, all transferors received instruction on the pivot transfer technique, using both the interlaced and straddle leg positions (Appendix B). Transferors were encouraged to pre-rotate the dummy to minimize the total bending and twisting required, orient their body along the centerline of the transfer angle, and keep their lumbar spine static while rotating primarily at the hips and ankles. The results suggest that this technique effectively mitigated the twisting that would otherwise have been required at the more extreme 90º and 180º wheelchair-to-toilet angles.

Transferors were discouraged from carrying the dummy. Carrying might also have allowed transferors to reduce their lumbar twisting. Caregivers in assisted living environments have reportedly carried the transferee when the wheelchair could not be positioned in close proximity to the toilet (Owen and Garg 1991). Some designs for "accessible lavatories" require the transferor to elevate transferees to a standing position and then spin/carry them through a 180º rotation before placing them on the toilet. It was, however, hypothesized that such transfers would increase the risk of injury to both the transferor and transferee in excess of any benefit derived from a reduction in lumbar twisting. The act of lifting alone has been found to reduce the transferor's ability to avoid a fall in response to external perturbation (Oddsson *et al.* 1999). Carrying is believed to be even more dangerous, as stepping reduces the transferor's base of support while, at the same time, lifting has increased their sensitivity to an external perturbation. Based upon this, all transfers conducted as part of this study used a pivot transfer; transferors rotated their feet but did not step or carry. This is important to keep in mind in interpreting the results of the present study, particularly with respect to the 180° transfers.

In addition to the wheelchair-to-toilet angle, the direction of assisted transfer affected the transferor's kinematic risk factors for lower back disorder. Specifically, the direction of assisted transfer affected the transferor's maximum load moment arm, maximum lumbar bending angle, maximum lumbar extension velocity, and the average lumbar bending and twisting velocities. For each of these risk factors for lower back disorder, assisted transfers from the toilet to the wheelchair resulted in greater values than transfers from the wheelchair to the toilet. This suggests that, despite the fact that the experimental lavatory was unconstrained, an inherent asymmetry exists between the transfers in the two directions. One factor that likely

contributed to this asymmetry is that the seat height of the toilet was 4 cm lower then the wheelchair seat height. Assisted transfers from the wheelchair to the toilet thus resulted in a net lowering of the dummy by 4 cm, whereas transfers in the opposite direction resulted in a net lifting. While small, this environmental difference in seat height could have, by itself, affected the kinematics associated with the assisted transfer. Previous research has found that lowering strength is approximately 50% greater then lifting strength and that, for a given weight, lowering is associated with greater spinal compression and lower shear forces than lifting (Davis *et al.* 1998).

Beyond environmental asymmetries, previous research has suggested that factors related to the transferors themselves affect the kinematics of transfers in different directions. In this study, the side of the transferee from which the assisted transfers were conducted was fixed across participants to simplify the spatial map calculations. During wheelchair-to-toilet transfers, the dummy was transferred to its left at the 0°, 45°, and 90° angles and to its right at the 180° angle. Toilet-to-wheelchair transfers were conducted in the opposite direction. In a previous study, transferors conducting assisted transfers from the left side of the transferee experienced greater spinal compression than those lifting from the right (Marras *et al.* 1999). It was also reported that some transferors expressed a preferred side from which to conduct an assisted transfer. These differences were attributed to differences in muscle cross-sectional area, trunk and hip kinematics, and patterns of muscle activation (Marras *et al.* 1999). Logically, dominant arm neuromuscular control factors could also have been a factor. However, if factors within the transferor did underlie the difference in transfer kinematics between directions, it would have been expected that more interactive effects between wheelchair-to-toilet angle and

direction would have been found, as the 180° transfers were conducted in the opposite direction from the perspective of the transferor. Factors within the transferor are thus assumed to have had a relatively minor role in the observed effects of transfer direction on the magnitude of the transferor's lower back disorder risk factors.

While the primary emphasis of this study was on the effects of environmental factors of the risk of lower back disorder during toilet transfers, it was also thought that characteristics of the transferor, such as whether he or she was experienced in performing transfers, might influence his or her risk. A meta-analysis of research investigating lower back disorder risk has suggested that, across all lifting tasks, education in proper lifting technique has no effect on lower back disorder risk (Martimo *et al.* 2008). However, contrary to this, compelling evidence exists that education in proper lifting technique should reduce the risk of lower back disorder associated with assisted transfers. A study in which transferors received extensive training (5 hrs) prior to performing assisted transfers between a bed and wheelchair found a 60% reduction in the probability that the transferor was at high risk for lower back disorder risk relative to transferors receiving only minimal training (Hess *et al.* 2007). Further compelling evidence for the benefits of training have been shown in two separate studies where ergonomic alterations in manual lifting technique were found to result in large reductions in the magnitude of spinal compression experienced by the transferor (Garg *et al.* 1991b, Schibye *et al.* 2003). It is thus believed that, if transferors are well trained in an ergonomically sound transfer technique, they will have a reduced risk of lower back disorder when compared to untrained transferors. Prior to participation in this study, all transferors received basic instruction in the pivot transfer technique. Transferors were also asked to report any prior experience in conducting assisted transfers during the preceding year; 27.6% of

the participants reported having such prior experience. Self-reported prior transfer experience was not, as a whole, associated with the magnitude of the lower back disorder risk factors examined. In fact, the only risk factor that was associated with prior transfer experience was integrated load moment arm and this, surprisingly, suggested that transferors reporting prior transfer experience were at increased risk for lower back disorder. This suggests that, in this study, regardless of prior experience in conducting assisted transfers, all transferors had approximately the same level of proficiency following instruction in the pivot transfer technique.

To control for the possible effects of transfer technique, the pivot transfer technique was used for all assisted toilet transfers (Appendix A). This transfer technique is commonly used (Garg *et al.* 1992) and easily learned (Hess *et al.* 2007). The transferors were taught two variants of this technique with regards to leg placement: an interlaced leg placement and a straddle leg placement. Transferors self-selected which leg placement to use for each transfer. The wheelchair-to-toilet angle and the direction of assisted transfer were not associated with the transferor's choice of leg position. However, the transferors' choice in leg placement was found to be associated with both their standing height and their self-reported prior experience in conducting assisted transfers. Taller transferors and those with prior experience were more likely to use the straddle leg position during assisted transfers. A potential confounding factor in these relationships is that all but one of the transferors reporting prior experience were in the upper half of the transferors by standing height. The short experienced transferor always used the interlaced leg position, whereas the tall experienced transferors were approximately 8.1 times more likely to use the straddle leg position than the interlaced leg position. Thus, the association between the

transferors' self-reported prior experience and leg position may, in part, reflect an association between prior experience and transferor standing height.

Use of the interlaced leg position was associated with slightly greater magnitudes of five of the transferor's kinematic risk factors for lower back disorder, compared to use of the straddle position. Using the logistic regression model developed by Marras *et al.* (1995), it is estimated that using the interlaced leg technique instead of the straddle technique during assisted transfers from the toilet to the wheelchair increases the transferor's odds of being at high risk for lower back disorder by a factor of 2.07. Mechanistically, it is unclear exactly why the change in leg position affected the transferor's kinematics. The connection between transfer technique and transferor standing height is suggestive. It suggests that the effect modeled by the straddle leg position disproportionally affects taller transferors and that the resulting regression model can be thought of as describing three primary groups; a group of short transferors who always used the interlaced leg position, a group of tall transferors who used the interlaced leg position, and a group of tall transferors who used the straddle position. Figure 15 supports this hypothesis. It shows that transferors with standing heights less then 1.741 m used only the interlaced leg position, whereas transferors with a standing height greater than or equal to 1.741 m used both techniques. The main effect of the leg position would thus model the predicted effect if a tall transferor were to switch from the use of one leg position to the other. For tall transferors, factors such as the transferor's leg length or the dummy's hip joint stiffness could have restricted the ability of transferors to move in close proximity to the dummy when using the interlaced leg position. In contrast, transferors conducting assisted transfers using the straddle leg position would logically be unaffected by their leg length or the dummy's hip joint stiffness. If

this hypothesis is correct, it is unclear why the effect of leg position was only observed for transfers originating on the toilet.

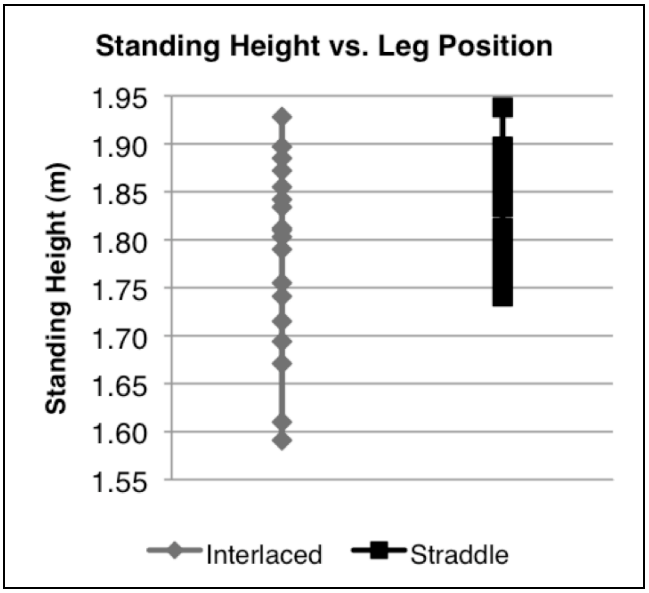

Figure 15 – Standing height vs. transfer leg position

Anthropometry conducted on people with and without back pain has suggested that greater pelvis height is associated with elevated lower back disorder risk (Merriam *et al.* 1983). The standing height of the transferor was associated with the magnitude of nine of the fourteen risk factors for lower back disorder analyzed. Of the examined factors, standing height was associated with more individual risk factors than any other explanatory measure. Greater standing height was found to have two primary opposing effects on the magnitude of lower back disorder risk factors. It increased lower back disorder risk through elevation of the maximum load moment arm and the maximum angle of lumbar flexion, and it decreased lower back disorder risk through its effect on all measures of lumbar bending and twisting. A logistic regression model developed by Marras *et al.* (1995) was used to assess the combined effects of standing height on the load moment arm, average twisting

velocity, maximum flexion angle, and maximum bending angle on the risk of lower back disorder. According to this model, a 10 cm increase in standing height would increase the transferor's odds of being at high risk for lower back disorder by a factor of 3.53. Based upon this, transferors who are short in stature, well trained, and physically able to conduct assisted toilet transfers are predicted to have the lowest relative risk of developing lower back disorder as a result of assisted toilet transfers. Although individuals short in stature are predicted to be at the lowest relative risk, the model estimates that their overall risk of developing lower back disorder is still high. The model estimates that the probability of being at high risk for lower back disorder of transferors in bottom quartile by standing height, 1.59 m – 1.76 m, was 0.977 (SD 0.016) across wheelchair-to-toilet angles. Based upon this, it is estimated that, irrespective of the wheelchair-to-toilet angle, only 1 out of approximately every 43.5 individuals with a standing height in the aforementioned range would be at low risk for lower back disorder. This further supports the suggestion made earlier that, ultimately, a "no-lift" solution to toilet transfers is needed.

Assisted patient transfers between a wheelchair and toilet have been reported to have the highest perceived stress of all transfers conducted in assisted care environments (Garg *et al.* 1992). Perceived stress is known to increase lower back disorder risk during lifting through its effect on lower back muscular co-contraction (Herrin *et al.* 1986, Marras *et al.* 2000b). Following the present assisted transfers, the transferor was asked to report his or her rating of perceived exertion (RPE) for the transfer just completed. In reporting RPE, transferors often expressed difficulty in differentiating between the awkwardness of a transfer and the physical exertion of a transfer. It is thus unclear how representative the transferor's reported RPE was of his or her true level of exertion, and thus how comparable it is to the RPE reported in

other studies. Across all angles, the mean RPE reported as part of this study were 1.4 to 2.1 points greater than values previously reported for assisted transfers of actual people between a wheelchair and a bed (Hess *et al.* 2007) or toilet (Garg and Owen 1992). A very small, statistically significant increase in transferor RPE was found for transfers at the 180º wheelchair-to-toilet angle relative to transfers at the 0º, 45º, and 90º angles. While small, this is suggestive that the 180º transfer was more physically demanding, suggesting in turn that a slightly smaller number of people would be capable of performing the 180º transfer. As part of a review of lifting injury models, it has been reported that the number of individuals capable of carrying out the most difficult portion of a lift is inversely related to the lift's overall injury potential (Herrin *et al.* 1986). Based upon this single psychometric, the 180º wheelchair-to-toilet angle is estimated to expose the transferor to a slightly greater risk of lower back disorder than transfers at the 0º, 45º, and 90º orientations.

Upon completion of the experiment, participants were asked which wheelchair-to-toilet angle they would prefer if they were to be routinely conducting assisted transfers at a single wheelchair-to-toilet angle. The 0º and 45º wheelchair-to-toilet angles were each preferred by 48% of the transferors, the 90º wheelchair-to-toilet angle was preferred by 4% of the transferors, and none of the transferors expressed preference for the 180º wheelchair-to-toilet angle. This suggests that, although the maximum load moment arm, and hence likely the risk of low back injury, was the smallest during the 180º transfers, the transferors based their preferences on other factors. Previous research has suggested that humans are more responsive to muscular strain than spinal compression (Davis *et al.*). Given this, it could be that factors such as the duration of the transfer, which was the greatest for the 180º transfer, influenced the transferors' preferred angle of transfer.

Few studies have examined assisted transfers from the perspective of the transferee. Two studies have reported the subjective comfort and perception of safety of the transferee during assisted transfers (Owen and Garg 1991, Hess *et al.* 2007) and no studies have quantified either the forces or associated accelerations experienced by the transferee. This study found that the maximum vertical acceleration experienced by the transferee was not affected by the wheelchair-to-toilet angle. Across all wheelchair-to-toilet angles, the mean maximum vertical acceleration experienced by the dummy was 0.38 Gs. This suggests that, when assisted transfers are properly conducted, the risk of injury to the transferee from forces acting vertically is low. However, it is possible that factors other than the maximum vertical force experienced by the transferee during an assisted transfer could pose as vectors for injury. Over the course of the experiment, it was observed that if the gait belt was loosely secured around the waist of the dummy, it would slip upward on the dummy. If, on the other hand, the gait belt was secured too tightly around the waist of the dummy, the transferors expressed difficulty in securely grabbing the belt. Similar problems were reported as part of an ergonomic intervention in a nursing home environment (Owen and Garg 1991). It was reported that traditional gait belts tended to slide upward over the course of an assisted transfer on transferees who were smaller in the chest and waist than at hip level. When tightened securely around the transferee's waist, the transferor's knuckles would dig into the side of the transferee and cause discomfort (Owen and Garg 1991). Of greater concern, it was reported that assisted transfers using a gait belt resulted in skin irritation and rib fracture for some individuals (Garg *et al.* 1992). It is, however, unclear exactly what components of the transfer caused these problems. A modified gait belt, with a "V" shape, larger contact area, and lifting handles was

reported to largely mitigate these problems (Owen and Garg 1991). Based upon this, it is assumed that these modified gait belts would have mitigated the observed upward sliding of the gait belt during the present assisted toilet transfers. Nevertheless, while the observed upward sliding of the gait belt would likely have caused discomfort for a human transferee, it is not believed that it affected either the spatial requirements of the assisted transfers or the transferor's risk of lower back disorder in the present study.

Limitations

This study used a 95th percentile male anthropometric dummy to model the transferee, whereas previous studies investigating assisted transfers have used actual humans to represent the transferee (Garg *et al.* 1991b, Owen and Garg 1991, Marras *et al.* 1999, Hess *et al.* 2007). The dummy was used to represent the transferee to control for the effect of the transferee across all components of the experiment. While designed to approximate the dimensions of a 95th percentile male, the dummy's torso was rigid and the joint articulations were much looser at the knees and much stiffer at the hips than what would be encountered when transferring an actual human. These differences could have altered the spatial volume employed during the assisted transfers and/or the transferor's kinematics from what would have been observed in transferring an actual human.

A key design decision behind the choice to use a dummy was to control for the ability of the transferee to provide active assistance to the transferor in conducting the assisted transfers. Through the use of the dummy, the transferee simulated in this study was never able to actively assist in the mechanics of the assisted transfer. In contrast, a recent study investigating assisted transfer techniques reported that the

human transferees provided assistance in conducting the transfers (Hess *et al.* 2007). It is likely that the level of assistance provided by a human transferee would differ across transfers both within and between transferors, introducing variability into the results. Furthermore, a transferee without mobility disabilities might provide different active assistance than a transferee with mobility disabilities. By using the dummy, the current study controlled for the ability of the transferee to actively affect the kinematics of the assisted toilet transfers and required the transferor to conduct the transfers with only passive assistance from the transferee. Thus, the present estimates of both the spatial requirements and the risk of injury are logically a superset of those experienced when transferring individuals capable of providing assistance. Based upon this, the use of the dummy enabled the spatial model to describe a spatial volume through which all transferees could likely be transferred, regardless of the level of assistance provided. In addition, with regards to injury risk, the use of the dummy enabled the determination of worst-case estimates for the effect of the wheelchair-to-toilet angle on the risk of injury to the transferor and transferee.

The pivot transfer technique used in this study (Appendix A) was different from pivot transfer techniques previously reported in the literature (Garg *et al.* 1991b, Garg *et al.* 1991a, Owen and Garg 1991, Marras *et al.* 1999, Hess *et al.* 2007). Previous studies using human transferees have described using a rocking motion to reduce the peak power required to lift the transferee. In general, rocking prior to the lifting phase of an assisted transfer is recommended and has been reported to decrease the transferor's overall risk of injury (Garg *et al.* 1991a, Owen and Garg 1991, Hess *et al.* 2007). In this study, rocking was not used due to the trunk stiffness of the dummy and the inability of the dummy to assist in either rocking or the stability of the assisted transfer. However, it is not believed that the rocking motion immediately preceding

the pivot transfer would have altered the observed effect of the wheelchair-to-toilet angle or significantly altered the reported spatiotemporal volumes.

The other primary difference between the toilet transfers implemented in this study and those reported in prior work is that this study did not attempt to simulate the associated toileting tasks. In an ergonomic evaluation of caregivers conducting assisted toilet transfers, Owen *et al.* (1991) reported that caregivers elevated the patient to standing position and the patient then supported at least part of their weight while the caregiver conducted the tasks associated with toileting, after which the patient was lowered using a pivot transfer. In contrast, in the present study, the dummy was transferred directly between the wheelchair and toilet. However, as indicated, patients in the assisted care environment reported by Owen *et al.* were able to support at least a fraction of their weight once standing. In contrast, the dummy used in this study to represent the patient was highly unstable when elevated into a standing position. It is assumed that real-world caregivers attending to individuals representative of the dummy used in this study would conduct the tasks associated with assisted toileting with the individual in the seated position on either the wheelchair or toilet.

It is believed that the spatial volume required for the assisted toileting of an individual who is able to support a portion of his or her weight will be similar to that required for individuals who are incapable of assisting in a toilet transfer. If, in the present study, the dummy had been transferred into the standing position, as in the above described toilet transfers observed by Owen *et al.* (1991), the dummy and transferor would logically have used portions of the total spatial volume already used during other parts of the transfer. This would have changed the percentage of the

overall transfer time that different portions of the transfer volume would have been occupied but would not have affected the total volume required for the movement.

The mean maximum lumbar flexion, bending, and twisting angles observed in this study were, in general, lower than values reported from an ergonomic evaluation of caregivers conducting wheelchair-to-toilet transfers and the associated assisted toileting tasks in an assisted living environment (Owen and Garg 1991). This suggests that tasks not modeled by the current research, such as removal of the pants or cleaning, could be responsible for the more extreme joint angles. Since greater magnitudes of these kinematic measures correspond to increased risk of lower back disorder, these additional tasks could, if requiring the same patient support, expose the assisted caregiver to greater injury risk than the assisted transfer itself. This is particularly concerning when considering assisted toilet transfers in a constrained environment, as studies examining tasks in such environments have suggested that they accentuate the time spent in awkward positions (Kilbom 1985). This would suggest that a constrained lavatory would accentuate the risk of injury associated with carrying out tasks related to assisted toileting. With regards to this study, the addition of constraints that reduce the spatial volume of the lavatory below that presently determined could accentuate the transferor's kinematic risk factors for lower back disorder.

This study measured the spatial volume required for assisted toilet transfers in an unconstrained environment. The addition of constraints would have logically affected the total spatial volume used by the transferor and possibly the transferor's risk of lower back disorder. It is likely that, in the presence of physical constraints that encroached upon the lavatory spatial volumes presently determined, transferors would have altered their kinematics and conducted assisted transfers using a smaller

total spatial volume. The lack of spatial constraints in the current study provides the foundation from which future studies investigating assisted transfers within spatially constrained environments can be conducted. The results from this study further provide strong suggestive evidence that if the spatial volumes measured are provided at a specific wheelchair-to-toilet angle, then the assisted transferor should be able to conduct an assisted transfer within that volume. Whether the assisted transfer could occur within a smaller volume is a topic for future research.

Future Research

The results of this study strongly suggest that the spatial volume required to conduct an assisted toilet transfer is non-rectangular and varies over the height of the transfer volume. Future research should expand upon this by developing prototype lavatory configurations in which the lavatory spatial volume is constrained and lavatory features are positioned within the transfer volume in positions that have been identified in this research as being unused portions of the overall lavatory volume. Experimental assisted toilet transfers could then be conducted in these prototype lavatories to investigate the effect of the constraints on the transferor's ability to safely perform assisted toilet transfers.

This research examined only the spatial requirements and risk of injury presented by assisted toilet transfers. Accessible lavatories should, however, facilitate the greatest level of accessibility possible. To accomplish this, they should support both independent and assisted toilet transfers. Independent toilet transfers are poorly understood. Neither the spatial volume required for independent toilet transfers nor the effect that the wheelchair-to-toilet angle has on the ease and safety of these transfers is well understood. Traditional accessible lavatories have

reportedly been designed to facilitate sliding transfers in which the wheelchair is placed adjacent to the toilet and the wheelchair user pulls him- or herself from the wheelchair to the toilet or vice versa using the grab bars. However, it has been reported that approximately 90% of elderly individuals who transfer independently stand during this process and the greatest percentage of these individuals, 33%, prefer the 180º transfer angle (Stanford 2001). To truly create accessible spaces, the factors influencing both assisted and independent toilet transfers must be understood. Future studies should investigate how the transfer technique and wheelchair-to-toilet angle affect the spatial volume requirements and injury risk during independent toilet transfers.

As previously stated, to control for the effect of the transfer technique, the pivot transfer technique was used for all assisted toilet transfers conducted as part of this study. However, the use of other innovative transfer techniques could potentially reduce the spatial requirements and/or risk of lower back disorder below what was estimated as part of this study. Previous research has suggested that sliding board transfers expose the transferor to a marginally lower risk of lower back disorder than do pivot transfers (Hess *et al.* 2007). The same research found that both transferors and transferees reported a greater perception of safety and comfort when performing a sliding board transfer compared to a pivot transfer (Hess *et al.* 2007). This suggests that the use of sliding board transfers could potentially reduce both the spatial volume required and the risk of lower back disorder associated with the assisted toilet transfers. This technique deserves further investigation.

Another technique that deserves biomechanical investigation is a novel transfer technique proposed by a participant in this study. The technique was not tested, but might potentially reduce the transferor's risk of lower back disorder by

transferring a portion of the transferee's weight directly to the legs of the transferor. The technique suggested by the participant is as follows. The transferor slides the transferee forward. The transferor assumes a squat position and drapes the legs of the transferee over the top of his/her thighs. Grasping the gait belt behind the transferee, the transferor scoots the transferee as far forward as possible and lifts them to the extent necessary with their legs. The transferor then shifts his or her body laterally and lowers the transferee to the toilet. Biomechanically, this technique would increase the total weight lifted by the transferor over what is assumed to be lifted using the pivot technique. During a pivot transfer, it is assumed that the transferor lifts the head-arms-torso of the transferee and that the legs of the transferee are neutrally self-supported. As part of this new technique, the transferor clearly lifts the whole body weight of the transferee. However, this transfer technique appears to be potentially advantageous in that the weight of the transferee is supported primarily using the legs of the transferor and not by the transferor's upper body. Furthermore, to the extent that the transferor's upper body does provide lifting support, the magnitude of the maximum load moment arm of the transferee about the transferor's lumbar spine appears to be reduced to the maximum extent possible. Together, this suggests that the maximum lumbar load moment experienced by the transferor in using this technique should be lower than that experienced by the transferor when using the pivot transfer technique. Again, while not practical for transfers in excess of the 0^{o} wheelchair-to-toilet angle, this novel transfer technique could potentially lower the transferor's risk of lower back disorder when conducting the 0^{o} transfer.

Finally, further research is needed to investigate no-lift assisted transfer devices. Recognizing the risk from manually-performed assisted transfers,

occupations such as nursing have adopted no-lift transfer protocols and have embraced the use of assistive lifting devices (Hudson 2005, Engkvist 2006). However, these devices are, in general, both expensive and not portable. Inexpensive assistive lifting devices, such as a sling and compound pulley system, could potentially be integrated as part of an accessible lavatory design. Assistive transfer devices such as these would ideally both mitigate the injury risk faced during assisted toilet transfers and reduce the spatial requirements of assisted transfers below what is required for manually-performed assisted transfers. Furthermore, the integration of assistive lifting devices within the lavatory could potentially allow some disabled travelers who would have otherwise required an assisted transfer to self-transfer and thus achieve a significantly greater level of independence. However, even if assistive lifting devices are included within some lavatory designs, these devices will be far from ubiquitous. Further research should ideally attempt to design inexpensive portable assistive lifting devices that wheelchair-bound individuals can easily carry with them and use to conduct assisted transfers in a variety of environments.

Conclusion

A major barrier to air travel for people with disabilities is the general lack of accessible lavatories on board commercial passenger aircraft. A primary reason for this lack of greater accessibility is related to space. To design an airplane lavatory that is both accessible and consistent with the restrictive spatial requirements of airplane environments, a broader understanding was needed as to how the relative angle of the wheelchair to the toilet affected the spatial requirements of assisted toilet transfers.

Beyond meeting the spatial requirements of assisted transfers, to be truly accessible, a lavatory design must also attempt to minimize the risk of injury to both the transferor and transferee during assisted toilet transfers. Biomechanical analysis has previously found that assisted transfers induce spinal forces at or above the level recognized to cause spinal damage (Garg and Owen 1992, Marras *et al.* 1999). However, it was unknown how the orientation of the wheelchair to the toilet during an assisted toilet transfer affected the transferor's risk of developing lower back disorder and the risk of injury to the transferee.

The purpose of this study was thus to investigate how the wheelchair-to-toilet angle affects both the spatial consumption required for assisted toilet transfers and the risk of injury to the transferor and transferee. Twenty-nine participants (transferors) were motion captured in a laboratory environment while conducting assisted toilet transfers using a pivot transfer technique at relative wheelchair-to-toilet angles of 0º, 45º, 90º, and 180º. A 95th percentile male dummy represented the transferee. A novel, three-dimensional computer-based spatial mapping technique

was developed to compute the spatial volume requirements of assisted toilet transfers from the motion capture data.

The wheelchair-to-toilet angle directly affected the total spatial volume needed to conduct an assisted toilet transfer. The total rectangular area required to perform an assisted toilet transfer using a pivot transfer technique progressively increased with increases in the wheelchair-to-toilet angle from 0° to 180°. Based purely on total rectangular area, the 0º transfer orientation required the least space. However, the three-dimensional volume required for an assisted transfer differs between transfer angles, is non-rectangular, and varies in spatial area over the height of the transfer volume. Spatiotemporal maps taken at various heights across the transfer volume strongly suggest that the total spatial volume required for an accessible lavatory could be minimized by designing a lavatory to support assisted transfers at a specific wheelchair-to-toilet angle and by placing lavatory fixtures in those portions of the lavatory volume that are unused during assisted transfers.

Beyond allowing sufficient space to support assisted toilet transfers, the spatial volume provided by an accessible lavatory should, to the extent possible, mitigate the injury risk to both the transferee and transferor. The wheelchair-to-toilet angle affected eight of the fourteen kinematic risk factors for lower back disorder to the transferor that were analyzed. Of these risk factors, the wheelchair-to-toilet angle primarily affected the transferor's odds of being at high risk of lower back disorder through its effect on the transferor's maximum load moment arm. Surprisingly, the magnitude of the transferor's maximum load moment arm was inversely related to the wheelchair-to-toilet angle. Through this effect, the transferor's odds of being at high risk of lower back disorder was 14.9-fold higher for the 0º transfer than when performing assisted transfers at the 180º orientation. As a whole, the kinematic

results suggest that assisted transfers at the larger wheelchair-to-toilet angles were safer for the transferor than at smaller angles.

After accounting for the effects of the wheelchair-to-toilet angle and the direction of assisted transfer, characteristics of the assisted transferor were investigated for associations with the magnitude of the transferor's kinematic risk factors for lower back disorder. The primary purpose of this analysis was to identify characteristics by which transferors at lower risk for lower back disorder could be selected. Associations were found between the transferor's kinematic risk factors for lower back disorder and both the transferor's leg position during the assisted transfers and his/her standing height. Of these associations, the association with transferor height was the strongest and suggested that transferors who are short in stature have a reduced risk of being at high risk for lower back disorder.

All together, the results of this study suggest that accessible lavatories can be designed for use in constrained environments by designing the lavatory to support assisted transfers at a single optimal wheelchair-to-toilet angle. The study further suggested that the transferor's risk of injury during assisted toilet transfers is the lowest at a wheelchair-to-toilet angle of 180º. This suggests that if lavatories are going to be designed to support a single optimal transfer angle, then they should be designed to support the 180º transfer. Transferors short in stature and physically able to conduct assisted transfer should be preferentially selected to perform assisted transfers, as they are predicted to have a lower risk of lower back disorder injury than taller transferors. However, the findings of this research also suggest that, regardless of the wheelchair-to-toilet angle and transferor selection, assisted toilet transfers place the transferor at high risk. The Marras *et al.* (1995) model for lower back disorder estimates that the probability of being at high risk for lower back disorder of

transferors in bottom quartile by standing height, 1.59 m – 1.76 m, at the 180º transfer angle was 0.955 (SD 0.033). Based upon this, it is estimated that even under the most optimum conditions only 1 out of approximately every 22.4 individuals would be at low risk for lower back disorder. Given the high risk this study finds that assisted wheelchair-to-toilet transfers should ideally be conducted using a no-lift transfer technique.

References

ATAA, 1992. *Suggested guidelines for accessible lavatories in twin aisle aircraft.* Washington D.C.: Air Transport Association of America.

Banaag, J., 1988. *Maximum acceptable weights, heart rates, ratings of perceived exertion and static strengths for one-hour repetitive symmetric and asymmetric lifting*. Master's thesis, University of Wisconsin.

Barondess, J.A., Cullen, M.R., De Lateur, B., Deyo, R.A., Donaldson, S.K., Drury, C.G., Feuerstein, M., Fischhoff, B., Frymoyer, J.W., Katz, J.N., Kroenke, K., Lotz, J.C., Mackinnon, S.E., Marras, W.S., Radwin, R.G., Rempel, D.M., Szabo, R.M., Vlahov, D., Wegman, D.H., Mavor, A.S., Mcgee, J.P., Mccutchen, S.R., Wigdor, A.K., Pope, A.M., Manning, F.J., Howell, W.C., Carroll, J.M., Drury, C.G., Grabowski, M., Ilgen, D.R., Jagacinski, R.J., John, B.E., Kraiger, K., Parasuraman, R., Roberts, K., Vicente, K.J., Zacharias, G.L., Mavor, A.S. & Mccutchen, S.R., 2001. *Musculoskeletal disorders and the workplace : Low back and upper extremities* Washington, D.C.: National Academy Press.

Binckmann, P., Johnnleweling, N., Hilweg, D. & Biggemann, M., 1987. Fatigue fracture of human lumbar vertebrae. *Clin Biomech,* (2), 94-96.

Borg, G., 1998. *Borg's perceived exertion and pain scales,* 1 ed. Champaign, IL: Human Kinetics.

Borg, G.A., 1982. Psychophysical bases of perceived exertion. *Med Sci Sports Exerc,* 14 (5), 377-81.

Bureau of Transportation Statistics, 2006. http://www.transtats.bts.gov/. Bureau of Transportation Statistics, U.S. Department of Transportation, Washington D.C.

Chaffin, D.B. & Park, K.S., 1973. A longitudinal study of low-back pain as associated with occupational weight lifting factors. *Am Ind Hyg Assoc J,* 34 (12), 513-25.

Charles, R. 1999. Handicap access needed in the air. *Christian Science Monitor*, 4/19/1999.

Chernew, M.E., Goldman, D.P., Pan, F. & Shang, B., 2005. Disability and health care spending among medicare beneficiaries. *Health Affairs,* 24 Suppl 2, W5R42-52.

Cummings, S.R., Bates, D. & Black, D.M., 2002. Clinical use of bone densitometry: Scientific review. *JAMA,* 288 (15), 1889-97.

Davis, K.G., Jorgensen, M.J. & Marras, W.S., 2000. An investigation of perceived exertion via whole body exertion and direct muscle force indicators during the determination of the maximum acceptable weight of lift. *Ergonomics,* 43 (2), 143-59.

Davis, K.G. & Marras, W.S., 2000. The effects of motion on trunk biomechanics. *Clin Biomech,* 15 (10), 703-17.

Davis, K.G., Marras, W.S. & Waters, T.R., 1998. Evaluation of spinal loading during lowering and lifting. *Clin Biomech,* 13 (3), 141-152.

Decker, H.B.J., 1993. *Letter Sent to all Major and National U.S. Passenger Air Carriers.* Office of Intergovernmental and Consumer Affairs, U.S. Department of Transportation.

Engkvist, I.L., 2006. Evaluation of an intervention comprising a no lifting policy in Australian hospitals. *Appl Ergon,* 37 (2), 141-8.

Freedman, V.A., Crimmins, E., Schoeni, R.F., Spillman, B.C., Aykan, H., Kramarow, E., Land, K., Lubitz, J., Manton, K., Martin, L.G., Shinberg, D. & Waidmann, T., 2004. Resolving inconsistencies in trends in old-age disability: Report from a technical working group. *Demography,* 41 (3), 417-41.

Freedman, V.A., Martin, L.G. & Schoeni, R.F., 2002. Recent trends in disability and functioning among older adults in the United States: A systematic review. *JAMA,* 288 (24), 3137-46.

Garg, A. & Owen, B., 1992. Reducing back stress to nursing personnel: An ergonomic intervention in a nursing home. *Ergonomics,* 35 (11), 1353-75.

Garg, A., Owen, B., Beller, D. & Banaag, J., 1991a. A biomechanical and ergonomic evaluation of patient transferring tasks: Bed to wheelchair and wheelchair to bed. *Ergonomics,* 34 (3), 289-312.

Garg, A., Owen, B., Beller, D. & Banaag, J., 1991b. A biomechanical and ergonomic evaluation of patient transferring tasks: Wheelchair to shower chair and shower chair to wheelchair. *Ergonomics,* 34 (4), 407-19.

Garg, A., Owen, B.D. & Carlson, B., 1992. An ergonomic evaluation of nursing assistants' job in a nursing home. *Ergonomics,* 35 (9), 979-95.

Goemaere, S., Van Laere, M., De Neve, P. & Kaufman, J.M., 1994. Bone mineral status in paraplegic patients who do or do not perform standing. *Osteoporos Int,* 4 (3), 138-43.

Goktepe, A.S., Yilmaz, B., Alaca, R., Yazicioglu, K., Mohur, H. & Gunduz, S., 2004. Bone density loss after spinal cord injury: Elite paraplegic basketball players vs. paraplegic sedentary persons. *Am J Phys Med Rehabil,* 83 (4), 279-83.

Granata, K.P. & Marras, W.S., 1999. Relation between spinal load factors and the high-risk probability of occupational low-back disorder. *Ergonomics,* 42 (9), 1187-99.

Greenberger, R.S. 1999. For disabled passengers, flying can be a nightmare. *The Wall Street Journal*, Monday, June 21.

Herrin, G.D., Jaraiedi, M. & Anderson, C.K., 1986. Prediction of overexertion injuries using biomechanical and psychophysical models. *Am Ind Hyg Assoc J,* 47 (6), 322-30.

Hess, J.A., Kincl, L.D. & Mandeville, D.S., 2007. Comparison of three single-person manual patient techniques for bed-to-wheelchair transfers. *Home Healthc Nurse,* 25 (9), 577-9.

Hignett, S. & Evans, D., 2006. Spatial requirements in hospital shower and toilet rooms. *Nurs Stand,* 21 (3), 43-8.

Hudson, M.A., 2005. Texas passes first law for safe patient handling in America: Landmark legislation protects health-care workers and patients from injury related to manual patient lifting. *J Long Term Eff Med Implants,* 15 (5), 559-66.

Kilbom, A., Ljungberg, S., Hägg G., 1985. Lifting and carrying in geriatric care. A comparison between differences in workspace layout, work organization and use of modern equipment. *Ergonomics International Association. Congress 1985*, Bournemouth, England, 550-552.

Lakdawalla, D.N., Goldman, D.P. & Shang, B., 2005. The health and cost consequences of obesity among the future elderly. *Health Affairs,* 24 Suppl 2, W5R30-41.

Lotz, J.C., Colliou, O.K., Chin, J.R., Duncan, N.A. & Liebenberg, E., 1998. Compression-induced degeneration of the intervertebral disc: An in vivo mouse model and finite-element study. *Spine,* 23 (23), 2493-506.

Marras, W.S., 2000. Occupational low back disorder causation and control. *Ergonomics,* 43 (7), 880-902.

Marras, W.S., Allread, W.G., Burr, D.L. & Fathallah, F.A., 2000a. Prospective validation of a low-back disorder risk model and assessment of ergonomic interventions associated with manual materials handling tasks. *Ergonomics,* 43 (11), 1866-86.

Marras, W.S., Davis, K.G., Heaney, C.A., Maronitis, A.B. & Allread, W.G., 2000b. The influence of psychosocial stress, gender, and personality on mechanical loading of the lumbar spine. *Spine,* 25 (23), 3045-54.

Marras, W.S., Davis, K.G., Kirking, B.C. & Bertsche, P.K., 1999. A comprehensive analysis of low-back disorder risk and spinal loading during the transferring and repositioning of patients using different techniques. *Ergonomics,* 42 (7), 904-26.

Marras, W.S. & Granata, K.P., 1995. A biomechanical assessment and model of axial twisting in the thoracolumbar spine. *Spine,* 20 (13), 1440-51.

Marras, W.S., Lavender, S.A., Leurgans, S.E., Fathallah, F.A., Ferguson, S.A., Allread, W.G. & Rajulu, S.L., 1995. Biomechanical risk factors for occupationally related low back disorders. *Ergonomics,* 38 (2), 377-410.

Martimo, K.P., Verbeek, J., Karppinen, J., Furlan, A.D., Takala, E.P., Kuijer, P.P., Jauhiainen, M. & Viikari-Juntura, E., 2008. Effect of training and lifting equipment for preventing back pain in lifting and handling: Systematic review. *BMJ,* 336 (7641), 429-31.

Mcconnell, E.A., 1995. Transferring a patient from bed to chair. *Nursing,* 25 (11), 30.

Mcconnell, E.A., 2002. Using proper body mechanics. *Nursing,* 32 (5), 17.

McGill, S.M., Norman, R.W. & Cholewicki, J., 1996. A simple polynomial that predicts low-back compression during complex 3-d tasks. *Ergonomics,* 39 (9), 1107-18.

Merriam, W.F., Burwell, R.G., Mulholland, R.C., Pearson, J.C. & Webb, J.K., 1983. A study revealing a tall pelvis in subjects with low back pain. *J Bone Joint Surg Br,* 65 (2), 153-6.

Miller, A., Engst, C., Tate, R.B. & Yassi, A., 2006. Evaluation of the effectiveness of portable ceiling lifts in a new long-term care facility. *Appl Ergon,* 37 (3), 377-85.

NIOSH, 1981. *Work Practices for Manual Lifting*. National Institute for Occupational Safety and Health, U.S. Department of Health and Human Services.

Norman, R., Wells, R., Neumann, P., Frank, J., Shannon, H. & Kerr, M., 1998. A comparison of peak vs cumulative physical work exposure risk factors for the reporting of low back pain in the automotive industry. *Clin Biomech,* 13 (8), 561-573.

Oddsson, L.I., Persson, T., Cresswell, A.G. & Thorstensson, A., 1999. Interaction between voluntary and postural motor commands during perturbed lifting. *Spine,* 24 (6), 545-52.

Owen, B.D., 2000. Teaching students safer methods of patient transfer. *Nurse Educ,* 25 (6), 288-93.

Owen, B.D. & Garg, A., 1991. Reducing risk for back pain in nursing personnel. *AAOHN J,* 39 (1), 24-33.

Pinheiro, J.C. & Bates, D.M., 2002. *Mixed Effects Models in S and S-Plus,* 3rd ed. New York, NY: Springer.

Punnett, L., Fine, L.J., Keyserling, W.M., Herrin, G.D. & Chaffin, D.B., 1991. Back disorders and nonneutral trunk postures of automobile assembly workers. *Scand J Work Environ Health,* 17 (5), 337-46.

Santaguida, P.L., Pierrynowski, M., Goldsmith, C. & Fernie, G., 2005. Comparison of cumulative low back loads of caregivers when transferring patients using overhead and floor mechanical lifting devices. *Clin Biomech,* 20 (9), 906-16.

Schibye, B., Hansen, A.F., Hye-Knudsen, C.T., Essendrop, M., Bocher, M. & Skotte, J., 2003. Biomechanical analysis of the effect of changing patient-handling technique. *Appl Ergon,* 34 (2), 115-23.

Stanford, J.A., 2001. *Best practices in the design of toileting and bathing facilities for assisted transfers*. U.S. Access Board, Washington D.C.

Strickman, N., 2005. *Providing accurate information to consumers about accessible aircraft lavatories*. Aviation Consumer Protection Division, U.S. Department of Transportation.

Syed, Z. & Khan, A., 2002. Bone densitometry: Applications and limitations. *J Obstet Gynaecol Can,* 24 (6), 476-84.

Takeda, K., 1977. [illustrated instruction on transfer techniques. 13. Patients with spinal cord injuries. 7. Transfer from a wheelchair to the toilet]. *Kangogaku Zasshi,* 41 (3), 305-8.

U.S. Census Bureau, 2000. *Disability Status by Sex, Census 2000.* U.S. Census Bureau. Washington D.C.

U.S. Census Bureau, 2004. American Community Survey. U.S. Census Bureau. Washington D.C.

U.S. Government, 1986. *Air Carrier Access Act*. 49 U.S.C. § 41705

U.S. Government, 1990. *ADA Standards for Accessible Design*. U.S. Department of Justice, Washington D.C.

U.S. Department of Transportation, 1993. *Lavatory accessibility in single-aisle aircraft final report.* U.S. Department of Transportation, Washington D.C.

Wald, M.L. 2003. U.S. Moves to aid disabled who fly. *New York Times*, Sunday, October 26.

Warren, G.C. & Valois, T., 1991. *Functional categories of persons with disabilities and operational dimensions for designing accessible aircraft lavortories.* Seattle: Air Transport Association of America.

Winter, D.A., 2005. *Biomechanics and motor control of human movement,* 3rd ed. Hoboken, N.J.: John Wiley & Sons.

Zurada, J., Karwowski, W. & Marras, W.S., 1997. A neural network-based system for classification of industrial jobs with respect to risk of low back disorders due to workplace design. *Appl Ergon,* 28 (1), 49-58.

Appendices

Appendix A

Pivot Transfer Technique

The spatial volume required to conduct an assisted transfer and the transferor's risk of injury is logically affected by the transfer technique used to conduct the assisted transfer. To control for this, all experimental transfers conducted in this study used the same general single-transferor pivot transfer technique. Using this technique, the transferors transferred the dummy from the wheelchair to the toilet using the following steps (Figures 16 – 22).

Step 1

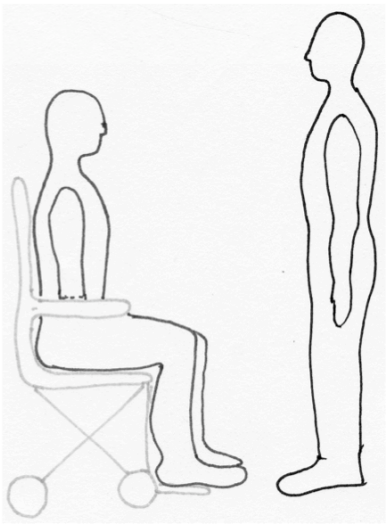

Figure 16 – The transferor positioned the wheelchair for the assisted transfer.

Step 2

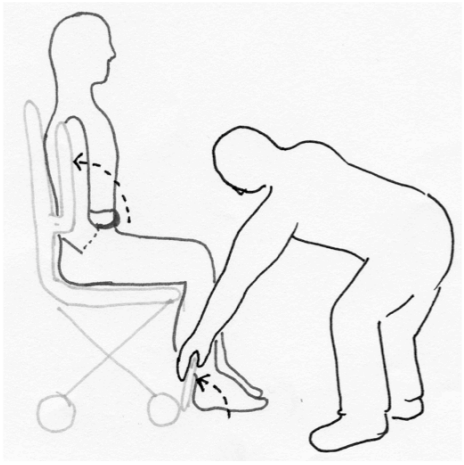

Figure 17 – The transferor raised the armrests, moved the feet to the floor, and raised the footrest.

Step 3

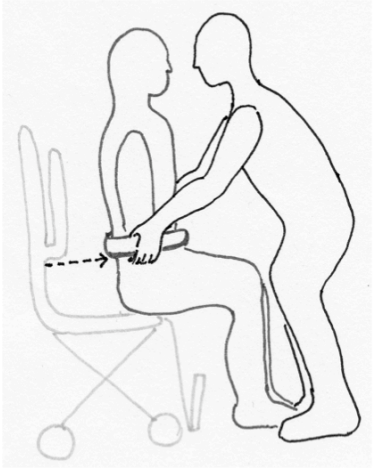

Figure 18 – Grasping the gait belt, the transferor slid the transferee forward.

Step 4

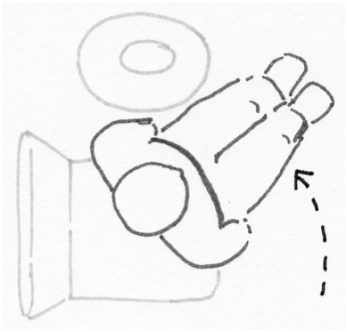

Figure 19 – The transferor rotated the transferee towards the toilet, keeping the transferee seated on the wheelchair.

Step 5

Figure 20 – The transferor positioned him/herself halfway between the wheelchair and toilet using either the straddle or interlaced leg position. The interlaced leg position is shown.

Step 6

Figure 21 – Grasping the gait belt, the transferor lifted the dummy, keeping his/her back straight. The straddle leg position is shown.

Step 7

Figure 22 – Starting with his/her pelvis oriented to divide the transfer angle in half, the transferor kept his/her back straight and pivoted, twisting at the arms and legs, to transfer the transferee from the wheelchair to the toilet. The straddle leg position is shown.

Appendix B

Select High Resolution Spatiotemporal Maps

The spatiotemporal mapping software generates high-resolution color and grey-scale spatiotemporal maps. Color maps taken at 1 cm and 75 cm from the floor for transfers conducted bi-directionally at each of the four wheelchair-to-toilet angles follow (Figures 23 – 30).

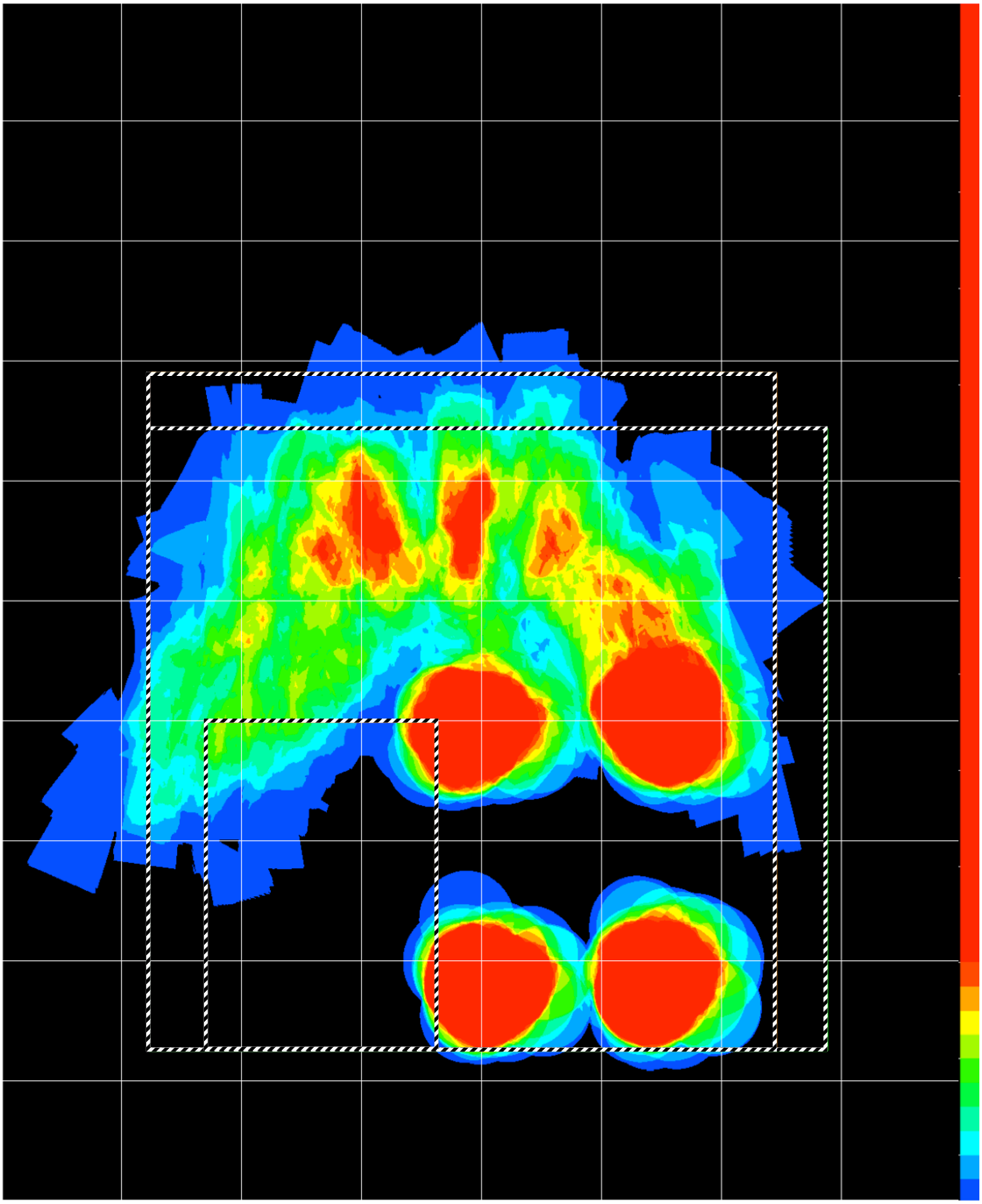

Grid Scale: 20 cm

Percent Occupation

0%	4% >= 6%	10% >= 12%	16% >= 18%
0% >= 2%	6% >= 8%	12% >= 14%	18% >= 20%
2% >= 4%	8% >= 10%	14% >= 16%	20% >= 100%

Lavatory and Toilet Boundary

Figure 23 – Spatial Consumption at 1 cm for 0° Transfer

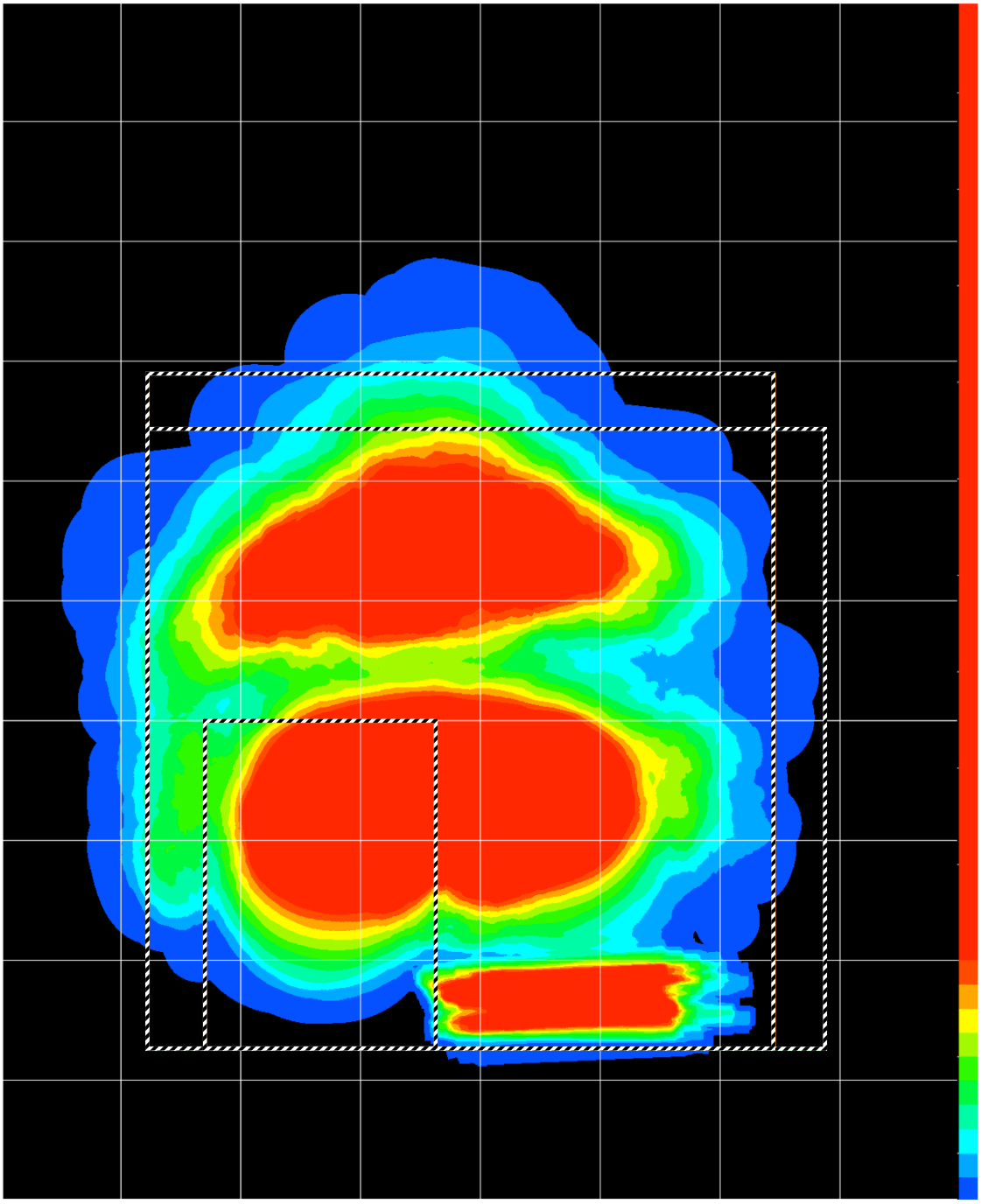

Grid Scale: 20 cm

Percent Occupation

0%	4% >= 6%	10% >= 12%	16% >= 18%
0% >= 2%	6% >= 8%	12% >= 14%	18% >= 20%
2% >= 4%	8% >= 10%	14% >= 16%	20% >= 100%

Lavatory and Toilet Boundary

Figure 24 – Spatial Consumption at 75 cm for 0° Transfer

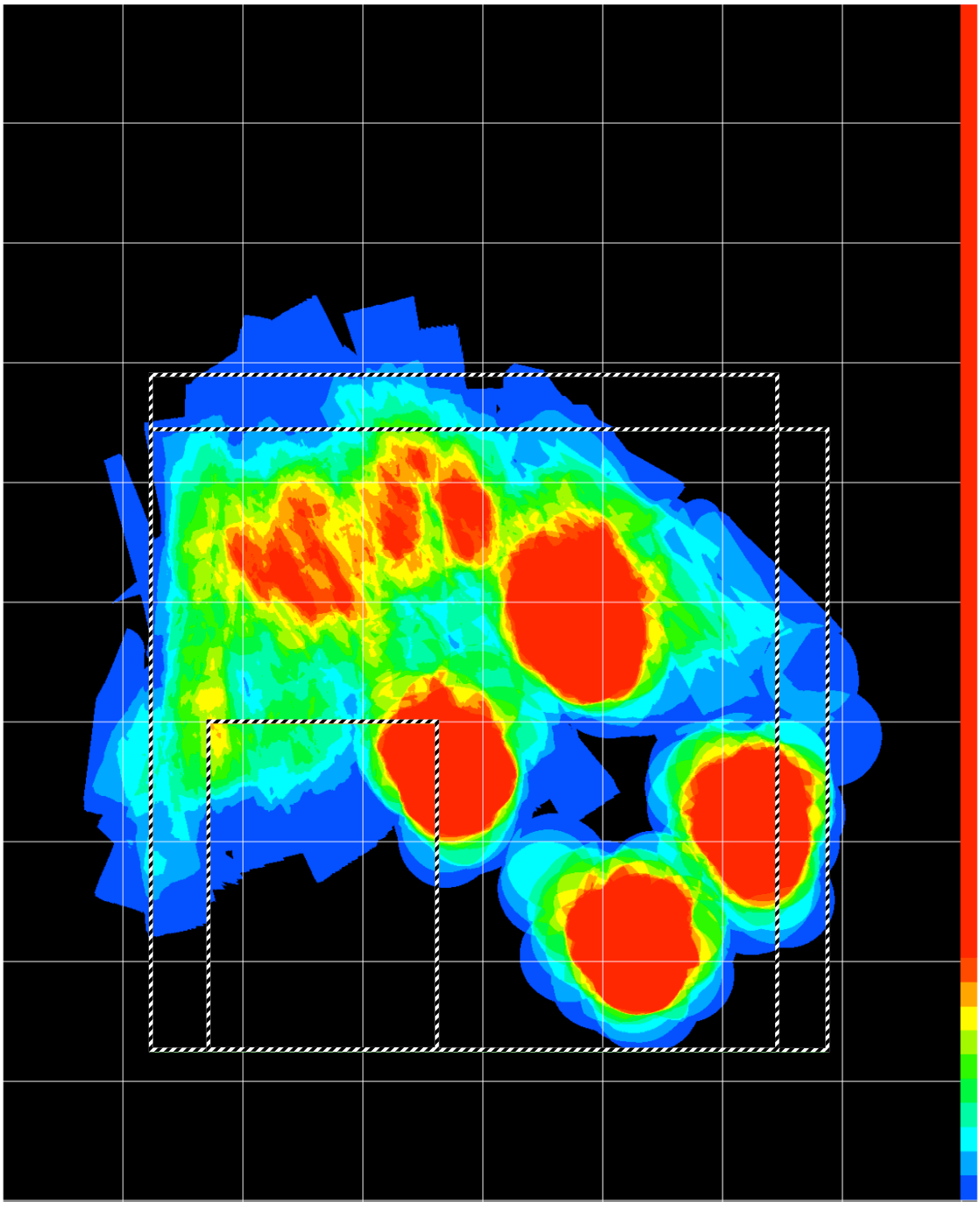

Grid Scale: 20 cm

Percent Occupation

0%	4% >= 6%	10% >= 12%	16% >= 18%
0% >= 2%	6% >= 8%	12% >= 14%	18% >= 20%
2% >= 4%	8% >= 10%	14% >= 16%	20% >= 100%

Lavatory and Toilet Boundary

Figure 25 – Spatial Consumption at 1 cm for 45° Transfer

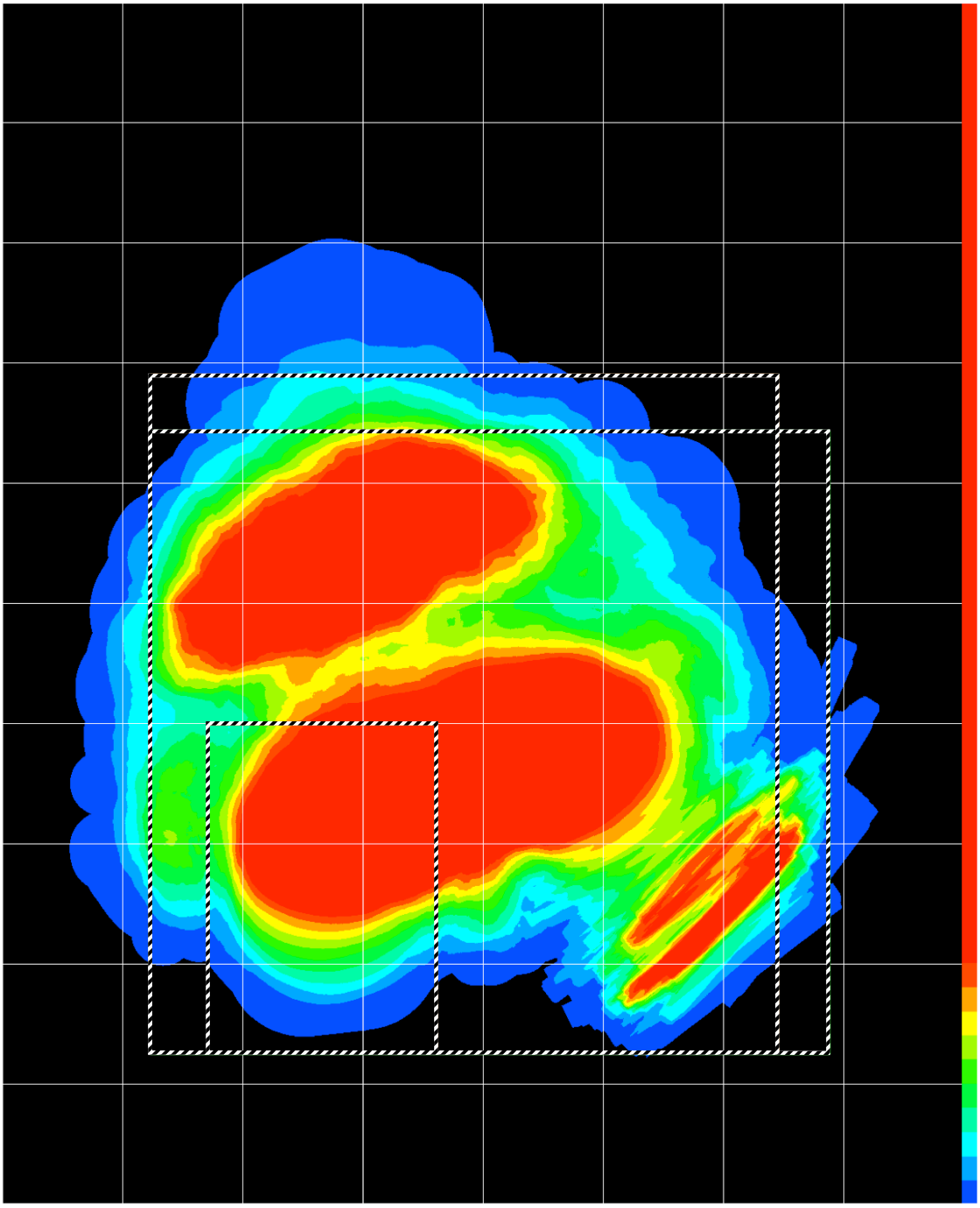

Grid Scale: 20 cm

Percent Occupation

0%	4% >= 6%	10% >= 12%	16% >= 18%
0% >= 2%	6% >= 8%	12% >= 14%	18% >= 20%
2% >= 4%	8% >= 10%	14% >= 16%	20% >= 100%

Lavatory and Toilet Boundary

Figure 26 – Spatial Consumption at 75 cm for 45° Transfer

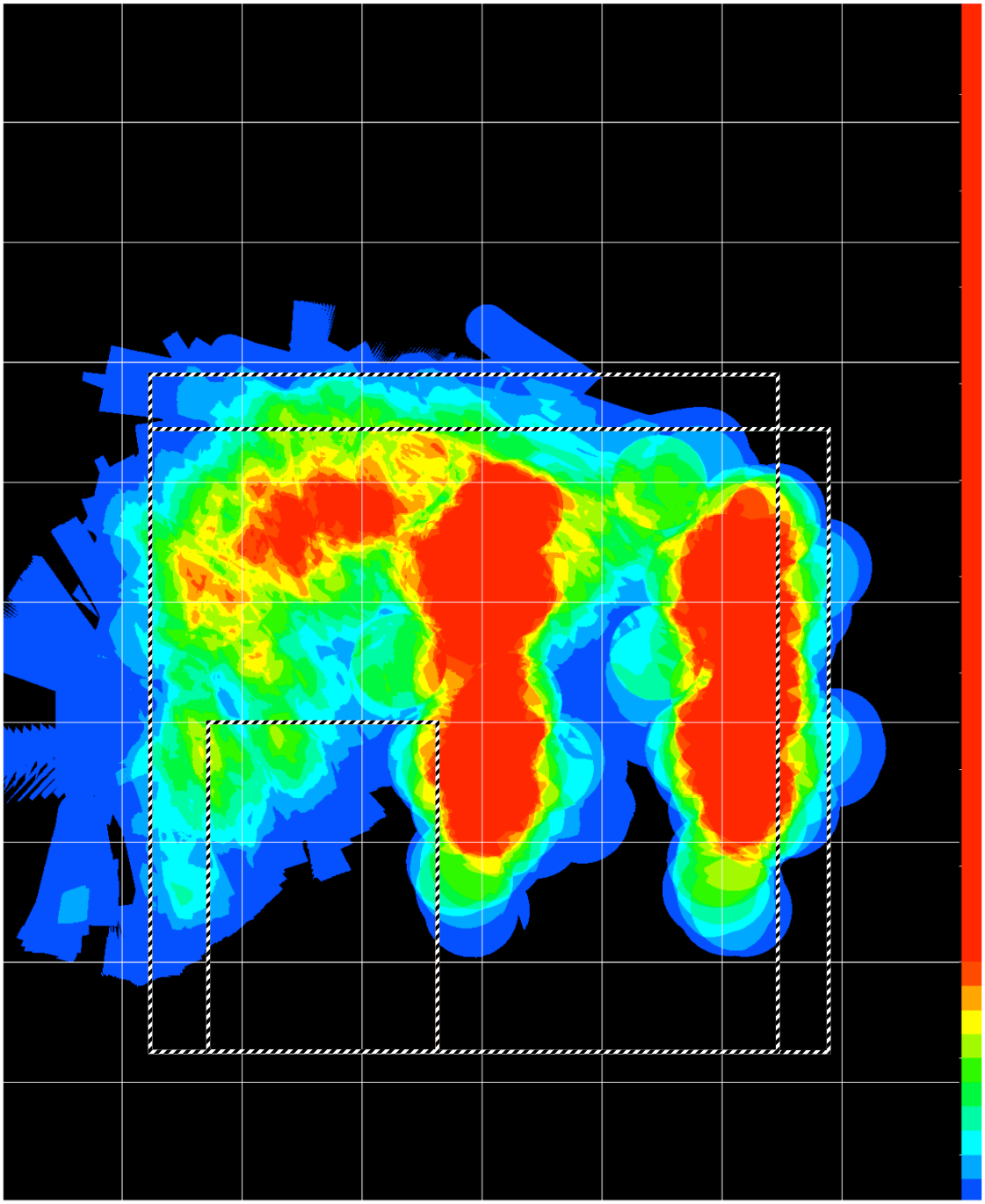

Grid Scale: 20 cm

Percent Occupation

0%	4% >= 6%	10% >= 12%	16% >= 18%
0% >= 2%	6% >= 8%	12% >= 14%	18% >= 20%
2% >= 4%	8% >= 10%	14% >= 16%	20% >= 100%

Lavatory and Toilet Boundary

Figure 27 – Spatial Consumption at 1 cm for 90° Transfer

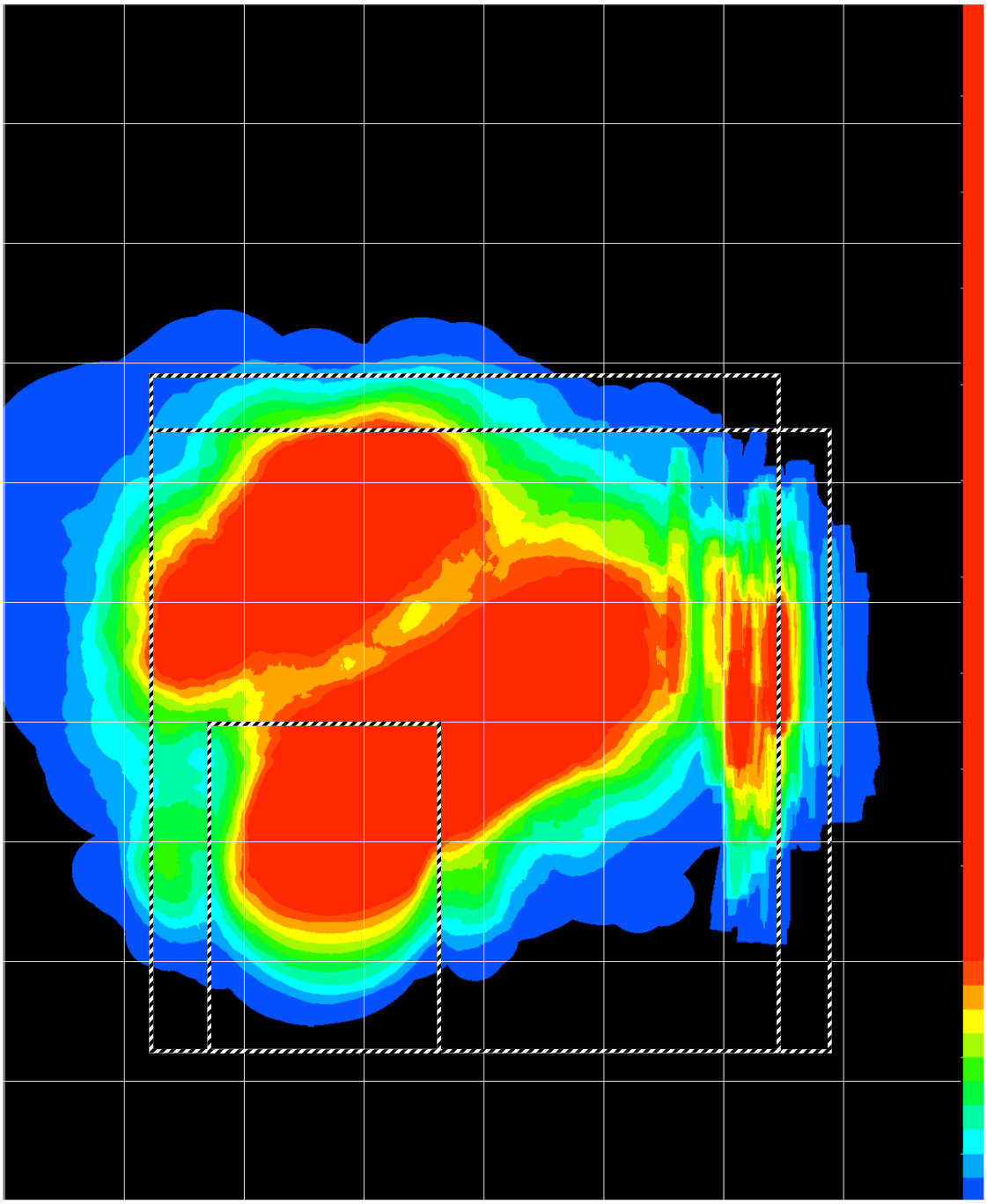

Grid Scale: 20 cm

Percent Occupation

0%	4% >= 6%	10% >= 12%	16% >= 18%
0% >= 2%	6% >= 8%	12% >= 14%	18% >= 20%
2% >= 4%	8% >= 10%	14% >= 16%	20% >= 100%

Lavatory and Toilet Boundary

Figure 28 – Spatial Consumption at 75 cm for 90° Transfer

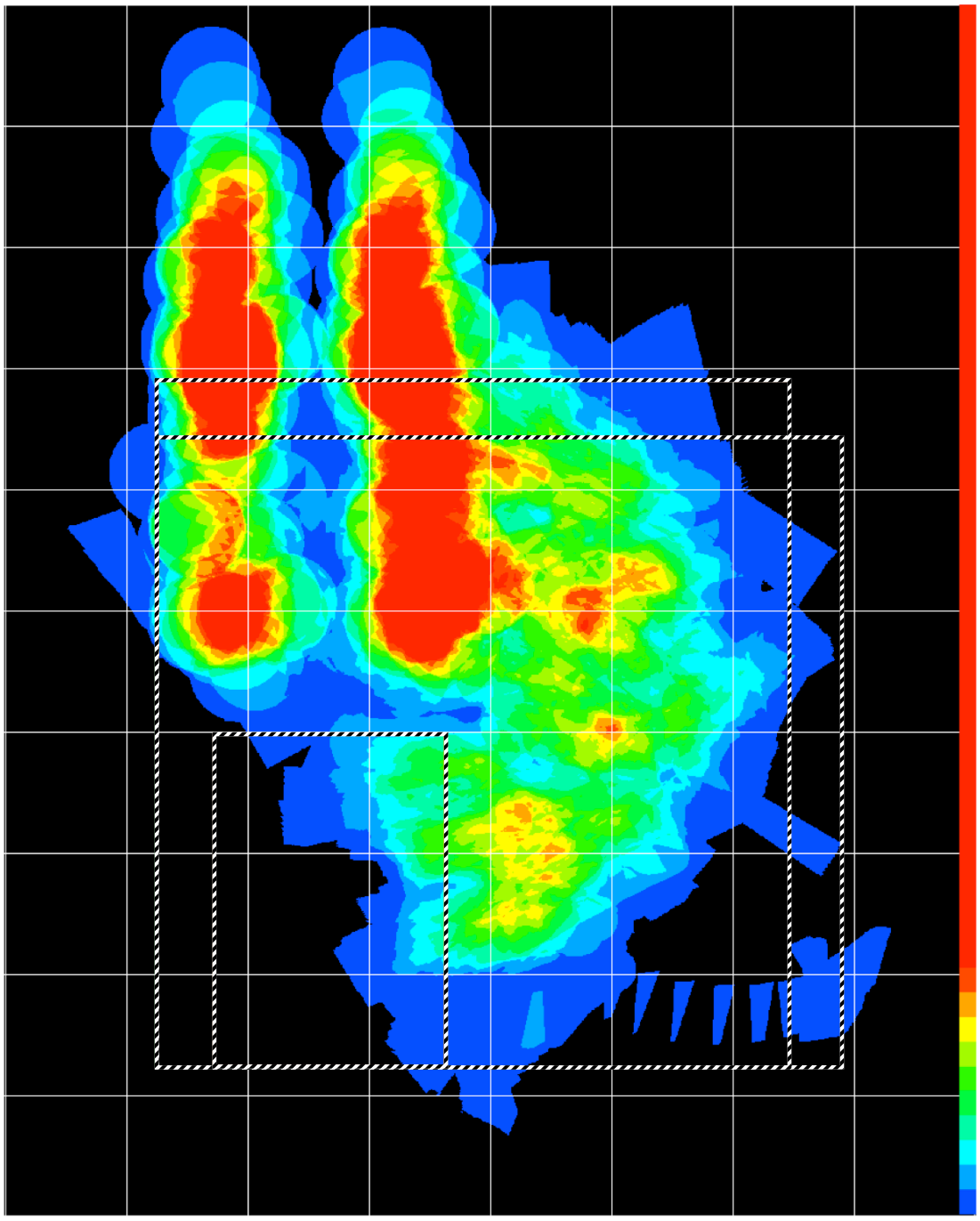

Grid Scale: 20 cm

Percent Occupation

0%	4% >= 6%	10% >= 12%	16% >= 18%
0% >= 2%	6% >= 8%	12% >= 14%	18% >= 20%
2% >= 4%	8% >= 10%	14% >= 16%	20% >= 100%

Lavatory and Toilet Boundary

Figure 29 – Spatial Consumption at 1 cm for 180° Transfer

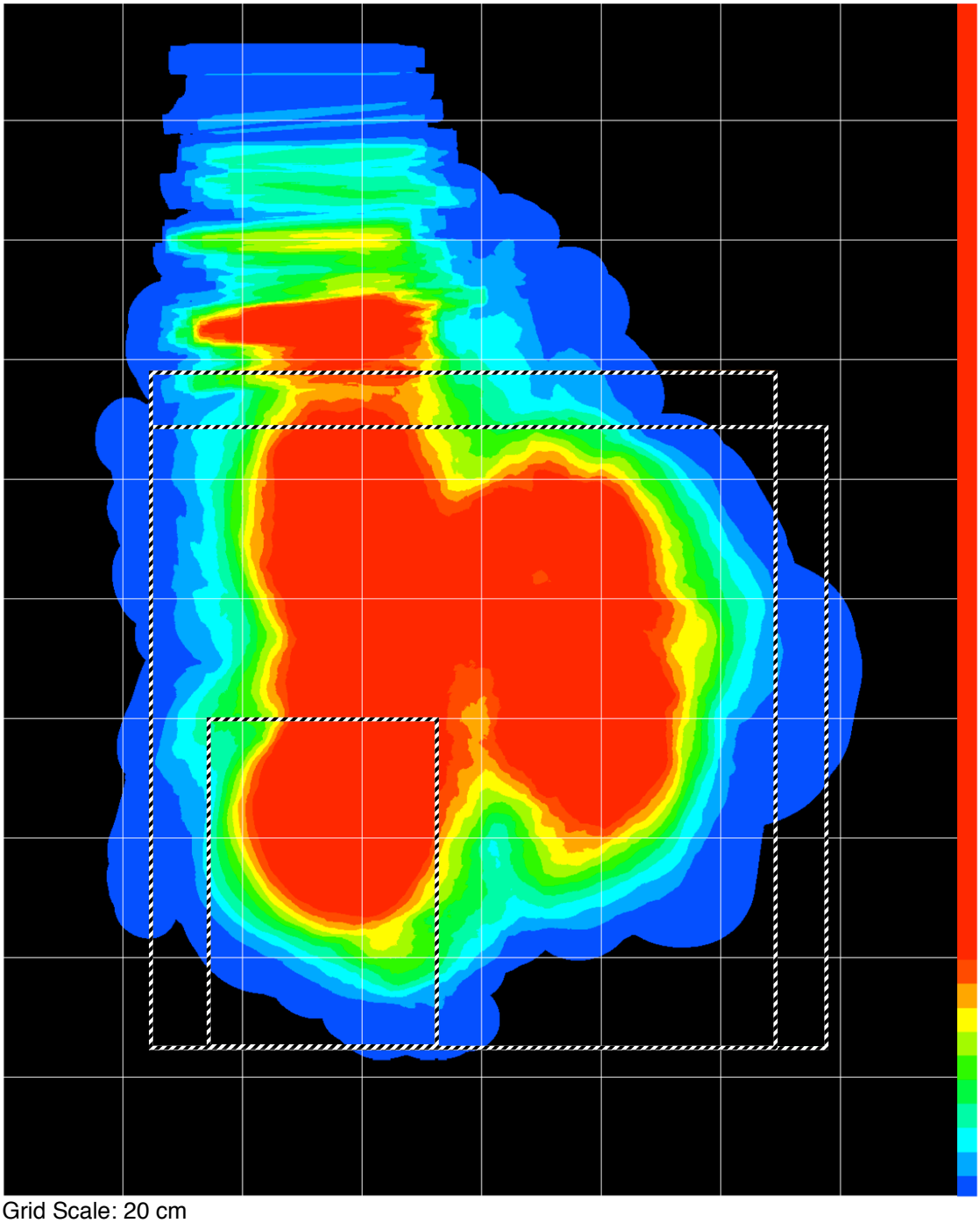

Grid Scale: 20 cm

Percent Occupation

0%	4% >= 6%	10% >= 12%	16% >= 18%
0% >= 2%	6% >= 8%	12% >= 14%	18% >= 20%
2% >= 4%	8% >= 10%	14% >= 16%	20% >= 100%

Lavatory and Toilet Boundary

Figure 30 – Spatial Consumption at 75 cm for 180° Transfer

Appendix C

Spatial Modeling Software

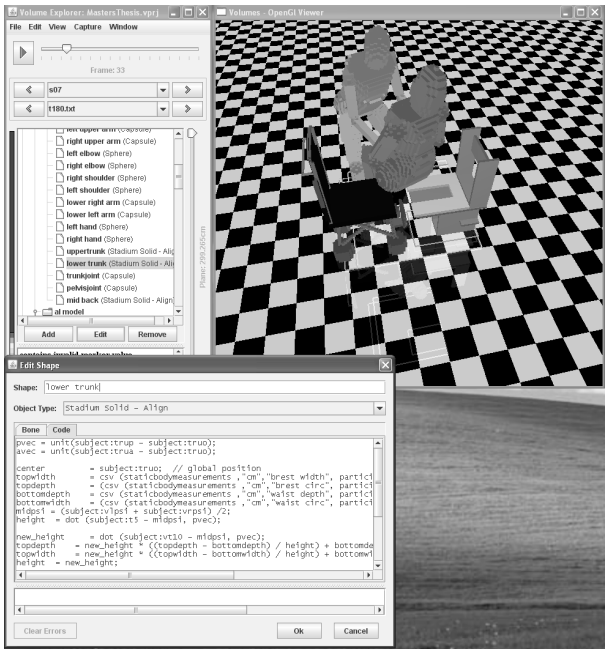

Figure 31 – Screen shot of user interface of the spatial modeling software

Custom spatial modeling software was developed to conduct the spatial analysis in the attached thesis. A screenshot of this software is shown above in Figure 31. This appendix outlines key aspects of the software's design and implementation. As a whole, the software was designed to be a general tool to facilitate the investigation of the spatial requirements of any dynamic task recorded using motion capture equipment.

A core goal underlying the spatial modeling software was to develop general-purpose software that enables the percentile spatial volume requirement questions to be investigated using dynamic motion capture data and static measurements as inputs. The spatial volume of objects of interest, "volume objects", is modeled for each frame of motion capture data. The volume objects themselves are modeled as

a collection of geometric bounding solids. The position, dimensions, and orientation of each of the geometric bounding solids are dynamically defined for each frame of motion capture data through the execution of a custom computer language designed explicitly to describe the geometric bounding solids. A user's guide for the custom programming language used to define the position, dimensions, and orientation is in Appendix D. By defining the properties of the geometric bounding solids for each frame of motion capture data, the position, dimensions, and orientation of the solids can be modified per-frame to best model the actual volume of the underlying physical system. The percentile spatial volume used across a trial is modeled and reported as a collection of planar area intersection maps taken at multiple discrete heights parallel to the floor. Each of the respective maps represent the percentage of time that each respective area in the map was inside the volume described by the volume model across one or more motion capture trials. By examining spatial maps taken across a range of heights, the percentile spatial volume requirements of a task can be both visualized and analyzed.

Overview

The software was developed using the model-view paradigm and a multi-language approach to leverage the strengths of both C++ and Java. The underlying model and the three-dimensional visualization components were written in C++; approximately 12,000 lines of source code. The user interface, "view", and the parsing engine were written in Java; approximately 8,000 lines of source code. Java Native Interfaces (JNI) were used to connect the managed Java user interface (UI) to the underlying native C++ model within a single process. Existing code bases and generative programming techniques were used whenever possible to reduce the time

associated with development and debugging; improve execution performance; and support greater software portability. As a whole, the software was developed as a collection of component blocks. A high-level block diagram for the software is pictured in Figure 32.

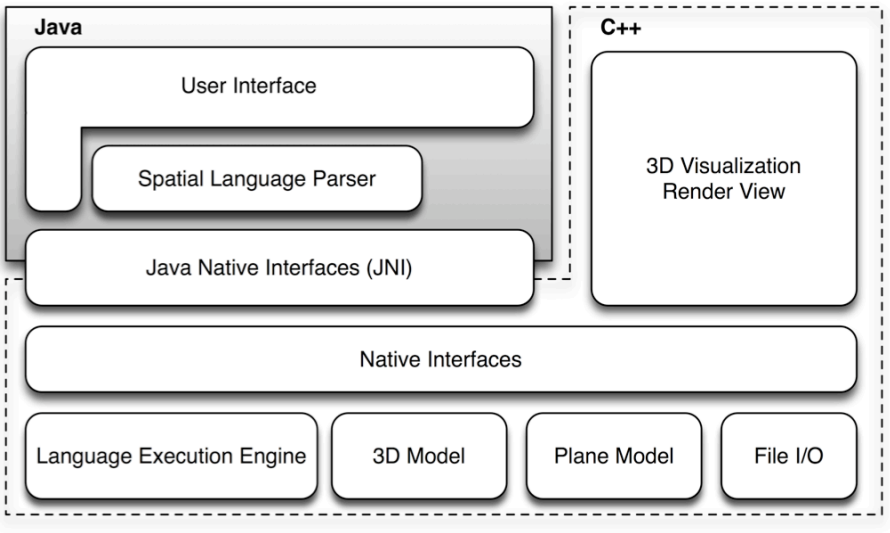

Figure 32 – High-level block diagram of the spatial modeling software

The User Interface (UI) and Spatial Language Parsing components were developed in Java. The UI enables the user to define and debug spatial model parameters, volume objects, and references objects and to interact with the model's properties visually. The UI was implemented using Java's cross platform Swing UI framework. To define the position, dimensions, and orientation of objects, the user describes these properties of the objects comprising the volume model in the Spatial Language, a custom computer language. The Spatial Language Parser component translates the user-generated Spatial Language into a representation that can be efficiently executed in C++. Appendix D describes the Spatial Language and describes the implementation of both the Java and C++ language processing components.

The Java Native Interface (JNI) and Native Interface components are the glue layer that binds the Java language based components to the native C++ based components. All cross-language communication is marshaled through these layers.

The Three-Dimensional Visualization and Render View displays three-dimensional graphical representations of the volume model for single motion capture frames, across entire motion capture trials, and across multiple motion capture trials. In addition to displaying the three dimensional volume, this component also visualizes the percentile planar area of intersection that occurs between the volume model and a plane of interest. This component was written in C++ using the OpenGL graphics library to provide cross-platform hardware accelerated rendering.

The Language Execution Engine component executes Spatial Language execution streams generated by the spatial language parser. Both the Three-Dimensional Model and Plane Model components use the language execution engine component to define the position, dimension, and orientation of the three-dimensional objects comprising the volume model for each frame of motion capture data. The Language Execution Engine component is used by the Three-Dimensional Visualization component to render reference objects.

The Three-Dimensional Model component models the spatial volume used by the volume objects comprising the volume model. The working memory of the model is separate from that used by the Render View. As such, most volume model operations do not affect or interrupt model visualization.

The Plane Model component is the core component that implements the two-dimensional volume object-plane intersection testing. Like the related Three-Dimensional Model component, the working memory for the Plane Model is separate from that used for visualization.

The File I/O component performs abstract read/write operations from CSV (comma separated value) motion capture data files. This component provides the framework for both the internal model's and Spatial Language's access to these data files. On access, CSV data files are completely loaded into memory and cached using a smart pointer, queue-based caching algorithm.

Geometric Bounding Solids

The spatial volume required for complex three-dimensional objects is modeled as the union of the volume required by a set of core geometric bounding solids. The dimensions, position, and orientation of each geometric solid are determined at run time through execution of the solid's attached Spatial Language code. The spatial modeling software supports modeling convex geometric solids, and the software has built-in support for the following basic solids: boxes, tapered boxes, tapered aligned boxes, capsules, cones, cylinders, domes, ellipsoids, spheres, stadium solids, aligned stadium solids, and a custom foot object. A subset of these geometric solids is pictured in Figure 33.

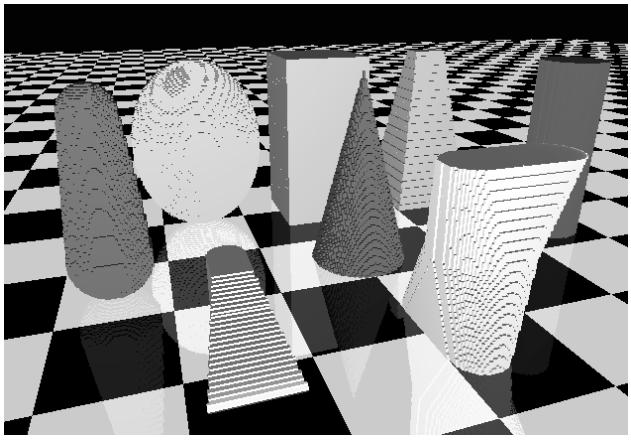

Figure 33 – A subset of the geometric solids supported by the spatial modeling software, visualized using the spatial modeling software (left to right): capsule, ellipsoid, box, and tapered box (back row); capsule, cone, and cylinder (middle row); custom foot object, and aligned stadium (front row)

Internally, the geometric solids are implemented in C++ as members of a single inheritance class hierarchy. At their core, the spatial volume described by a geometric solids class is defined through the implementation of two core methods, a "bounding box" method which returns a bounding box for the solid in the solid's local coordinates and an "inside" method which returns "true" if a test point in the solid's local coordinates is inside the volume described by the solid. Defining the geometric solid's spatial volume in its local coordinate system allows both the bounding box definition and intersection test to be agnostic to the solid's global position and orientation. This separation allows the solid to be defined within its local coordinate system in an orientation that minimizes the computational costs associated with determining the intersection status of a point and the solid's bounding box. Figure 34 shows a two-dimensional graphical representation of how complex volumes could be described from a set of geometric solids.

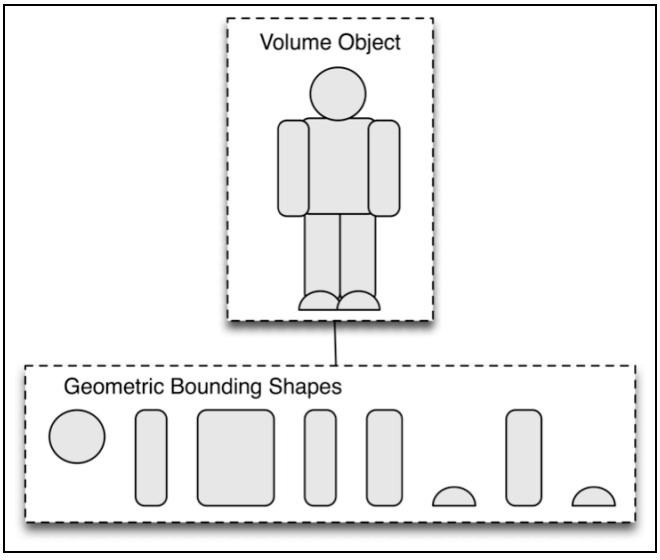

Figure 34 – Volume objects are represented as a union of the core geometric bounding solids.

Percentile Planar Intersection Map

A percentile planar intersection map represents the percentage of time a specific area at a specific height above the floor is occupied by volume objects. Percentile planar intersection maps can represent the spatial area occupied across one motion capture trial or the mean percentile occupation across multiple trials.

To construct a percentile planar intersection map, a height from the floor is designated. Starting with the first motion capture trial of interest, planar intersections for all visible volume objects are then calculated across motion-captured frames of interest. The result of this is a set of binary planar intersection maps, one for each motion capture frame, each designating the area in the plane that intersected with a volume object (Figure 35). The binary planar intersection maps are then integrated and normalized into a single map representing the relative percentage of time that a given area in map was occupied (Figure 36). Averaging the percentile planar intersection maps for the trials of interest creates multi-trial mean percentile planar intersection maps.

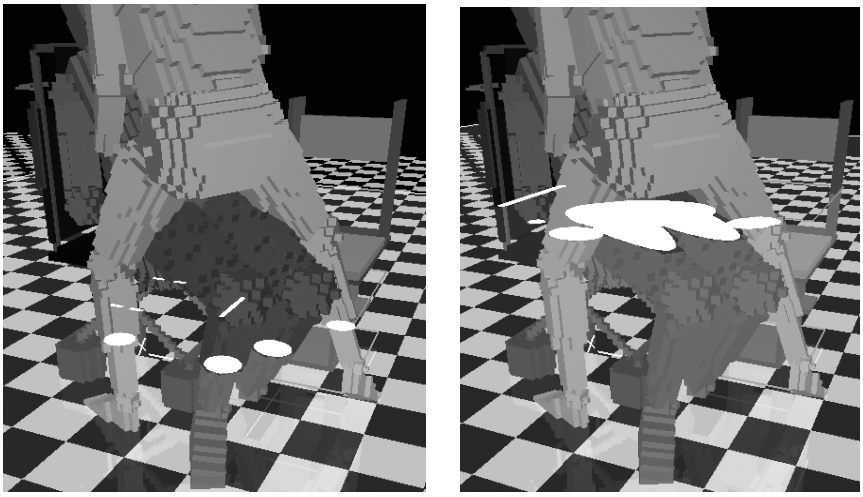

Figure 35 – Visualization of the binary area occupied by the participant, wheelchair, and dummy for a single frame at two experimental heights. The area of intersection is illustrated in white.

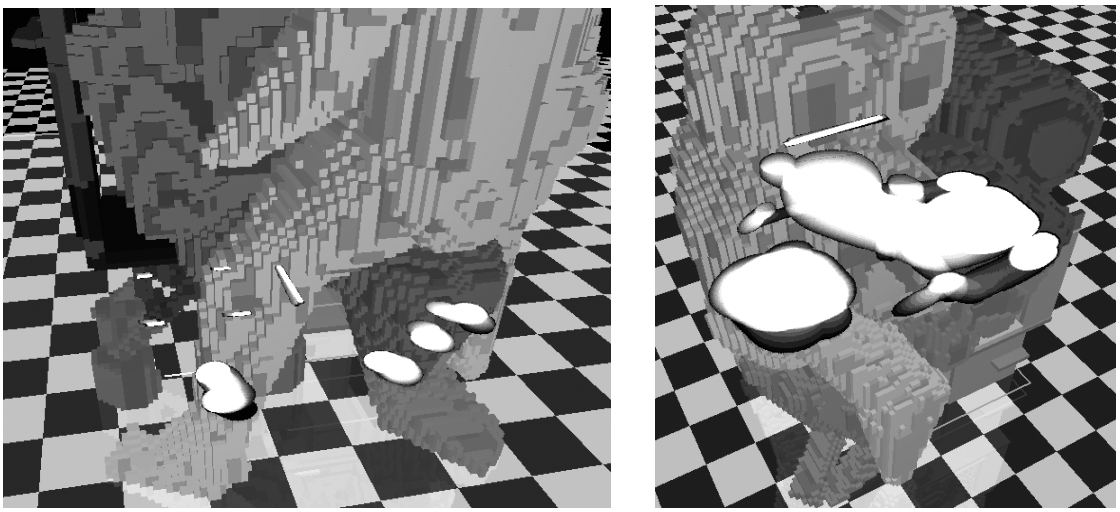

Figure 36 – Percentile planar intersection map taken below and above the knee for a single trial.

The key algorithmic step in terms of both complexity and efficiency during percentile spatial map creation is the determination of the binary area of intersection for a single frame of motion capture data between the plane and the geometric solids comprising a volume object. The first step in determining plane-solid intersections is to test if the geometric solid's bounding sphere and the plane intersect. If a plane-bounding sphere intersection does not occur, then no further plane-solid intersection testing is done. Otherwise, if an intersection occurs, then the geometric bounding solid's axis-aligned bounding box is computed in global coordinates and projected onto the plane. The rectangular region defined by the projection is then tested using one of three algorithms for intersection with the geometric bounding solid. The algorithm used is determined based upon characteristics of the geometric bounding solid. The algorithms will be described from least to most complex.

The algorithm with the lowest complexity is the least efficient but most general in computing plane-solid intersections between both convex and concave geometric

bounding solids. This algorithm has a Big (O) efficiency of approximately N^2. Assuming an N x N projection, this algorithm requires approximately N^2 comparisons. Solid-plane intersections are computed by stepping through each point in the plane within the rectangular region defined by the geometric solid's bounding box projection. The global position of each of the test points is then transformed into the local coordinates of the geometric bounding solid and tested for intersection with the solid using the solid's "inside" method.

The algorithm of intermediate complexity computes intersections between bounding box projections from convex geometric solids and the plane. This algorithm has best to worst case Big-O efficiency of N to N^2. Solid-plane intersections are computed by identifying the leading and trailing edge for each scan line in the solid's axis-aligned bounding box projection. After identifying the leading and trailing edge positions, all points in between the two edge points are marked as intersecting. The key advantage here is that points in between the two edge positions can be marked as intersecting without conducting further intersection tests. Similar to the basic algorithm, to test if a point in the plane intersects with the geometric solid, the global position of the point in the plane is determined and transformed into the local coordinate system of the geometric solid. The geometric solid's "inside" method is then used to test the point for an intersection in the local coordinate system of the solid. Two algorithms are used to efficiently identify the leading and trailing edges.

If no previous leading edge position has been identified, then a breadth-wide search of the scan line is conducted to search the scan line for a point of intersection with the solid. Best case, this search will locate the solid on the first comparison resulting in a single intersection test. Worst case, the solid will not intersect with the scan line and every point will be tested resulting in N comparisons. A breadth-wise

search is used based upon the heuristic that the mid-point of the scan line is a likely point of intersection and that points near each other are likely to have a similar solid intersection status. Upon finding a point of intersection, a binary search is used to identify the leading and trailing edge on the scan line. The binary search will identify both edge positions using a worst case of $Log_2 N$ companions. With no prior knowledge, the leading and trailing edge along a single scan line can thus be found with a best case of approximately $Log_2 N + 1$. The worst case of no intersection will again result in N comparisons. On finding the leading edge position, the position of the leading edge in the scan line is cached.

If a prior leading edge position was identified, it is assumed that an adjacent scan line will have a similar leading edge position. Using the old leading edge position as a starting heuristic position, the 5 points on either side of the cached position are sequentially tested as leading edge points. If a leading edge point is identified, then a binary search is used to identify the trailing edge. If, after ten comparisons, no leading edge point is found, the algorithm reverts to the previously described breadth-wise search heuristic. Using this algorithm, optimally the leading edge is found using an average of 5 comparisons and the trailing edge is identified using $Log_2 N$ comparisons.

The algorithm with the greatest complexity uses ray tracing to directly compute the geometric bounding solid's edge positions for each scan line. This algorithm has a best and worst case Big-O efficiency of N and, unlike the previous two algorithms, does not call the solid's "inside" method. The algorithm works by mathematically solving for the leading and trailing edge intersection points of the geometric bounding solid along each scan line. If edge points are identified, points in the scan line between the edge points are marked as being points of intersection

without further intersection testing. To directly solve for the given scan line's leading and trailing edge points, a vector describing the scan line is computed by converting the two points along the scan line into the solid's local coordinate system. The geometric bounding solid's edge is then expressed as one or more parametric equations and the intersection points of the scan line's vector and the solid's parametric equations are solved for. This technique is used to compute sphere, ellipsoid, cone, cylinder, and capsule intersections.

Visualization of a Volume Object's Three Dimensional Volume

The spatial modeling software produces visualizations of the spatial volume used during a single frame of motion capture data, across an entire motion capture trial, and the percentile spatial volume used across multiple motion capture trials. Three separate algorithms were written to visualize each of these unique spatial volumes.

Single Motion Capture Frame Visualization

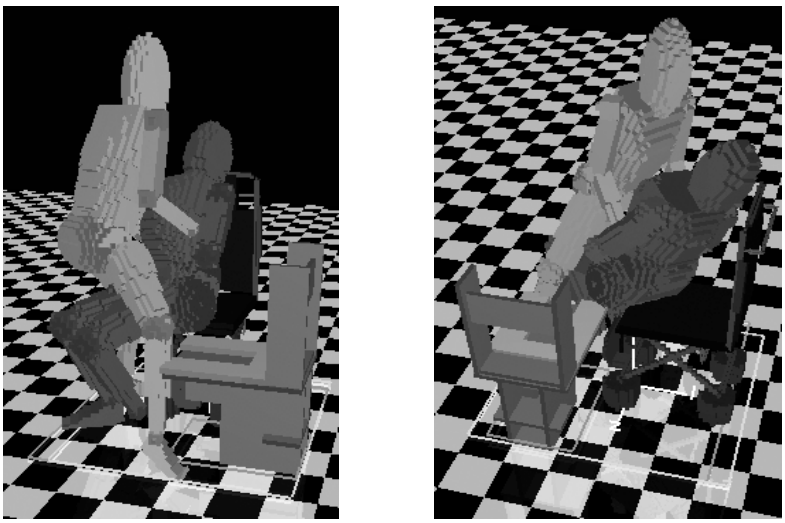

Figure 37 – Graphical representation of the assisted transfer three-dimensional model.

To visualize the spatial volume used during a single frame of motion capture, each of the geometric solids making up each of the volume objects is rendered independently (Figure 37). To render a given geometric solid, two planar height maps are created. The planar height maps generated represent the respective maximum and minimum heights of the geometric solid in its local coordinate system. To visualize the volume defined by the two height maps, the rendering environment's coordinate system is transformed into the local coordinate system of the geometric solid. Scaled rectangular volumes are then drawn between the two height maps at each position within the height map. While all the geometric solids used as bounding volumes are convex, a key limitation of this technique is that it is only a valid technique for convex geometric solids. Concave solids can have more then two edge positions for any X, Z pair and thus cannot be described completely using just two planar height maps (Figure 38).

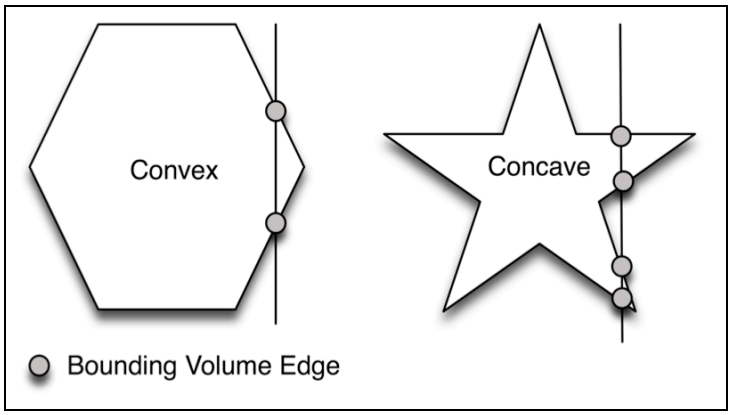

Figure 38 – Convex geometric solids have only two edge points (top and bottom), concave solids can have more than two.

Single Trial Visualization

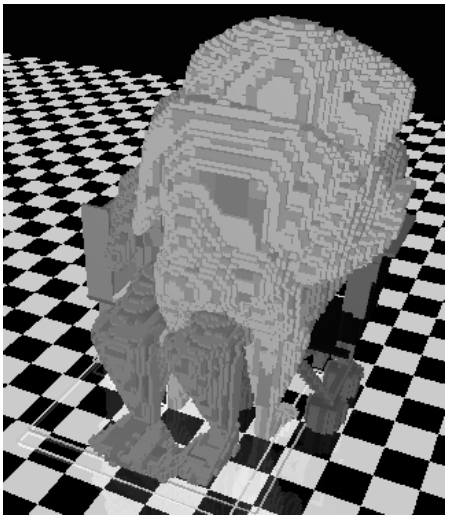

Figure 39 – Graphical representation of the total volume of a single trial of assisted transfer.

The total spatial volume required across an entire motion capture trial is modeled by combining the spatial volumes used across each motion capture frame in an adaptive oct-tree volume model (Figure 39). To store a single motion capture frame in the oct-tree, the parameters for each volume object and their associated geometric bounding volumes are initialized. Following initialization, the volume object's volume is modeled by adding each of the geometric bounding solids comprising the volume object to the adaptive oct-tree. To reduce the oct-tree's total memory requirement, only the volume occupied by the total volume object is tracked.

The oct-tree data structure is a tree data structure that's root node is a cube bounding the entire motion capture volume. Each node in the oct-tree data structure defines eight equal-sized, non-overlapping, cube-shaped child nodes, each describing a unique sub-volume of the parent node. To store the volume defined by a geometric bounding solid in the oct-tree data structure, starting with the root node, the oct-tree's nodes are recursively tested for intersection with the geometric bounding

solid. At the root level, this intersection test in effect tests for an intersection between the geometric solid and the entire motion capture volume. If an intersection occurs, then the tested oct-tree node is marked as intersecting with the geometric object and the test is repeated on each of the child nodes, eight total, not already marked as touching the volume object. The recursive step of this algorithm is repeated until the tested node's volume falls completely within the geometric bounding primitive, completely outside, or the node is sufficiently small and intersects the geometric bounding primitive's volume. Leaf nodes intersecting the geometric bounding solid are marked as touching the volume object. Figure 40 represents a two-dimensional version of the oct-tree generated to touch the area in grey with a level 4 sub-division, resulting in nodes being sufficiently small to be classified as "touching" the volume.

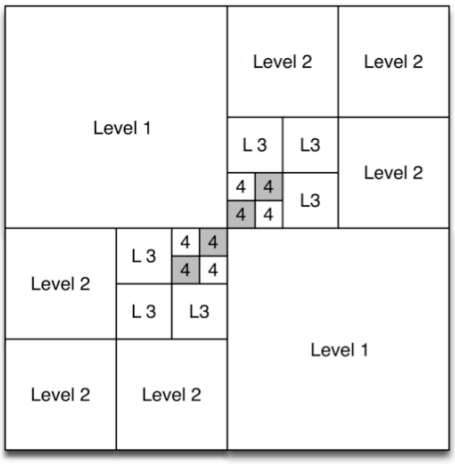

Figure 40 – A two dimensional representation of the oct-tree expanded to describe the nodes in grey is shown below, the numbers within each node represent the node's level of sub-division

To reduce the oct-tree's total memory requirement and improve it's rendering efficiency, the oct-tree's nodes are designed to adaptively recycle their leaf nodes when the child nodes for a given node all touch the same set of volume objects. This adaptive leaf node pruning step occurs as part of the geometric bounding solid's oct-

tree intersection testing after a node's child nodes have been tested for intersection with the geometric bounding volume. This pruning of the volume model allows the oct-tree to be adaptively collapsed as multiple volume bounding solids fill in an object's volume for a given frame of motion capture data or as the volume object moves through space across multiple frames of motion capture data. Figure 41 demonstrates this in two dimensions using a quad-tree. When the bounding area is positioned over the quad-tree at frame one, twenty-nine nodes are allocated at the conclusion of node expansion (L1 = 1, L2 = 4, L3 = 8, L4 = 16). For frame two, the bounding area is moved right resulting in the entire L1 space being marked and thus the recycling of its 28 child nodes.

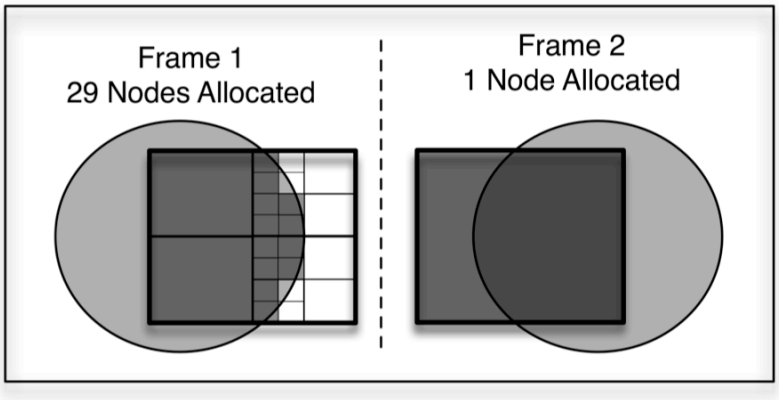

Figure 41 – A two-dimensional representation of an adaptive oct-tree.

Once the adaptive-oct-tree's volume has been defined, the visualization of the volume can be accomplished by recursion. Starting with the root node of the oct-tree, nodes marked as intersecting a volume object are entered, and nodes marked as touching the volume object are visualized. To visualize a given node, a cube with the global position and dimensions of the node is drawn using OpenGL.

Percentile Spatial Volume used Across Multiple Motion Capture Trials

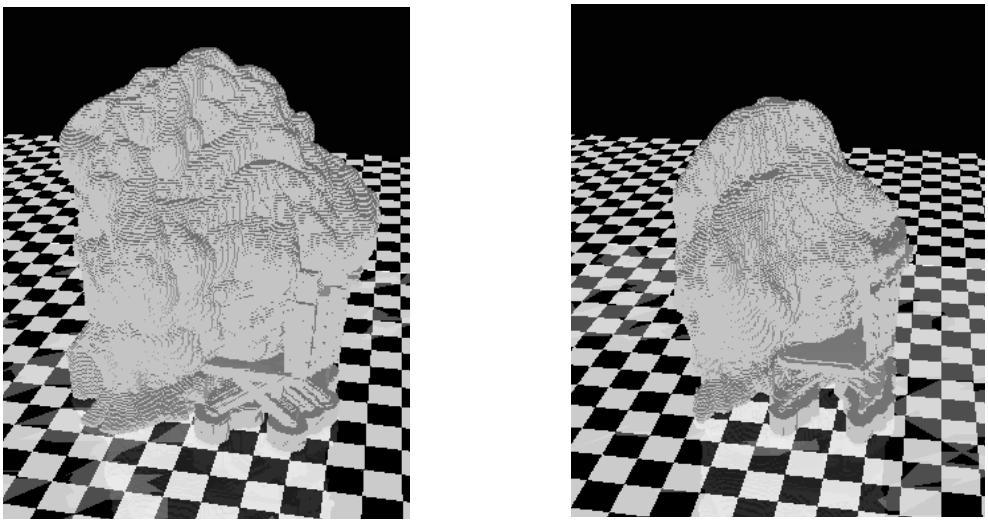

Figure 42 – Total spatial volume and 95% spatial volume for 29 assisted transferors conducting two assisted transfers between the wheelchair and toilet at the 90° wheelchair-to-toilet angle.

The percentile spatial volume used by one or more participants across one or more trials is visualized by creating percentile planar intersection maps at a selection of heights from the floor across the desired spatial volume (Figure 42). Using the planar intersection maps, the percentile volume is rendered using a voxel spatial representation by assuming that the volume between two planes is used if the area described by a given (X, Z) position in both planes is used at the desired percentile threshold. The occupied space between contiguous planes is then rendered as box-shaped voxels. To accelerate rendering for a given percentile threshold, vertically adjacent voxels are cached and rendered as a single large voxel.

Implementing Spatial Language Parser and Execution Engine

The spatial language is a context free computer language designed to facilitate the dynamic description of the position, dimensions, and orientation of geometric bounding solids for each frame of motion capture data. Context free

languages are commonly used to provide a powerful descriptive language for human computer control; C++, Java, Pascal are all examples of context free computer languages. However, while common, the implementation of these language parsers is far from trivial. Parsing has received considerable attention in both academic and commercial circles and, at this point, is a well-understood design problem [1]. Numerous generative programming tools have been created to generate custom language parsers based upon a language grammar [2].

The spatial language interpreter was implemented as two distinct components, a Java based language parser which translates raw spatial language source code into a tokenized polish notation style tokenized execution stream that can be efficiently read and executed in C++ using a stack-based execution. The Java based component is run once for each code segment to generate the code segment's execution stream. The resulting execution stream is repeatedly executed in C++, once for each modeled frame, to define the position, dimensions, and orientation of the code segment's respective geometric bounding solid.

Implementing the Java Component

Traditionally, context free language parsing is thought of as being composed of two discrete tasks, lexical analysis and language parsing of the lexical output. During lexical analysis, the white space in the input stream is removed and the raw characters composing an input stream are blocked into a series of descriptive tokens.

---

[1] Aho, A.V., Sethi, R., Ullman, J.D. 1986. Compilers: Principles, Techniques, and Tools. Boston: Addison Wesley.

[2] Generative programming tools for language parsers: ANTLR, Lex and Yacc, Flex and Bison

To interpret the meaning of the tokens within the resulting token stream, the token stream is parsed by the parsing component into a parse tree based upon the language's grammar. Grammar elements are executed as grammar elements are matched. A number of generative programming tools have been developed to accelerate development of both the lexical analysis and language parsing components of language parsers. Examples of these tools include lex, yak, visul, flex, bison, and ANTLR (ANother Tool for Language Recognition). Both the lexical analysis components and language parsing components of the Java based component were developed using the ANTLR parser generator.

Generative programming tools define lexical tokens as a collection of regular expressions. A partial example of an ANTLR regular expression used to define floating point numbers in the spatial language is "DIGIT: '0'..'9'; NUMBER : (DIGIT+ | DIGIT* '.' DIGIT+)". This definition first describes a digit as being the characters that range from '0' to '9'. The definition then describes a number as being first composed of either one or more digits or zero or more digits, followed by a '.', followed again by one or more digits. Using a set of unique regular expressions as input, the generator creates source code for a custom lexical analyzer that accepts a raw character input stream and returns a stream of descriptive tokens. By limiting tokens to a set of unique regular expressions, the lexical analyzer can provably translate the character input stream into a token stream using a constant amount of memory. Figure 43 shows a graphical representation of the input and output of lexical analysis.

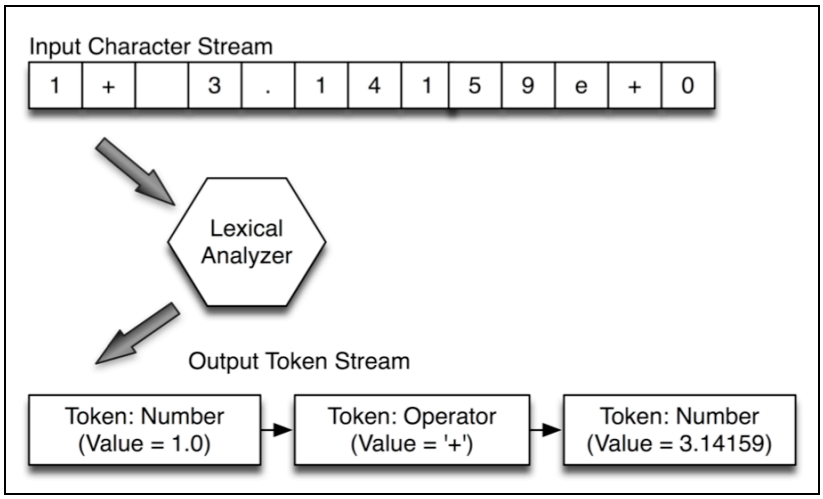

Figure 43 – Lexical analysis, conversion of the input stream into token blocks.

Once tokenized, the context free language described by the tokens is parsed into a parse tree and interpreted using the language's parser. Parser generators for context free languages, e.g. ANTLR, generate custom source code for language parsers based on an input language grammar. The input grammar both describes the context free language as a series of nested language constructs and provides mechanisms through which custom source code can be inserted into the parser and executed as language constructs are parsed. An example of the ANTLR syntax used to identify function calls in the spatial language is:

```
function: IDENTIFIER '(' ( expr (',' expr)* )? ')'  { printf ("Expression Parsed\n"); }
```

This syntax, describes a function definition as being an identifier token, followed by a '(' token, zero or more comma separated expressions, and terminating with a ')' token. An important aspect of this is that the expression syntax, not shown, defines expressions as being arithmetic, variables, and function calls. This recursive definition allows the token parser to decode nested function calls of arbitrary complexity and construct a parse tree that captures the order of construct execution. In the above example, a C style printf statement has been embedded into the

grammar statement. When the parser matches the function grammar definition the embedded C code will be called. While the C printf statement isn't terribly interesting, this ability to embed source code into the grammar that is conditionally executed when language constructs are parsed is what gives these tools their real power. Unlike lexical analysis, parsing of a context free language requires an undefined amount of memory.

C++ Spatial Language Parser

The Java based spatial language parsing component translates raw spatial language source code into a tokenized polish notation style tokenized execution stream. The stream is generated through a pseudo execution of the spatial language in the Java based parsing component. During pseudo execution, the Java based parser generates a stream of tokens to represent the operations that were to have been conducted in the order they were to have been conducted. The execution stream is passed to the C++ component using JNI (Java Native Interfaces). The C++ based parser then executes the execution stream associated with each geometric solid to define its position, dimensions, and orientation based upon a given frame of motion capture data. The C++ based parser executes the execution stream using a simple stack-based execution paradigm, executing the commands in the order they occur within the stream. Figure 44 shows a graphical representation of the parser's execution starting from the input stream and culminating in execution.

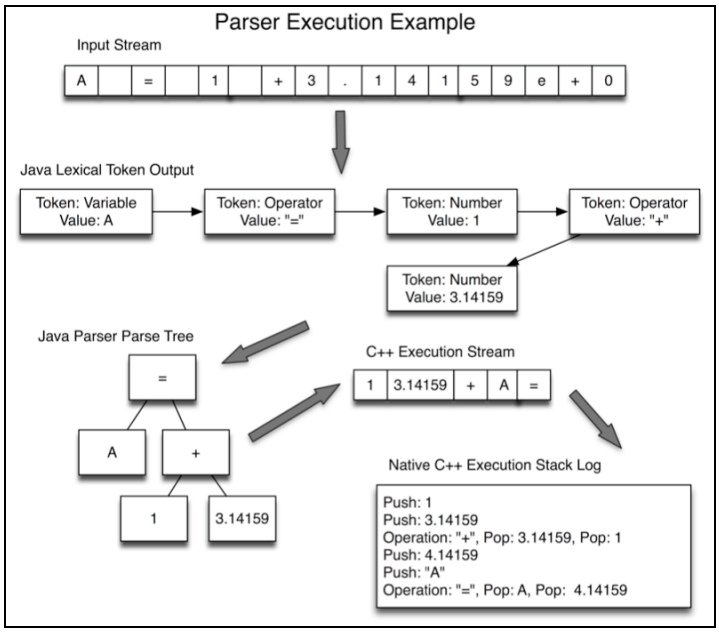

Figure 44 – The stages of parsing, raw text, lexical analysis, generation of parse trees, creation of the optimized C++ execution stream, and finally stack based execution.

Antler 3 Spatial Language Grammar

The Java component of the spatial consumption language interpreter was developed using the ANTLR 3.0 parser generator. The core grammar for the Java lexical analyzer and parser components is listed below.

```
//------------------------------------------
//  PARSER
//------------------------------------------
/*          Defines Expression Syntax  All Expressions are Assignments      */

mstat   :sourceline*;
sourceline : topstat->^(LINE topstat);
topstat :IDENTIFIER '=' hiddenStat ';' -> ^('=' IDENTIFIER hiddenStat) | function ';' -> function;

hiddenStat        : (IDENTIFIER '=')=> (IDENTIFIER '='^ hiddenStat) | expr;

/*          Defines Vectors and Vector Opps           */
vector        :   '[' vectoritem (',' vectoritem)* ']' -> ^(VECTOR vectoritem*);
vectoritem   :     expr -> ^(VITEM expr);

/*          Defines Expressions      */
expr      : (term -> term) (('+' i=term -> ^('+' $expr $i)) | ('-' i=term -> ^('-' $expr $i)) )*;
term      : power (('*' power)=>('*'^ power)  | ('/'^ power))*;
power               :  uminus ('^'^ power)?;
```

```
uminus          :  ('-' uminus) -> ^(UMINUS uminus) | atom;

atom    :       HEX     |     NUMBER  | (function)=>function |'('! expr ')'!  |  IDENTIFIER |
        vector |  STRING;

/*      Defines Functions       */
function :      IDENTIFIER '(' ( formalParameter (',' formalParameter)* )? ')' -> ^(FCALL
IDENTIFIER formalParameter*);
formalParameter :       (expr)=>expr -> ^(EPARAM expr);

//-------------------------------------------
//  LEXER
//-------------------------------------------

NUMBER          :       (DIGIT+ | DIGIT* '.' DIGIT+)(('E' | 'e')('+' | '-')?DIGIT+)?;
HEX     :       ('0x')(DIGIT | ('a'..'f') | ('A'..'F'))+;
IDENTIFIER :    ('_' | LETTER)('.' | ':' | '_' | LETTER | DIGIT)*;
STRING          :       '"' ~('"' | '\r' | '\n')*  ('"'| '\r' | '\n');
SL_COMMENT :    ('//' ~('\r' | '\n')*) { $channel = HIDDEN; };
ML_COMMENT :    '/*' (options {greedy=false;} : .)* '*/' {$channel=HIDDEN;};
WHITESPACE :('\t' | ' ' | '\r' | '\n' | '\u000C')+ { $channel = HIDDEN; } ;
fragment LETTER         :       'a'..'z' | 'A'..'Z';
fragment DIGIT :        '0'..'9';
```

Appendix D

Spatial Consumption Language Programming Guide

Language Overview

The spatial consumption language is a high-level interpreted scene definition language designed to define the position, dimensions, and orientation of both volume and reference objects for each frame of motion capture data based on motion capture marker data and static measurements. Volume objects are defined as a set of geometric bounding solids and the spatial volume enclosed by these solids defines the volume object's spatial volume. Reference objects provide visual references as part of both three-dimensional volume visualizations and two-dimensional planar visualizations. While these objects are drawn as reference points, the spatial volume contained within them is not tracked.

End of Line and Comment Syntax

The spatial consumption language uses the same end-of-line and comment syntax as those used in both Java and C++. Semicolons ';' designate the end of source code lines. Comments allow non-interpreted text to be included with the source. The language supports both C++ style single-line and multi-line commenting. The syntax for single-line commenting is '//'. The syntax for multi-line comments wraps the desired lines in '/*' and '*/' operators. Examples of these two comment styles are shown in Table 13.

Table 13 – Examples of comment syntax

```
A = 1 + 2; // Single Line Comment

/*  This
    Is an example of a Multi-Line
    Comment*/
```

Variable and Types

The language has no structured notion of variable type. Variable type is automatically determined internally on assignment. The language is not case sensitive; variables such as “VARIABLE_1” and “variable_1” reference the same internal variable. Variables are defined at their declared source hierarchy level using the “=” operator and can be reassigned using the “=” operator. The left side of the “=” operator must reference a valid variable name. Similar to C++, the “=” operator supports multiple variable assignments, allowing assignment statements to be chained together. Liberal usage of variables is encouraged and will result in slightly higher performance execution (Table 14).

Variables can reference numbers, strings, and vectors of numbers. Variables are always copied by value and passed into functions by value. The language has no support for references, pointers, and dynamic memory outside what is provided internally through the built-in string and vector types. Beyond variable assignment with the “=” operator, each variable type supports a type-specific operator set.

Table 14 – Examples of variable usage

```
Superior                    Inferior
A = 1 + 2;                  PrintLn (1+2);
Println (A);                PrintLn (1+2);
Println (A);

Functionally Equivalent Statements
A = 1 + 2;                  A = B = 1 + 2;
B = A;
```

Numbers

Syntactically, numbers can be expressed as integer values in hexadecimal or decimal format and as floating point values in decimal format (Table 15). Regardless of input format, numbers are stored internally as 32-bit double-precision floating-point numbers and all arithmetic is computed using double-precision floating-point arithmetic.

Table 15 – Examples of correct number syntax

Expression	Result
123	123.0
123.00	123.0
1.23e2	123.0
0x7B	123.0

The numeric data type supports traditional arithmetic operators: + (addition), - (unary minus), - (subtraction), / (division), * (multiplication), ^ (power), and ( )(precedence). Traditional operator precedence rules apply (Tables 16 – 17). Operators having equal precedence are executed left to right.

Table 16 – Operator precedence (first to last executed)

1: precedence
2: unary minus
3: power
4: multiplication and division
5: addition and subtraction

Table 17 – Examples of expression and resulting value based upon operator precedence

Expression	Result
123 + 0x7B + 10.0	256
123 - 0x7B – 10	-10
10 / 2 * 4^0.5 * 2	20
5^2	25
(2+3) * 4	20

Strings

Strings represent arbitrary-length character sequences and are used as input variables for I/O routines to specify file name paths, column names, and debug output messages. Static strings are syntactically declared by quoting the desired character sequence (Table 18). Escaping characters such as tab or quote characters are not supported and strings cannot extend beyond one source line. Internally, strings are represented as a vector of 8-bit ASCII characters. Unicode is not supported. The "+" operator is supported for concatenation and can be used to append strings, numbers, and numeric vectors to a string.

Table 18 – Examples of string syntax

Expression	Result
"Hello World"	"Hello World"
"Hello " + "World"	"Hello World"
"Number " + 1	"Number 1.0"

Numeric Vectors

Numeric vectors are arbitrary-length sequences of numbers. Typically, numeric vectors are used to represent three positions and orientations. When used as position vectors, vector indices 0, 1, and 2 correspond with the X, Y, and Z coordinates. Syntactically, numeric vectors are declared by the following syntax, [A, B, C, D, …. Nth], where A corresponds to the first element in the vector. When declared, each element of the vector's declaration can be a: number, equation, or function call that returns a number.

Numeric vectors support arithmetic operators. The precedence properties of the vector operators are identical to the precedence of the corresponding numeric operators. The usage and meaning of the operators is as follows. Unary minus, '-',

negates the values contained in the vector. Addition, '+', and Subtraction, '-', operators take two vectors of identical size and return a vector in which the corresponding elements of the two input vectors have had the desired operation conducted on them, e.g. [2, 3, 4] – [1, 0, 4] results in [1, 3, 0]. Multiplication, '*', and division,'/', are supported as numeric vector-number operations. These operations return a vector in which the elements of the new vector have been computed as outlined in the example below (Table 19).

Table 19 – Examples of numeric vector arithmetic

Expression	Result
A / [v1, v2, v3]	[A/v1, A/v2, A/v3]
[v1, v2, v3] / A	[v1/A, v2/A, v3/A]
A * [v1, v2, v3]	[A*v1, A*v2, A*v3]
[v1, v2, v3] * A	[v1*A, v2*A, v3*A]

Volume Objects

Volume objects define the objects for which spatiotemporal volume is tracked across one or more frames of motion capture data. Volume objects themselves are defined as collections of geometric bounding solids. Each geometric solid's object has two code blocks: a "bone" and a "code" section. For a solid's volume to be tracked, both the bone and code sections must execute without error.

The "bone" section defines the solid's orientation. Spheres are the only geometric bounding solid that does not require a bone definition, as they have no orientation. The orientation of a solid is defined through the definition of two vector variables, "LongAxis" and "MinorAxis". The long axis refers to the vector orientation of the long axis of the solid. Since the spatial volume of capsules, cylinders, and cones is unaffected by rotation about the long axis, they only require a long-axis definition to define their orientation. For solids such as stadium solids, ellipsoids, and

cubes that are affected by rotation about the long axis, a second vector, “MinorAxis” should also be defined. The only requirement for this second vector is that it not be parallel with the “LongAxis” vector. Note that there are no requirements for the length of either the “LongAxis” vector or the “MinorAxis” vector; the sole purpose of these vectors is to define the orientation of the solid.

A geometric solid’s “code” section defines the solid’s position and dimensions. Each solid has a unique set of required variable definitions. All solids, except for aligned stadium solids and aligned boxes, are defined about a center point located at the midpoint of the solid’s long axis; a box having side lengths (1,1,1) would have its virtual local center at (0,0,0) and side dimensions would extend from (-0.5 to +0.5) along each axis. The global position of this center point is defined by assigning the point’s desired global position vector to the “Center” variable. Aligned solids use the global center point to define the aligning point. The variable “LocalCenterOffset” is an optional vector parameter for all solids except spheres that describes a 3D translation performed on the solid prior to orientation with the bone rotation matrix. The primary purpose of this setting is to enable the definition of solids that rotate around a point other than their center. Source code examples for both “bone” and “code” blocks follow the internal function reference section.

Box

Variables	Type	Definition
Center	Vector	Global position of the center of the solid
Local Center Offset	Vector	Translation applied to the solid prior to bone orientation; modifies the center of rotation
Width	Number	Width of the box along its minor axis
Depth	Number	Depth of the box
Height	Number	Height of the box along its long axis

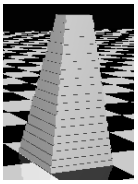

Tapered Box

Variables	Type	Definition
Center	Vector	Global position of the center of the solid
Local Center Offset	Vector	Translation applied to the solid prior to bone orientation; modifies the center of rotation
TopWidth	Number	Top width of the box along its minor axis
TopDepth	Number	Top depth of the box
BottomWidth	Number	Bottom width of the box along its minor axis
BottomDepth	Number	Bottom depth of the box
Height	Number	Height of the box along its long axis

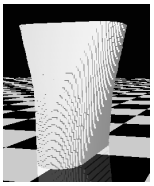

Stadium Solid

Variables	Type	Definition
Center	Vector	Global position of the center of the solid
Local Center Offset	Vector	Translation applied to the solid prior to bone orientation; modifies the center of rotation
TopWidth	Number	Top width of the stadium solid along its minor axis
TopDepth	Number	Top depth of the stadium solid
BottomWidth	Number	Bottom width of the stadium solid along its minor axis
BottomDepth	Number	Bottom depth of the stadium solid
Height	Number	Height of the stadium solid along its long axis

Solid Code Block Reference (Continued)

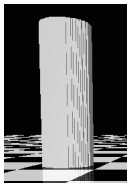

Cylinder

Variables	Type	Definition
Center	Vector	Global position of the center of the solid
Local Center Offset	Vector	Translation applied to the solid prior to bone orientation; modifies the center of rotation
Height	Number	Height of the cylinder along its long axis

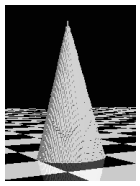

Cone

Variables	Type	Definition
Center	Vector	Global position of the center of the solid
Local Center Offset	Vector	Translation applied to the solid prior to bone orientation; modifies the center of rotation
Height	Number	Height of the cone along its long axis
Radius	Number	Radius of the base of the cone
Up	Boolean (True/False)	Does the long axis point in the direction of the cone's tip (True) or its base (False)?

Ellipsoid

Variables	Type	Definition
Center	Vector	Global position of the center of the solid
Local Center Offset	Vector	Translation applied to the solid prior to bone orientation; modifies the center of rotation
XRadius	Number	X-axis radius of the ellipsoid along its minor axis
YRadius	Number	Y-axis radius of the ellipsoid along its long axis
ZRadius	Number	Z-axis radius of the ellipsoid

Solid Code Block Reference (Continued)

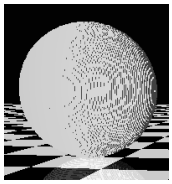

Sphere

Variables	Type	Definition
Center	Vector	Global position of the center of the solid
Local Center Offset	Vector	Translation applied to the solid prior to bone orientation; modifies the center of rotation
Radius	Number	Radius of the sphere

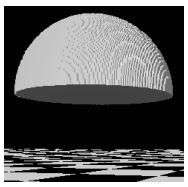

Dome

Variables	Type	Definition
Center	Vector	Global position of the center of the solid
Local Center Offset	Vector	Translation applied to the solid prior to bone orientation; modifies the center of rotation
Radius	Number	Radius of the dome
Up	Boolean (True/False)	Does the long axis point in the direction of the dome's curve (True) or its base (False)?

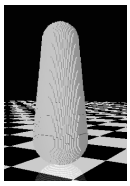

Capsule

Variables	Type	Definition
Center	Vector	Global position of the center of the solid
Local Center Offset	Vector	Translation applied to the solid prior to bone orientation; modifies the center of rotation
TopRadius	Number	Radius of the top of the capsule
BottomRadius	Number	Radius of the bottom of the capsule
Height	Number	Height of the capsule along its long axis; height must be at least as big as the top radius + bottom radius

Solid Code Block Reference (Continued)

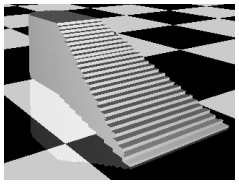

Custom Foot Object

Variables	Type	Definition
Center	Vector	Global X,Z position of the center of the ankle, at the height, Y position, of the sole of the foot.
Local Center Offset	Vector	Translation applied to the solid prior to bone orientation; modifies the center of rotation
FootLength	Number	Length of the foot, toe to heel
ToeWidth	Number	Width of the front of the foot, 1st to 5th metacarpal. Dimension runs along the minor axis of the foot.
AnkleLength	Number	Length of the ankle
AnkleHeight	Number	Height of the ankle from the sole of the foot. Dimension runs along the long axis of the foot.
AnkleWidth	Number	Width of the ankle. Dimension runs along the minor axis of the foot. Note: If toe width is set to a value less then the ankle width the ankle width is set to the same value as the toe width.

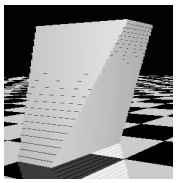

Aligned Tapered Box

Variables	Type	Definition
Center	Vector	Global X, Z position of the point of alignment at the mid-height, Y position, of the solid.
Local Center Offset	Vector	Translation applied to the solid prior to bone orientation, modifies the center of rotation
TopWidth	Number	Top width of the box along its minor axis
TopDepth	Number	Top depth of the box
BottomWidth	Number	Bottom width of the box along its minor axis
BottomDepth	Number	Bottom depth of the box
Height	Number	Height of the box along its long axis
AlignFront	Boolean	Is the Center located at the Front face (True) or the Rear face (False)?
AlignTop	Boolean	Is the AlignOffset being applied to the Top face (True) or the Bottom face (False)?
AlignOffset	Number	Offset the designated face (Top/Bottom) forward from the Center by this amount.

Solid Code Block Reference (Continued)

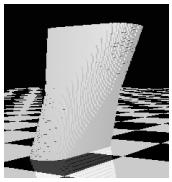

Aligned Stadium Solid

Variables	Type	Definition
Center	Vector	Global X, Z position of the point of alignment at the mid-height, Y position, of the solid.
Local Center Offset	Vector	Translation applied to the solid prior to bone orientation; modifies the center of rotation
TopWidth	Number	Top width of the stadium solid along its minor axis
TopDepth	Number	Top depth of the stadium solid
BottomWidth	Number	Bottom width of the stadium solid along its minor axis
BottomDepth	Number	Bottom depth of the stadium solid
Height	Number	Height of the stadium solid along its long axis
AlignFront	Boolean	Is the Center located at the Front face (True) or the Rear face (False)?
AlignTop	Boolean	Is the AlignOffset being applied to the Top face (True) or the Bottom face (False)?
AlignOffset	Number	Offset the designated face (Top/Bottom) forward from the Center by this amount.

Internal Variables

Internal variables are defined at runtime to communicate motion capture marker positions and the internal state of the spatial model. It is highly recommended that internally defined variables only be read from; writing to internal variables will result in undefined behavior.

Dynamic Motion Capture Marker Positions

The dynamic motion capture CSV data file associated with a trial is used to define the internal variables that represent the trial's dynamic raw data values and three-dimensional marker position vectors. It is assumed that columns within the CSV file correspond to variables and that rows correspond to frames. The column header name of each column in the trial data file is defined as an internal variable of

type “number” and, within the source code, represents the respective value stored in the column for a given modeled frame. Columns with header names ending in “:x”, “:y”, or “:z” that are otherwise identical are grouped into three-dimensional position vectors. The common column name is defined as an internal variable of type “numeric vector” which, within the source code, represents the three-dimensional marker position defined by the three grouped columns for the frame being modeled. The example in Table 20 illustrates the usage and naming convention.

The static motion capture CSV data file associated with a trial is used to define the static internal variables (Table 20). Static internal variables return the mean numeric or vector value for each respective column or marker position in the static data file, following the same file structure, variable type, and naming conventions described for the dynamic data files; undefined data points are ignored. Static internal variables are defined by prefixing “static:” to the respective variable name.

Table 20 – Example of input CSV data file and the resulting dynamically defined internal variables

CSV File

Sub:C7:X,	Sub:C7:Y,	Sub:C7:Z,	Sub:T10:X,	Sub:T10:Y,	Sub:T10:Z
1,	2,	3,	4,	6,	7
2,	5,	1,	8,	3,	0
4,	7,	4,	3,	9,	2

Dynamic Source

X = dist (Subj:C7, Subj:T10);	distance between two position vectors
Y = Subj:C7:Y – Subj:T10:Y;	difference in the Y position value
V = Subj:C7 - Subj:T10;	difference between two vectors

Internal Model State

The following internal variables are defined at runtime to return the spatial model state.

Variable:	**FrameNumber**
Alt Syntax:	Frame
Type:	Number
Value Description:	The frame number of the current frame being rendered by the spatial consumption engine.

Variable:	**ParticipantNumber**
Alt Syntax:	Participant
Type:	Number
Value Description:	The index number of the participant being rendered by the spatial consumption engine.

Variable:	**InvalidMarkerValue**
Type:	Number
Value Description:	The sentinel number used to represent an invalid internal marker value.

Internal Functions

The spatial language contains internal functions to support basic arithmetic operations, vector operations, data file access, debugging, and reference object drawing. There is currently no support for user-defined functions. All function parameter values are passed by value. Functions accept raw values, variables, expressions, and function output as parameter input. A list of the internal functions follows.

General Math Functions

Function:	**Abs (x)**
Returns:	The absolute value of x
Parameter (x):	Floating point value
Example:	value = Abs (-3.14159); // Value = 3.14159

General Math Functions (Continued)

Function:	**Floor (x)**
Returns:	The largest integer value that is not greater than *x*
Parameter (x):	Floating point value
Example:	value = Floor (3.14159); // Value = 3

Function:	**Ceil (x)**
Returns:	Returns the smallest integer value that is not less than *x*.
Parameter (x):	Floating point value
Example:	value = Ceil (3.14159); // value = 4

Function:	**Sqrt (x)**
Returns:	The square root of x.
Parameter (x):	Floating point value
Example:	value = Sqrt (4); // Value = 2

Function:	**Log (x)**
Returns:	Returns the natural logarithm of x
Parameter (x):	Floating point value
Example:	value = Log (4.0); // value = 1.38629…

Function:	**Log10 (x)**
Returns:	The base-10 logarithm of x
Parameter (x):	Floating point value
Example:	value = Log10 (100.0); // value = 2.0

Function:	**EXP (x)**
Returns:	The exponential function of x, i.e. e^x
Parameter (x):	Floating point value
Example:	value = EXP (1.0); // value = 2.71828…

General Math Functions (Continued)

Function:	**Pow (x, y)**
Returns:	x raised to the y power, i.e. x^y
Parameter (x):	Floating point value
Parameter (y):	Floating point value
Example:	Value = Pow(5, 2); // value = 25

Function:	**Min (x, y)**
Returns:	The minimum value of x and y
Parameter (x):	Floating point value
Parameter (y):	Floating point value
Example:	value = Min (1.0, 5.0); // value = 1.0

Function:	**Max (x, y)**
Returns:	The maximum value of x and y
Parameter (x):	Floating point value
Parameter (y):	Floating point value
Example:	value = Max (1.0, 5.0); // value = 5.0

Trig Functions

Function:	**Cos (x)**
Returns:	The cosine of the angle
Parameter (x):	Floating point value of angle in radians
Example:	angle = 0.0; value = cos (angle); // value = 1.0

Function:	**Sin (x)**
Returns:	The sine of the angle
Parameter (x):	Floating point value of angle in radians
Example:	pi = 3.14159; value = sin (pi / 4); // value = 0.70710…

Trig Functions (Continued)

Function:	**Tan (x)**
Returns:	The tangent of the angle
Parameter (x):	Floating point value of angle in radians
Example:	pi = 3.14159; value = tan (pi / 4); // value = 1.0

Function:	**ACos (x)**
Returns:	The principal value of the arc cosine of *x*, expressed in radians. Inverse of the Cos (x).
Parameter (x):	Floating point value from with a value ranging from -1 to + 1
Example:	value = ACos (0.5); // value = 1.04719…

Function:	**ASin (x)**
Returns:	The principal value of the arc sine of *x*, expressed in radians. Inverse of the Sin(x).
Parameter (x):	Floating point value from with a value ranging from -1 to + 1
Example:	value = ASin (0.5); // value = 0.52359…

Function:	**ATan (x)**
Returns:	The principal value of the arc tangent of *x*, expressed in radians. Inverse of the Tan(x).
Parameter (x):	Floating point value
Example:	value = ATan (1.0); // value = 0.78539…

Function:	**ATan2 (y, x)**
Returns:	The principal value of the arc tangent of y/*x*, expressed in radians. Inverse of the Tan(x).
Parameter (y): Parameter (x):	Floating point y coordinate value Floating point x coordinate value
Example:	value = ATan2 (4.0, 2.0); // value = 1.10714…

Trig Functions (Continued)

Function:	**CosH (x)**
Returns:	The hyperbolic cosine of (x)
Parameter (x):	Floating point value
Example:	value = CosH (2.0); // value = 3.76219…

Function:	**SinH (x)**
Returns:	The hyperbolic sine of (x)
Parameter (x):	Floating point value
Example:	value = SinH (2.0); // value = 3.62686…

Function:	**TanH (x)**
Returns:	The hyperbolic tangent of (x)
Parameter (x):	Floating point value
Example:	value = TanH (2.0); // value = 0.96402…

Vector Functions

Function:	**Vector (x, y, z, ..., n)** **Variable Parameter Number**
Returns:	A vector constructed from the vector parameters.
Parameter (x):	Floating point x value, vector element[0], or X vector element
Parameter (y):	Floating point y value, vector element[1], or Y vector element
Parameter (z):	Floating point z value, vector element[2], or Z vector element
Parameter (n):	Floating point n value, vector element[n-1]

Examples:	// Two Examples
	value = Vector(1,2,3); // value = [1,2,3];
	value1 = Vector(1); // value1 = [1];

Vector Functions (Continued)

Function:	**Distance (x, y)**
Alt Syntax:	Dist (x, y)
Returns:	The distance between x and y
Parameter (x):	Floating point value
Parameter (y):	Floating point value
or	
Parameter (x):	Vector value
Parameter (y):	Vector value

Example:	value = dist (1, 5); // Distance between double values (=4)
	value = distance ([1,1,1], [3, 4, 5]); // Distance between Vectors (=5.4)

Function:	**Dot (x, y)**
Returns:	The dot product of vectors x and y
Parameter (x):	Vector value
Parameter (y):	Vector value
Example:	value = dot ([1,1,1], [3, 4, 5]); // Dot product of two vectors (=12)

Function:	**Cross (x, y)**
Returns:	The cross product of two vectors (i.e. x **x** y)
Parameter (x):	Vector value
Parameter (y):	Vector value
Example:	value = cross ([1,1,1], [3, 4, 5]); // Cross product of vectors (=[1,-2,1])

Function:	**Unit (x)**
Returns:	The unit vector of vector x
Parameter (x):	Vector value
Example:	value = unit ([4, 3, 5]); // value = [0.566, 0.424, 0.707]

Function:	**ElementAt (vec, index)**
Returns:	The floating point value stored in the vector at the specified index
Parameter (vec):	Vector value
Parameter (index):	Integer index value
Example:	Value = ElementAt ([1,2,3], 0); // value = 1

Vector Functions (Continued)

Function:	**SetElement (vec, index, value)**
Returns:	Returns the vector created by setting the element at index parameter to the value parameter.
Parameter (vec):	Vector value; function call does not change vec parameter
Parameter (index):	Vector index of the value to change.
Parameter (value):	Value to set the index value to.
Example:	InVec = [1,2,3]; Value = SetElement (InVec, 0, 3.14159);
Result:	InVec (unchanged) = [1,2,3] value = [3.14159, 2, 3]

String Functions

Function:	**ToString (P1, P2, P3, ... N)**	**Variable Parameter Number**
Returns:	The string created by appending the strings created by each of the parameters.	
Parameter:	Any combination of strings values, vector values, and floating point values can be passed in as parameters.	
Example:	value = ToString (“Magic Number: ”, 42); // result value = “Magic Number: 42.0000”	

Function:	**CharAt (str, index)**
Returns:	The character stored at the specified index
Parameter (str):	String value;
Parameter (index):	Index of the character to return.
Example:	Value = CharAt (“hello”, 1); // value = “e”

Function:	**SetChar (str, index, char)**
Returns:	The string created by setting the character at index to the char parameter.
Parameter (str):	String value; function call does not change string parameter
Parameter (index):	String index of the value to change.
Parameter (char):	Char to set the index value to.

Example:	InStr = “Hello”;
	value = SetChar (InStr, 1, “H”);
	// result
	// InStr (unchanged) = “Hello” value = “HHllo”

Data Access Functions

Function:	**CsvFile (filename, units, column, row)**
Alt Syntax:	CSV (filename, units, column, row)
Returns:	Returns the value stored in the specified CSV file at the specified column name and row number
Performance Note:	CSV file read caches the CSV data to avoid repeated data file i/o
Parameter (filename):	String value specifying the CSV data file to open. CSV file format must conform to the previously defined CSV file format.
Parameter (units):	String parameter specifying the measurement units that the data file is stored in. Parameter Values: “cm”, “mm”, “dm”, “m”, “dkm”, “km”, “in”, “ft”
Parameter (column):	String value specifying the name of the column to return a value from. If the column specifies a full column name, a single value (String or floating point value) is returned. If the column string specifies a full valid data file column name excluding the ending “:X”, “:Y”, or “:Z” column specifier, then a vector containing the three values is returned.
Parameter (row):	An integer specifying the row of the column to return (excluding the header row). Row indices are zero base.
Example Data File:	Line, Hand:X, Hand:Y, Hand:Z LN1, 1, 2, 3 LN2, 4, 5, 6
Source Example (1):	value = CSV (“c:\datafile.csv ”, “cm”, “Hand”, 1); // value = [4, 5, 6]
Source Example (2):	value = CSV (“c:\datafile.csv ”, “cm”, “Hand:Y”, 1); // value = 5
Source Example (3):	value = CSV (“c:\datafile.csv ”, “cm”, “Line”, 0); // value = “LN1”

Data Access Functions (Continued)

Function:	**ViconCsv (filename, column, row)**
Alt Syntax:	Vicon (filename, column, row)
Returns:	The value stored in the specified Vicon CSV file at the specified column name and row number.
Performance Note:	CSV file read caches the CSV data to avoid repeated data file i/o
Parameter (filename):	String value specifying the Vicon CSV data file to open. CSV file format must conform to the previously defined CSV file format.
Parameter (column):	String value specifying the name of the column to return a value from. If the column specifies a full column name, a single value (String or floating point value) is returned. If the column string specifies a full valid data file column name excluding the ending ":X", ":Y", or ":Z" column specifier, then a vector containing the three values is returned.
Parameter (row):	An integer specifying the row of the column to return (excluding the header row). Row indices are zero base.
Example Data File:	Hand:X, Hand:Y, Hand:Z 1, 2, 3 4, 5, 6
Source Example (1):	value = Vicon ("c:\vicondatafile.csv ", "Hand", 1); // value = [4, 5, 6]
Source Example (2):	value = Vicon ("c:\vicondatafile.csv ", "Hand:Y", 1); // value = 5

Function:	**StaticViconCsv (filename, column)**
Alt Syntax:	StaticVicon (filename, column)
Returns:	The mean value stored in a column
Performance Note:	CSV file read caches the CSV data to avoid repeated data file i/o
Parameter (filename):	String value specifying the Vicon CSV data file to open. CSV file format must conform to the previously defined CSV file format.
Parameter (column):	String value specifying the name of the column to return a value from. If the column specifies a full column name, a single value (String or floating point value) is returned. If the column string specifies a full valid data file column name excluding the ending ":X", ":Y", or ":Z" column specifier, then a vector containing the three values is returned.
Example Data File:	Hand:X, Hand:Y, Hand:Z 1, 2, 3 4, 5, 6
Source Example (1):	value = StaticVicon ("c:\vicondatafile.csv ", "Hand"); // value = [2.5, 3.5, 4.5]
Source Example (2):	value = StaticVicon ("c:\vicondatafile.csv ", "Hand:Y"); // value = 3.5

Debug Output Function

Function:	**PrintLn (str)**
Returns:	Nothing. Function prints the string to standard out. Standard out is normally controlled by the Java Console. If the Java application has been started without a console, then the output will not normally be visible.
Parameter (str):	String to print to standard out.
Example:	PrintLn (“Test ”, 123); // Outputs “Test 123.0000”

Model State Functions

Function:	**GetStaticViconCSVPath ()**
Alt Syntax:	GetStaticPath ()
Returns:	The path to the current Static Vicon CSV data file, as a string.
Example:	value = GetStaticPath (); // value = “c:\viconstatic.csv”

Function:	**GetViconCSVPath ()**
Alt Syntax:	GetViconPath ()
Returns:	The path to the current Vicon CSV data file, as a string.
Example:	value = GetViconPath (); // value = “c:\vicon.csv”

Function:	**GetPlaneHeight ()**
Returns:	The height of the plane selected in the UI.
Example:	value = GetPlaneHeight (); // value = 12.23

Reference Object Drawing Functions

These Functions are used to draw reference objects and are only valid for reference objects.

Function:	**Line (x1,y1,z1, x2, y2, z2)**
Returns:	Nothing. Draws a line from coordinate (x1, y1, z1) to coordinate (x2, y2, z2)
Parameter (x1, y1, z1):	Floating point values
Parameter (x2, y2, z2):	Floating point values
Example:	Line (1,2,4, 3, 6, 7);

Reference Object Drawing Functions (Continued)

Function:	**Line (x1, x2)**
Returns:	Nothing. Draws a line from coordinate (x1) to coordinate (x2)
Parameter (x1):	Vector values
Parameter (x2):	Vector values
Example:	Line ([1,2,4], [3, 6, 7]);

Function:	**LineWidth (x)**
Returns:	Nothing. Sets the current line drawing width to x
Parameter (x):	Floating point value
Example:	LineWidth (1.5);

Function:	**Color (r, g, b)**
Alt Syntax:	RGB (r, g, b)
Returns:	Nothing. Sets the current drawing color to the one specified by R, G, B
Parameter (r):	Floating point value in range 0 to 1.0 or 0 to 255
Parameter (g):	Floating point value in range 0 to 1.0 or 0 to 255
Parameter (b):	Floating point value in range 0 to 1.0 or 0 to 255
Note:	r, g, b parameters must be on the same range scale.
Example (1):	RGB (1.0, 0.5, 0.75);
Example (2):	RGB (75, 30, 255);

Function:	**Color (color)**
Alt Syntax:	RGB (color)
Returns:	Nothing. Sets the current drawing color to the one specified by the parameter color
Parameter (color):	Vector value containing r, g, and b values.
Note:	r, g, b parameters must be on the same range scale, 0.0 - 1.0 or 0.0 – 255.0.
Example (1):	RGB ([1.0, 0.5, 0.75]);
Example (2):	RGB ([75, 30, 255]);

Reference Object Drawing Functions (Continued)

Function:	**Point (x, y, z)**
Returns:	Nothing. Draws a point at position x, y, z
Parameter (x):	Floating point value, global x position.
Parameter (y):	Floating point value, global y position.
Parameter (z):	Floating point value, global z position.
Example:	Point (400, 23, 23);

Function:	**Point (vec)**
Returns:	Nothing. Draws a point at position vec
Parameter (vec):	Vector value, containing x, y, z values
Example:	Point ([400, 23, 23]);

Function:	**PointSize (x)**
Returns:	Nothing. Sets the current point drawing size to x
Parameter (x):	Floating point value
Example:	PointSize (1.5);

Function:	**Bone (p, a, l, o, or)**
Returns:	Nothing. Draws a segment's orientation vector
Parameter (p):	Vector value, proximal position vector [x, y, z]
Parameter (a):	Vector value, anterior position vector [x, y, z]
Parameter (l):	Vector value, lateral position vector [x, y, z]
Parameter (o):	Vector value, origin position vector [x, y, z]
Parameter (or):	Vector value, origin [x, y, z]
Note:	lines drawn = (p - o) + or, (a - o) + or, (l - o) + or line color = RGB

Function:	**Box (center, width, height, depth)**
Alt Syntax:	Cube (center, width, height, depth)
Returns:	Nothing. Draws a box centered at "center" with dimensions (width, height, depth)
Parameter (center):	Vector value, center position of the box (vector [x,y,z])
Parameter (width):	Floating point value, box width dimension
Parameter (height):	Floating point value, box height dimension
Parameter (depth):	Floating point value, box depth dimension
Example:	Box ([12, 3, 2], 2 , 3, 4);

Reference Object Drawing Functions (Continued)

Function:	**Box (center, dim)**
Alt Syntax:	Cube (center, dim)
Returns:	Nothing. Draws a box centered at “center” with dimensions “dim”
Parameter (center):	Vector value, center position of the box (vector [x,y,z])
Parameter (dim):	Vector value, dimensions of the box (vector [width, depth, height])
Example:	Box ([12, 3, 2], [2 , 3, 4]);

Function:	**scale (width_scale, height_scale, depth_scale)**
Returns:	Nothing. Adjust the drawing scale.
Parameter (width_scale):	Floating point value, width scale value
Parameter (height_scale):	Floating point value, height scale value
Parameter (depth_scale):	Floating point value, depth scale value
Example:	Scale (2.0, 2.0, 2.0); // draw at x2 size

Function:	**scale (s);**
Returns:	Nothing. Adjusts the drawing scale.
Parameter (s):	Vector value, s = [width scale, height scale, depth scale]
Example:	Scale ([2.0, 2.0, 2.0]); // draw at x2 size

Function:	**DrawMarkerSet (prefix);**
Returns:	Nothing. Draws the dynamic motion capture markers for the current frame that have a name starting with the prefix parameter.
Parameter (prefix):	Prefix of markers names to draw
Example:	DrawMarkerSet(“subject:”);

Function:	**DrawMarkerSet ();**
Returns:	Nothing. Draws the entire dynamic motion capture marker set for the current frame
Example:	DrawMarkerSet();

Language Execution Model

The spatial consumption language is directly integrated with the broader spatial consumption software engine; the engine controls exactly what code modules

are executed and the order of execution. The source contained within volume objects and reference objects is executed independently and their state is not accessible across executions.

The source code attached to a volume object is executed to initialize and define the object's properties during three-dimensional rendering, during plane intersection testing, and during generation of output. The execution of the volume object source code follows the volume object project hierarchy: project, object, solid bone, and solid source. The volume language itself has no syntax for defining execution scope; however, the execution of the volume objects' source is internally scoped following the object hierarchy. The net effect of this is that child objects can access parent object state but cannot directly access the state of fellow sibling objects. In pseudo code, the volume object hierarchy can be thought of as executing as shown in Table 21.

Table 21 – Pseudo code representation of volume object hierarchy execution.

```
Execute "Volume Project Source"
        ForEach "Volume Object"
        Begin
                Execute "Volume Object Source"
                ForEach "Geometric Solid Object"
                Begin
                        Begin
                                Execute "Geometric Solid Bone Source"
                        End
                        Begin

                                Execute "Geometric Solid Source"
                        End
                End
        End
```

In contrast with the volume object execution hierarchy, reference object execution occurs in isolation. Reference objects' state cannot be shared across

reference objects and reference objects cannot share their state with volume objects. In short, reference object source is executed in an entirely self-contained environment.

Runtime errors are raised as a result of both language syntax errors and the use of undefined internal variables. The undefined internal variable errors can occur when internal variables used to reference motion capture data are accessed and are undefined due to missing or invalid data for the frame in which they are being accessed. All errors, both syntax and missing data, are logged in the UI. Once an error is raised, the execution of the currently executing code block is halted and execution proceeds to the next code block. All errors, both syntax and missing data, are logged in the UI.

Example Source

The following examples demonstrate actual valid source code. The examples demonstrate initialization of two volume objects and two reference objects.

Volume Objects

Capsule

Bone

```
longaxis = al:alrsjc - al:alrejc;
```

Code

```
center         = al:alrejc;  // global position
topradius      = csv (staticbodymeasurements ,"cm","upper arm circ", 29) / (2*pi);
bottomradius   = csv (staticbodymeasurements ,"cm","elbow width", 29) / 2;
height         = distance (al:alrsjc,al:alrejc);
localcenteroffset = [0,height/2,0];  // optional local offset to global center
```

Aligned Stadium Solid

Bone

```
longaxis = al:altrup-al:altruo;
minoraxis = -(al:altrul - al:altruo);
```

Code

```
pvec = unit(al:altrup - al:altruo);
avec = unit(al:altrua - al:altruo);
center        = al:altruo;  // global position
topwidth      = csv (staticbodymeasurements ,"cm","brest width", 29);
topdepth      = 2*(csv (staticbodymeasurements ,"cm","brest circ", 29) –
                  2*topwidth)/(-4 + 2* pi);
bottomdepth   = csv (staticbodymeasurements ,"cm","waist depth", 29);
bottomwidth   = (csv (staticbodymeasurements ,"cm","waist circ", 29) –
                  pi*bottomdepth)/2 + bottomdepth;
midpsi = (al:allpsi + al:alrpsi) /2;
height  = dot (al:alt5 - midpsi, pvec);
new_height     = dot (al:alt5 - al:alt10, pvec);
voffset = (height-new_height);
bottomdepth    = voffset * ((topdepth - bottomdepth) / height) + bottomdepth;
bottomwidth    = voffset * ((topwidth - bottomwidth) / height) + bottomwidth;
height  = new_height;
alignfront     = false;
aligntop = true;
zoffset = dot (avec, al:alt10 - al:altruo);
alignoffset    = dot (avec, al:alt5 - al:alt10);
center = center + (zoffset *avec) + (voffset * pvec);
 // optional local offset
localcenteroffset = [0,height/2 + dot(midpsi - al:altruo, pvec), 0];
```

Reference Objects

referenceobject "orange lavatory”

```
lavatorymeasurements   = "f:\"+"lavatorydimension.csv";
color (0xff,128,0);
lavur = viconcsv (lavatorymeasurements, "orangelav:ur", 0);
lavbl = viconcsv (lavatorymeasurements, "orangelav:bl", 0);
lavul = [ ElementAt(lavbl,0), ElementAt(lavbl,1), ElementAt(lavur,2)];
lavbr = [ ElementAt(lavur,0), ElementAt(lavbl,1), ElementAt(lavbl,2)];

line (lavul, lavur);
line (lavul, lavbl);
line (lavbr, lavur);
line (lavbr, lavbl);

planeheight =  getplaneheight();
lavul = setelement (lavul, 1, planeheight);
lavbl = setelement (lavbl, 1, planeheight);
lavur = setelement (lavur, 1, planeheight);
lavbr = setelement (lavbr, 1, planeheight);

line (lavul, lavur);
line (lavul, lavbl);
line (lavbr, lavur);
line (lavbr, lavbl);
```

referenceobject "toilet"

```
linewidth (2);
drive = "f:\";
lavatorymeasurements   = drive+"lavatorydimension.csv";
pos = viconcsv (lavatorymeasurements, "toilet", 0);
x = elementat (pos,0);
z = elementat (pos,2);

// draw toilet outline on floor
color ([1.0, 0.5, 0.0]);
line ([x-7.5, 4, z],[x+7.5,4,z]);
line ([x-7.5, 4, z-21.5],[x+7.5,4,z-21.5]);
line ([x-7.5, 4, z],[x-7.5, 4, z-21.5]);
line ([x+7.5,4,z],[x+7.5,4,z-21.5]);
planeheight =  getplaneheight();
line ([x-7.5, planeheight, z],[x+7.5,planeheight,z]);
line ([x-7.5, planeheight, z-21.5],[x+7.5,planeheight,z-21.5]);
line ([x-7.5, planeheight, z],[x-7.5, planeheight, z-21.5]);
line ([x+7.5,planeheight,z],[x+7.5,planeheight,z-21.5]);
z = -z;

scale (1,1,-1);
color ([1.0, 0.5, 0.0]);

// toliet seat base
cube ([x, 16.0 + 0.75/2.0, z + 21.5 / 2.0], 15, 0.75, 21.5);

// toliet back left
cube ([x - (14.5 / 2) + (0.75 /2), 16.75 + 9.0, z+ 5.5 / 2.0],   [0.75,18.0,5.5]);
cube ([x + (14.5 / 2) - (0.75 /2), 16.75 + 9.0 , z + 5.5 / 2.0], [0.75,18.0,5.5]);

// toliet back middle
cube ([x, 27.0 + 5.5/2.0, z+1.5], 13.0, 5.5,0.75);

// toliet seat
cube ([x, 16.75 + 0.75/2.0, z + 5.5 / 2.0],[13.0,0.75,4.75]);
color ([1.0, 1.0, 1.0]);
cube ([x, 16.75 + 0.5, z + 5.5 + 3.5/ 2.0],[15.0,1.0, 3.5]);
cube ([x + 15.0 / 2 - 4.75 / 2, 16.75 + 0.5, z + 9.0 + 13.0/ 2.0], [4.75,1.0, 13.0]);
cube ([x - 15.0 / 2 + 4.75 / 2, 16.75 + 0.5, z + 9.0 + 13.0/ 2.0], [4.75,1.0, 13.0]);
color ([1.0, 0.5, 0.0]);

// support
cube ([x, 6.0 + 0.75 / 2.0, z + 3.0], [11.5,0.75, 6.0]);
cube ([x, 0.75 / 2.0, z + 13.25 / 2.0], [6.0,0.75, 13.25]);
cube ([x, 8.25 + 7.75 / 2.0, z + 6.75 + 0.75/ 2.0], [6.0, 7.75, 0.75]);
cube  ([x + 7.5 / 2 - 0.75 / 2, 11.0 / 2.0, z + 13.25/ 2.0], [0.75, 11.0, 13.25]);
cube ([x + 7.5 / 2 - 0.75 / 2, 11.0 + 2.5, z + 19.0/ 2.0], [0.75, 5.0, 19.0]);
cube ([x - 7.5 / 2 + 0.75 / 2, 11.0 / 2.0, z + 13.25/ 2.0], [0.75, 11.0, 13.25]);
cube ([x - 7.5 / 2 + 0.75 / 2, 11.0 + 2.5, z + 19.0/ 2.0], [0.75, 5.0, 19.0]);
scale (1,1,-1);
```

Appendix E

2007 Northwest Biomechanics Symposium Abstract

A METHOD FOR CALCULATING THE SPATIOTEMPORAL REQUIREMENTS OF A MOVEMENT TASK

Philbrick, K and Pavol, M
Department of Nutrition and Exercise Sciences, Oregon State University, Corvallis, OR USA
email: philbrik@onid.orst.edu

INTRODUCTION

A fundamental component of ergonomic workstation design is to ensure that sufficient spatial volume is provided to safely conduct the required tasks. Biomechanical analyses employing motion capture are a powerful tool for inferring the risk of injury during a task based on the associated joint angles, forces, and moments [1]. However, such analyses typically provide little information regarding the spatial volume used during a task, nor how much time different regions within that volume are used. To address this limitation, a novel method has been developed to efficiently compute the spatiotemporal requirements of a movement task using a combination of motion capture data and static body measurements.

METHODS

Geometric Model. The basis of the method is a model of the body as a set of geometric solids (bounding volumes) that approximate the size and shape of the body's segments. The algorithm uses as input the global position of each joint center and the three-dimensional orientation of each body segment of interest, derived from motion capture data. These data are used to position, orient, and scale the bounding volumes at each frame (i.e. sample time) across the movement task.

Five basic geometric shapes were selected to serve as bounding volumes for human segments. Tapered capsules are used to model the forearms, arms, legs, and thighs. Stadium solids [2] are used for the pelvis and trunk. The head is modeled as an ellipsoid. A custom foot shape was also developed. Finally, spheres at each joint are used to minimize gapping between body segments.

To accurately model the body segments, the dimensions of the bounding volumes are dynamically calculated, where feasible, from the instantaneous distances between joint centers. The remaining dimensions are determined from a set of 15 static measurements (e.g. knee circumference).

Planar Intersections. To determine the spatiotemporal requirements of a movement task, a set of planes of interest must be selected (e.g. at different height increments), along with the desired within-plane areal resolution. The space consumed within each plane in each individual frame of data is computed by calculating the intersection between the plane and each bounding volume that comprises the geometric model (Figure 1). The result is a binary spatial map of the areal elements that are (= 1) and are not (= 0) occupied for a given plane and frame.

The basic algorithm to calculate the intersection between a plane and volume is as follows. First, a bounding sphere for the volume is calculated and an intersection test is conducted between the bounding sphere and the plane of interest. If the bounding sphere is found to intersect the plane, the volume is projected onto the plane and the points inside this projection are tested for intersection. One of three algorithms is used in the intersection tests, as determined by the shape of the bounding sphere/volume. The first algorithm, used for spheres and tapered capsules, employs ray intersection techniques from ray-tracing. A second algorithm is designed to calculate intersections between convex bounding volumes using a combination of caching and/or a linear search. Finally, a general algorithm, in which each areal element is tested, was designed for concave shapes. These three algorithms have relative computational efficiencies, in big-O notation, of $O(N)$, $O(N \text{ Log}_2 N)$ to $O(N^2)$, and $O(N^2)$, respectively, where the area of intersection is defined by a NxN grid.

Spatiotemporal Mapping. The final step is to construct a spatiotemporal map which expresses the proportion of time during the movement task that each areal element within a given plane was occupied (Figure 2). This process essentially involves averaging the spatial maps, element-by-element, across all frames of a movement task. Spatiotemporal maps may similarly be averaged across trials, individuals, and/or tasks.

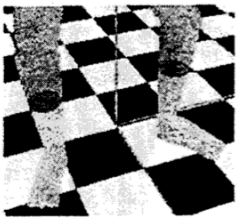

Figure 1: Space consumed at the mid-leg level during one motion capture frame.

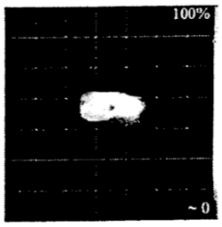

Figure 2: Spatiotemporal map taken near the level of the hip for a transfer task.

CONCLUSIONS

The spatial requirements for the safe performance of a task are a key variable in ergonomic design. This method represents a novel technique for using motion capture data to derive detailed three-dimensional spatiotemporal maps of movement task performance. These maps can provide ergonomists and designers with precise information regarding what space must be provided, how efficiently or effectively a given space is being utilized, and what space might potentially be eliminated. Thus, this method can complement traditional biomechanical analyses in creating safer, more efficient, and more accessible workplaces.

REFERENCES

1. Kingma I, et al. *Ergonomics* **47**, 1365-1385, 2004.
2. Yeadon MR. *J Biomech* **23**, 67-74, 1990.

ACKNOWLEDGEMENTS

Funded by grant H133E030009 from the U.S. Dept. of Education, NIDRR.